Direct, Quantitative Analysis of Organic Contaminants in Complex Samples Using Membrane Introduction Mass Spectrometry with Electron and Chemical Ionization

by

Gregory William Vandergrift
B.Sc., Vancouver Island University, 2016

A Dissertation Submitted in Partial Fulfillment
of the Requirements for the Degree of

DOCTOR OF PHILOSOPHY

in the Department of Chemistry

Supervisory Committee

Direct, Quantitative Analysis of Organic Contaminants in Complex Samples Using Membrane Introduction Mass Spectrometry with Electron and Chemical Ionization

by

Gregory William Vandergrift
B.Sc., Vancouver Island University, 2016

Dr. Chris Gill, Department of Chemistry
Co-Supervisor

Dr. J. Scott McIndoe, Department of Chemistry
Co-Supervisor

Dr. Alexandre Brolo, Department of Chemistry
Departmental Member

Dr. Erik Krogh, Department of Chemistry
Departmental Member

Dr. Mohsen Akbari, Department of Mechanical Engineering
Outside Member

Abstract

Supervisory Committee

Dr. Chris Gill, Department of Chemistry
Co-Supervisor

Dr. J. Scott McIndoe, Department of Chemistry
Co-Supervisor

Dr. Alexandre Brolo, Department of Chemistry
Departmental Member

Dr. Erik Krogh, Department of Chemistry
Departmental Member

Dr. Mohsen Akbari, Department of Mechanical Engineering
Outside Member

Condensed phase membrane introduction mass spectrometry (CP-MIMS) is a direct, *in situ* analysis technique that is well suited to persistent organic pollutants, pesticides, and other small molecules. In CP-MIMS, neutral analytes permeate a hollow fibre membrane, typically polydimethylsiloxane (PDMS), driven by a concentration gradient. Analytes are subsequently dissolved by a liquid (condensed) solvent acceptor phase that is continuously flowed through the membrane lumen, which finally entrains the analytes to a mass spectrometer for detection. The membrane rejects charged and particulate matrix components, therefore eliminating sample cleanup that is otherwise necessary for conventional (*i.e.*, chromatographic) techniques. However, larger analytes may suffer from relatively lengthy response times and lower sensitivity. A heptane cosolvent was therefore doped into the PDMS membrane, resulting in a polymer inclusion membrane (PIM). Through a system coupling CP-MIMS to electrospray ionization (ESI), the use of a PIM for model compounds resulted in faster response (~3×) and improved sensitivity (~3.5×, parts per trillion level detection limits).

While effective for the demonstration of the PIM, pairing ESI with CP-MIMS represents an inherent incongruity: ESI is effective for polar, hydrophilic analytes, whereas CP-MIMS (*i.e.*, PDMS membranes) is effective for hydrophobic analytes. CP-MIMS was therefore coupled with liquid electron ionization (LEI) as a more suitable ionization strategy. In LEI, the post-membrane solvent flow is entrained at nanolitre per minute flowrates to a LEI source, where the liquid is sequentially nebulized, vaporized, and ionized. The CP-MIMS-LEI coupling was optimized for the measurements of polycyclic aromatic hydrocarbon (PAH) isomer classes from aqueous samples, demonstrating low ng/L detection limits and response times (≤1.6 min). CP-MIMS-LEI was also applied to PAH isomer classes from soil samples, demonstrating rapid sample throughput (15 samples/hr) and low μg/kg detection limits, and additionally was quantitatively

comparable to conventional techniques. A similar CP-MIMS-LEI system was applied to online monitoring of catalytic oxidation and alkylation reactions, demonstrating quantitative, real-time results for harsh, complex organic reaction mixtures.

A significant analytical improvement was conducted by intentionally exploiting the already present liquid acceptor phase as an *in situ* means of providing liquid chemical ionization (CI) reagents for improved analyte sensitivity and selectivity (*i.e.*, CP-MIMS-LEI/CI). Acetonitrile and diethyl ether were used as a combination acceptor phase/CI reagent system (*i.e.*, proton transfer reagents) for the direct analysis of bis(2-ethylhexyl)phthalate from house dust (6 mg/kg detection limit). CP-MIMS-LEI/CI was then applied to PAHs from soils. Using methanol and dichloromethane combination acceptor phase/CI reagents, CP-MIMS-LEI/CI was shown to quantify and resolve PAH isomers from direct soil analyses via diagnostic PAH adduct ions: $[M+CH_2Cl+CH_3OH-HCl]^+$ or $[M+CHCl_2-HCl]^+$. Using these selective ions, CP-MIMS-LEI/CI was again shown to be rapid (15 soils/hr), sensitive (ng/g detection limits) and quantitatively comparable to gas chromatography-MS for PAH measurements (average percent difference of -9% across 9 PAHs in 8 soil samples). The results across this thesis present a compelling argument for direct, quantitative screening from complex samples using CP-MIMS-LEI/CI, particularly given the simple workflow and short analytical duty cycle.

Table of Contents

List of Tables

List of Figures

List of Equations

List of Abbreviations and Definitions

ACN	Acetonitrile
amu	Atomic mass unit
Ant	Anthracene
APCI	Atmospheric pressure chemical ionization
BaAnt	Benz[*a*]anthracene
BaPyr	Benzo[*a*]pyrene
BbFl	Benzo[*b*]fluoranthene
C_s	Concentration in sample
CE	Charge exchange
Chr	Chyrsene
CI	Chemical ionization
CP-MIMS	Condensed phase membrane introduction mass spectrometry
DART	Direct analysis in real-time
DBP	Dibutyl phthalate
DCM	Dichloromethane
DEHP	Bis(2-ethylhexyl)phthalate
DEI	Direct electron ionization
DEP	Diethyl phthalate
DESI	Desorption electrospray ionization
DI	Deionized
DL	Detection limit
D_m	Diffusivity in membrane
D	Deuterium
DMS	Direct mass spectrometry
EI	Electron ionization
EESI	Extractive electrospray ionization
ELDI	Electrospray assisted laser desorption ionization
ESI	Electrospray ionization
Fl	Fluoranthene
FT-IR	Fourier transform infrared spectroscopy
GC	Gas chromatography
GP-MIMS	Gas phase membrane introduction mass spectrometry
HES	High-efficiency source
HPLC	High pressure liquid chromatography
ID	Inner diameter
IE	Ionization efficiency

J	Flux across membrane
$K_{m\text{-}s}$	Relative solubility between membrane and sample
K_{ow}	Octanol-water partitioning constant
l	Membrane thickness
LC	Liquid chromatography
LEI	Liquid electron ionization
LEI/CI	Liquid electron ionization with *in situ* chemical ionization
MIMS	Membrane introduction mass spectrometry
MS	Mass spectrometry
MS/MS	Tandem mass spectrometry
m/z	Mass to charge ratio
N	Naphthalene
NA	Naphthenic acid
NMR	Nuclear magnetic resonance
OD	Outer diameter
P	Phenanthrene
P_m	Membrane permeability
PAH	Polycyclic aromatic hydrocarbon
Per	Perylene
PIM	Polymer inclusion membrane
PDMS	Polydimethylsiloxane
PS	Paper spray
POP	Persistent organic pollutant
Pyr	Pyrene
Q	Quadrupole
RPM	Revolutions per minute
S	Signal intensity
SIM	Selected ion monitoring
SPE	Solid phase extraction
SPME	Solid phase microextraction
SRM	Selected reaction monitoring
S/N	Signal-to-noise ratio
$t_{10\text{-}90\%}$	Signal risetime
UV-vis	Ultraviolet-visible

Acknowledgments

I would first like to thank Drs. Erik Krogh and Chris Gill for their patience, expert advice, and seemingly endless support. Additionally I would like to thank Drs. Scott McIndoe, Alexandre Brolo, and Mohsen Akbari for valuable feedback throughout my degree. I would like to thank the many AERL group members who have helped make my graduate experience highly enjoyable. In particular, I would like to thank Dr. Kyle Duncan for training me as an undergraduate student. I would like to thank Scott Borden and Joseph Monaghan for being great friends and even better 'colleagues.' I would like to thank my friends and collaborators Drs. Achille Cappiello, Pierangela Palma, and Veronica Termopoli for contributing greatly to the progression of my research. I would like to thank Agilent Technologies for their support of my research through the provision of instrumentation, resources, and scientific advice. To my family, Mom, Dad, Dianne, and Darren, thank you for your support and interest in my research projects, feigned or not. I would like to thank my late Uncle Dr. Larry Vandergrift, for being a great encouragement and advocate for advanced education for as long as I can remember. Thank you to my wife Jade, for being there for all the highs and lows. Thank you for providing celebrations, timely encouragements, and constant support. Finally, I would like to thank God for these incredible people and providing this life-changing experience.

Dedication

For Jade

Chapter 1

Introduction

Advances in direct mass spectrometry (DMS) have revolutionized analytical chemistry over the past several decades largely due to operational simplicity, widely varied applications, and the capability to collect real-time data. In DMS, a sample is directly interfaced to a mass spectrometer, obviating numerous sample preparation, cleanup, and separation steps that are otherwise associated with conventional, discrete sampling techniques such as liquid/gas phase chromatography couplings to mass spectrometry (LC-MS, GC-MS). While the simultaneous analysis of mixture components as part of DMS strategies presents inherent challenges (*i.e.*, component separation/identification, matrix effects, quantitative results), researchers have been refining DMS since the 1970s through the use of improved mass analyzers and the development of a broad variety of DMS ionization/sampling techniques.[1-5]

One such DMS technique that has been developed primarily by Drs. Chris Gill, Erik Krogh, and co-workers in recent years is condensed phase membrane introduction mass spectrometry (CP-MIMS).[6-8] In CP-MIMS, a semipermeable hollow fibre membrane, typically polydimethylsiloxane (PDMS), is mounted onto a probe, where the probe is then directly immersed into a sample (aqueous, solvent, slurry, etc.). Neutral analytes that are free in solution permeate the membrane, driven by a concentration gradient, whereas charged and particulate matrix components are rejected. Membrane permeants are dissolved by a solvent acceptor phase that continuously flows through the membrane lumen, entraining analytes towards a mass spectrometer for detection. Further advantages and general principles of CP-MIMS are discussed in detail as part of the subsequent chapters contained in this thesis.

CP-MIMS, along with the vast majority of current DMS techniques, often uses atmospheric pressure ionization strategies (*i.e.*, related to electrospray (ESI)) to place a charge on analytes prior to sorting/detection via a mass analyzer. While effective for numerous relevant analyte classes, ESI and related techniques are generally restricted to analytes that exhibit acid/base chemistry in the gas-phase. As a result, DMS analyses of neutral, hydrophobic analytes (e.g., polycyclic aromatic hydrocarbons (PAHs)) are generally limited. A central goal of this thesis was to therefore pair CP-MIMS, a technique already ideally suited to hydrophobic compounds due to the hydrophobic PDMS membrane, with electron and chemical ionization (EI, CI) techniques as a more ideal analytical coupling. This pairing, as shown in this thesis, ultimately helped to address a significant gap in the DMS literature and complement existing

methods for the quantitative analyses of neutral, hydrophobic compounds directly from complex samples.

Prior to demonstrating EI and CI couplings, Chapter 2 describes the optimization of membrane permeation via a CP-MIMS-ESI system by cosolvent additions to the CP-MIMS acceptor phase. The modified membrane/solvent systems as demonstrated in Chapter 2 were applied in principle to the rest of the studies presented in this thesis.[9] The results from Chapter 2 are also universally beneficial to other CP-MIMS projects that are beyond the scope of this thesis, improving both sensitivity and throughput for a wide variety of analytes. Chapter 3 describes the coupling of CP-MIMS to EI, termed CP-MIMS liquid electron ionization (CP-MIMS-LEI), and was applied to the analyses of PAHs from both aqueous, and notably soil samples.[10] This coupling was non-trivial due to the nature of pairing liquid flows from CP-MIMS with the vacuum environment of EI, but resulted in a complementary pairing for the analysis of hydrophobic, organic analytes as discussed earlier. The soil analyses as presented in Chapter 3 are especially significant, as there is a notable paucity of direct, quantitative methods for soil samples in the peer-reviewed literature. Building upon the analyses of organic compounds from complex and heterogeneous samples, Chapter 4 applies CP-MIMS-LEI to the analyses of synthetic reactions directly from harsh, complex mixtures.[11]

Results in Chapter 5 represent the evolution of CP-MIMS-LEI via the purposeful exploitation of the solvent acceptor phase from CP-MIMS as a means to generate chemical ionization reagents (*i.e.*, CP-MIMS-LEI/CI) while still using a conventional EI source.[12] Chapter 5 furthermore applied these principles of chemical ionization to the direct, quantitative analysis of phthalates from house dust, another heterogeneous sample phase. Finally, in Chapter 6, CP-MIMS-LEI/CI (using a CI source) is applied to the analysis of PAHs from soils, where individual PAH isomers were quantitated directly from soils through the use of unique gas-phase CI behaviour with dichloromethane and methanol reagent ions. CP-MIMS-LEI/CI represents the culmination of this thesis, being a technique that is not only capable of DMS of neutral hydrophobic compounds from various complex samples and phases, but furthermore exploits CI principles for additional sensitivity and selectivity. Chapter 7 discusses further conclusions of this work, and also presents opportunities and ideas for future work.

This thesis contains one appendix, which represents the exploration of paper-spray mass spectrometry (PS-MS), another DMS technique, for use in fentanyl and norfentanyl quantitation from complex samples.[13] While not directly related to the main contents of this thesis, the appendix further demonstrates the diversity and analytical capability of DMS methods. With the exceptions of Chapters 1 and 7, the entire contents of this thesis have been published in refereed journals.

Chapter 2

Polymer Inclusion Membranes with Condensed Phase Membrane Introduction Mass Spectrometry (CP-MIMS): Improved Analytical Response Time and Sensitivity

Reproduced with minor changes and permission from Vandergrift, G.W.; Krogh, E.T.; Gill, C.G. "Polymer Inclusion Membranes with Condensed Phase Membrane Introduction Mass Spectrometry (CP-MIMS): Improved Analytical Response Time and Sensitivity." *Analytical Chemistry*, **2017**, *89*, 5629-5636. G.W. Vandergrift designed the experiments, collected the data, and analyzed the data. G.W. Vandergrift drafted the manuscript, with intellectual and editorial contributions from all authors.

2.1 Introduction

Membrane introduction mass spectrometry (MIMS) is an online, *in situ* analytical technique that uses a membrane as a semipermeable interface between a sample and a mass spectrometer, allowing the simultaneous, direct, and continuous measurement of trace level analytes in real time. For further background, the reader is directed to several published reviews on MIMS.[14-17] The membrane is directly exposed to or immersed in a sample (gaseous, aqueous, and slurry), and analytes diffusing through the membrane (driven by a concentration gradient) are then transported to a mass spectrometer for their subsequent detection and measurement. Gas phase MIMS (GP-MIMS) uses a gaseous acceptor phase or vacuum to transfer permeating analytes and is well-suited for the measurement of relatively volatile analytes, whereas condensed phase MIMS (CP-MIMS) uses a condensed (liquid) acceptor phase and is tailored for low volatility analytes.[17] With either approach, analytes are resolved based on their permselectivity at the membrane, their ionization efficiency in the MS ion source, and their *m/z* ratio or *m/z* transition in MS/MS experiments. MIMS frequently uses polydimethylsiloxane (PDMS) membranes, which are selective for neutral hydrophobic analytes but are impermeable to ionized species (e.g., salts) and particulate matter present in complex samples. This direct MS sampling strategy largely eliminates the need for costly, time-consuming sample handling and cleanup procedures required for other (*i.e.*, chromatographic) methods. Overall, MIMS is a

sensitive, selective and cost-effective analytical method capable of directly and simultaneously analyzing a wide range of analytes in complex samples in real time.

The steady-state mass transfer of an analyte through an ideal one-dimensional polymer barrier is governed by a concentration gradient in the membrane as described by Fick's law.[18] If the analyte is swept away from the downstream side of the membrane by an acceptor phase, a concentration gradient is maintained and the flux across the membrane barrier is described as

Equation 2.1 $$J = \frac{C_s K_{m-s} D_m}{l}$$

where J is the analyte flux (moles per area per unit time), C_s is the concentration of analyte in the sample, K_{m-s} is the relative solubility of the analyte between the membrane and sample (a partition constant), D_m is the diffusivity of the analyte in the membrane, and l the membrane thickness. Overall membrane permeability is given by the product of K_{m-s} and D_m. In a CP-MIMS experiment, the signal intensity (S) from the mass spectrometer depends also on the ionization efficiency (IE) for a given analyte, therefore

Equation 2.2 $$S \propto C_s K_{m-s} D_m IE$$

While analytes with reduced volatility may be successfully measured by CP-MIMS, the time required for analytes to reach steady-state across the membrane can be considerable (e.g., > 10 min). This is especially true for larger analytes, where their lower diffusivities through a polymer membrane yield longer measurement response times.[7] This increases their analytical duty cycle and reduces the effectiveness of MIMS for the real time monitoring of dynamic processes occurring in the sample (*i.e.*, reacting systems, variable contaminant levels, etc.). Processes occurring at time scales faster than the analyte diffusion through the membrane will not be observable. Therefore, strategies to minimize response times are needed in order to both increase throughput and improve the temporal resolution of dynamic process monitoring. Modifications to reduce response times (such as sample heating) may be effective[17, 19] but can be undesirable because sample integrity and kinetic data may be compromised and/or biased by elevated temperatures.

The signal response time is related to the time required for analyte flux across a membrane to reach steady-state and is proportional to intrinsic properties of the membrane material and the analyte, including the membrane thickness (l) as shown in Equation 2.3:[20]

Equation 2.3 $$t_{10-90\%} \propto \frac{l^2}{D}$$

where response time may be referred to as $t_{10-90\%}$ (time required for the signal to rise from 10% to 90% of the maximum, steady-state signal intensity) and D represents the analyte diffusivity in

the membrane at specified conditions (*i.e.*, temperature). Alberici *et al.* used a thin (10 μm) membrane to decrease response times for the MIMS analysis of volatile organic compounds in water but experienced reduced sensitivity, which they attributed to increased permeation of water through the membrane in their GP-MIMS type experiment, resulting in lower ionization efficiency and/or ion−molecule chemistry.[21] Our group has also used very thin, supported PDMS membranes (500 nm) with CP-MIMS to successfully reduce response times, although we observe that these membranes are inherently more fragile and prone to damage.[7]

To utilize CP-MIMS effectively for analytes with slower response times, a robust membrane system with faster response times is desirable, and is potentially best achieved through manipulation of analyte diffusivity characteristics rather than by reducing membrane thickness. One strategy aimed at solving this issue is to employ polymer inclusion membrane (PIM) systems. To form a PIM, a polymer membrane is used to provide mechanical strength and a suitable solvent is doped in the polymer matrix to assist both analyte extraction and diffusion. PIMs have been used largely for the extraction of metal ions[22-24] but also have been employed for organic molecules.[25-27] For example, Gelotte and Listritto reported solvent interactions with PDMS to improve the membrane solubility and diffusion of benzocaine using a series of alkanol cosolvents.[25] Solvent/polymer interactions were observed to affect polymer swelling and were consistent with the corresponding Hildebrand solubility parameters.[28] In early MIMS experiments by our group, we observed the physical swelling of PDMS membranes when exposed to hexane and toluene rich samples and even "anomalous" signal response times and sensitivities for analytes in these instances (unpublished work). These experiments were very likely forming *in situ* PIM systems, although in an uncontrolled manner. Until the work reported here, we have not intentionally investigated or employed a PIM system to assist with MIMS performance.

The goal of the presented research was to develop a more robust CP-MIMS membrane system with improved analytical performance. In particular, we aim to achieve faster signal response times without compromising analytical sensitivity or altering the sample conditions by heating, etc. Presented is the development and characterization of the first CP-MIMS approach utilizing an *in situ* generated PIM resulting from the addition of a heptane cosolvent to a methanol acceptor phase. We demonstrate improved signal response times and sensitivity for a suite of biologically and environmentally relevant analytes in complex samples. Short duration, fixed sample exposure times have also been evaluated as a strategy to further decrease the analytical duty cycle for high throughput and rapid screening applications.

2.2 Experimental Section

2.2.1 Standard Solution and Sample Preparation

Stock solutions were prepared gravimetrically in methanol (HPLC grade, Fisher Scientific, Ottawa, ON, Canada). Gemfibrozil (99%), heptane (HPLC grade), nonylphenol (technical grade), 2,4,6-trichlorophenol (98%), and triclosan (5-chloro-2-(2,4-dichlorophenoxy)phenol, 97%) were obtained from Sigma-Aldrich (Oakville, ON, Canada). Table 2.1 gives the physicochemical properties of the analyte suite. Analytical standards were prepared as combined suites at low concentration levels such that inter-analyte ionization suppression effects with ESI were negligible. Analytes were also measured individually to ensure that the CP-MIMS signal response times were independent of the presence of other analytes. The refined Merichem Naphthenic Acids mixture (Merichem Company, Houston, TX) was supplied by Environment Canada. Heptane and methanol mixtures (0-20% heptane in methanol v/v) were prepared volumetrically and mixed thoroughly before use. Aqueous samples were prepared by gravimetric dilution using 18 MΩ deionized (DI) water (model MQ Synthesis A10, Millipore Corp., Billerica, MA) in 40 mL glass vials (EPA/VOA Type, Scientific Specialties Inc., Hanover, MD). The final methanol concentration in all aqueous samples was kept below 0.2% by mass. Complex matrices included surface water from a river in Northern Alberta, seawater collected at Lantzville, BC, Canada, and artificial urine (preparation described elsewhere[6]). Sample matrices were passed through a 0.45 μm filter (Durapore, Millipore Corp.) prior to analysis. Each sample analyzed by CP-MIMS was pH adjusted below 4 with 6 M HCl (Fisher Scientific). HCl was chosen for this purpose because it is a strong acid, with 100% dissociation, requiring minimal additions to lower the pH of samples. The pH was manipulated such that the vast majority of the analyte was in its neutral form and therefore able to partition through the PDMS membrane.[29]

Table 2.1: MS scan parameters and analyte physiochemical properties.

Target Analyte	Molar mass g mol^{-1}	Vapor pressure[a] Pa at 25 °C	pKa[a]	LogK_{ow}[a]	MS scan[b] *m/z*
Gemfibrozil	250.33	4.1×10^{-3}	4.5	4.3	249→120 (15)
Nonylphenol	220.35	3.1×10^{-3}	10.3	5.76	219→133 (30)
2,4,6-Trichlorophenol	197.45	1.1	6.23	3.67	197
Triclosan	289.54	8.6×10^{-5}	7.9	4.76	287

[a] SRC Physical Properties Database[30]

[b] Collision energy is eV listed in brackets

2.2.2 CP-MIMS System

A triple quadrupole mass spectrometer (Micromass Quattro Ultima LC, Waters-Micromass, Altrincham, U.K.) equipped with an ESI source was used in negative ion mode, with −3.2 kV applied to the capillary. The desolvation gas temperature was maintained at 225 °C. Nitrogen (UHP grade, Praxair, Nanaimo, BC, Canada) desolvation and curtain gas flow rates were maintained at 750 and 50 L/hr, respectively. Argon (UHP grade, Praxair) was maintained at approximately 3 mTorr in the collision cell for tandem mass spectrometry (MS/MS) experiments. Selected ion monitoring (SIM) (0.5 s dwell time) and fullscan (*m/z* 100−600, 1 s scan time) methods were used for the Merichem analyses. SIM (1 s dwell time) was used for 2,4,6-trichlorophenol and triclosan, while MS/MS (1 s dwell time) was used for gemfibrozil and nonylphenol, with pertinent MS scan parameters presented in Table 2.1. A 2.0 cm length of 170 μm thick (0.30 mm i.d., 0.64 mm o.d.) PDMS hollow fiber membrane (Silastic brand, Dow Corning, Midland, MI) was mounted on a CP-MIMS immersion "J-probe", with construction details described previously.[7-8] A syringe pump (Harvard Apparatus Pump 11 Elite, St. Laurent, QC, Canada) and gastight syringe (10 mL, Hamilton Corporation, Reno, NV) was used to supply the acceptor phase at 75 μL/min, first through a 20 μm inline filter (Upchurch Scientific A-313, Oak Harbor, WA), and then through the lumen of the hollow fiber membrane, and finally toward the mass spectrometer. All analyses were performed at ambient temperature and pressure (~25 °C and ~101 kPa). For all CP-MIMS measurements, the membrane probe was directly immersed into a magnetically stirred sample (LABDISC S56, Fisher Scientific, Waltham, MA), and after a stable baseline signal was established, analyte was spiked into the mixing sample with a micropipettor to achieve the desired concentration. The probe was either left in the sample until the analyte signals reached a steady-state or removed after a specific exposure time (10 s, 30 s), as noted. After each measurement, the membrane probe was removed from the sample and immersed in a magnetically stirred methanol rinse until signals returned to baseline levels.

2.2.3 Direct Infusion Experiments

To investigate any ionization effects from a mixed acceptor phase and to quantify membrane transport, direct calibration curves for gemfibrozil, nonylphenol, trichlorophenol, and triclosan were generated using standards prepared in both methanol and 0.046 mole fraction heptane in methanol solvent systems. These were analyzed by direct infusion to the ESI source at a flow rate of 75 μL/min, the same used in the CP-MIMS experiments. To eliminate any potential experimental bias, the membrane interface was removed for direct infusion studies.

2.2.4 Data Analysis

Microscopic images were obtained using a dissection microscope (model MDG 17, Wild Heerbrugg, Switzerland) equipped with a digital camera imaging system (model MD500, Amscope, Irvine, CA). All measurements were conducted in triplicate, with uncertainties reported as standard deviations, unless otherwise noted. All data was background-subtracted using the signals obtained for the corresponding unspiked sample matrix. In all cases, five-point

moving boxcar smoothing was applied to the signal chronograms, and signal intensities for non-steady-state measurements were evaluated as peak heights.

2.3 Results and Discussion

2.3.1 Signal Response Time Studies

A homologous series of aliphatic straight chain hydrocarbons (pentane, hexane, heptane, and octane) were initially tested for their suitability as cosolvents to generate PIM systems, adding them to the CP-MIMS methanol acceptor at modest mixing ratios, within their respective miscibility ranges. Heptane was chosen as the optimal cosolvent because of its solubility in methanol, green chemistry advantages, lower volatility compared to shorter chain aliphatic hydrocarbons, and the overall analytical performance of the PIM system. The interaction of the cosolvent acceptor phase system with the PDMS membrane alters its physiochemical properties, visually observed as a swelling of the membrane when forming the PIM. Figure 2.1 shows images of the physical changes of a PDMS hollow fiber membrane present in pure methanol, 0.046 mole fraction heptane in methanol, and pure heptane. Solvent-infused polymer membranes have been previously observed to enhance analyte flux.[25, 31] This was ascribed to a combination of increased permeant solubility and diffusivity in swelled PDMS, measured in a series of steady-state experiments using permeation cells. These effects can also be readily observed in real time via the CP-MIMS approach described here. For example, Figure 2.2 shows an overlay comparison of CP-MIMS measurements made with and without heptane in the methanol acceptor for 6 μg/L of gemfibrozil in aqueous solution. The time required for the signal to reach a steady-state is markedly reduced, and the signal intensity is significantly higher in the presence of the heptane-modified PDMS system (*i.e.*, the PIM system). This advantage is explored further in the non-steady- state measurements (see below).

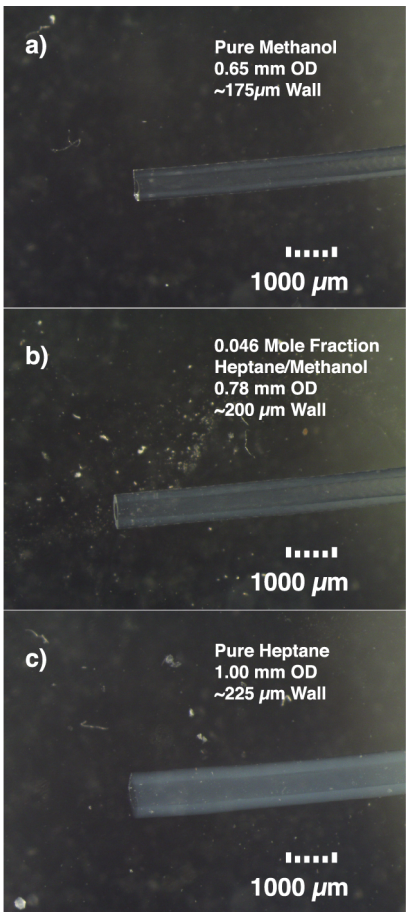

Figure 2.1: Microscope images obtained for PDMS hollow fiber membranes immersed in (a) pure methanol, (b) 0.046 mole fraction heptane in methanol, and (c) pure heptane. The swelling of the membrane is evident when heptane is present.

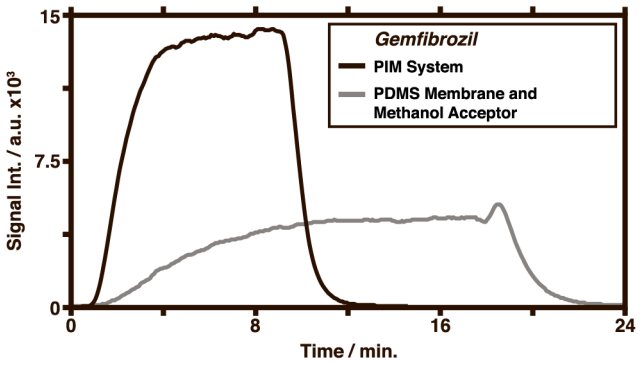

Figure 2.2: Comparison of the CP-MIMS signal responses observed for the direct measurement of 6 μg/L aqueous gemfibrozil using a PDMS hollow fiber membrane with a methanol acceptor phase and a PIM system formed by using 0.046 mole fraction heptane in methanol acceptor.

To optimize the PIM system for use with CP-MIMS, a series of experiments were conducted that measured a mixed suite of four target analytes (gemfibrozil, nonylphenol, 2,4,6-trichlorophenol, and triclosan) at 6 μg/L in DI. A series of heptane/methanol acceptor solutions was prepared at 0, 5, 10, 15, and 20% by volume (heptane mole fractions of 0 to 0.065) and evaluated for their effects upon signal response time (*i.e.*, $t_{10-90\%}$) and analytical sensitivity. For each acceptor phase composition, the measured analyte signals were allowed to reach a steady-state and the signal response times were determined as $t_{10-90\%}$. Figure 2.3 summarizes the results, showing a marked decrease in the $t_{10-90\%}$ for nonylphenol from 6.1 to 1.2 min as the heptane cosolvent concentration increases. Gemfibrozil and triclosan also exhibit significant improvements in their response times over this range. Trichlorophenol, the smallest of the analytes measured here, exhibits the least response time improvement in the presence of the heptane cosolvent. Relative response time improvements are summarized in Table 2.2. We attribute the decreased response time to a greater diffusivity of analytes in the swelled membranes. Heptane effectively increases membrane plasticity, reducing resistance to mass transport. Diffusivity depends on a variety of properties intrinsic to both the permeant (most notably it is size and shape parameters) and the medium (viscosity and tortuosity). Interestingly, we observe that the response times for all four analytes, which markedly differ without heptane, coalesce to more or less the same value (~1 min) when using the swelled PIM system. This "leveling" effect is consistent with the notion that the PIM removes analyte specific differences, and that at 0.046 mole fraction heptane, the remaining resistance is intrinsic only to the swelled membrane itself. Since membrane thickness actually increases with increasing heptane cosolvent concentration (Figure 2.1), the observed reduction in signal response times suggests that the increase in analyte diffusivities more than compensates the effect of increasing membrane thickness. From an analytical standpoint, faster response times that are independent of analyte identity are advantageous, particularly for high throughput, online, and rapid screening applications.

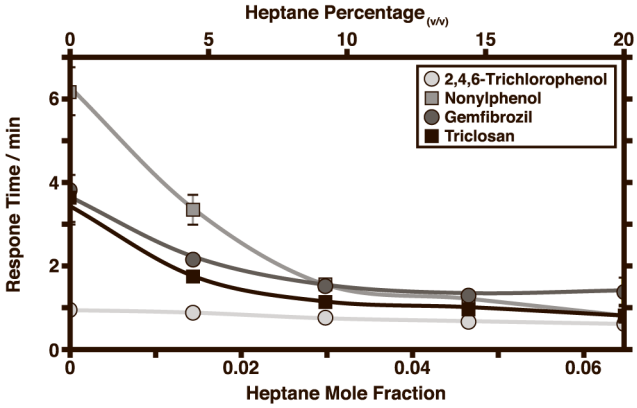

Figure 2.3: Effect of increasing the acceptor phase heptane composition upon CP-MIMS signal response times ($t_{10-90\%}$). Identical combined samples prepared in DI water (6 µg/L each of gemfibrozil, nonylphenol, 2,4,6-trichlorophenol, and triclosan in DI, pH < 4) were used to generate each data point.

Table 2.2: Detection limits, relative signal intensities, response times, ionization efficiencies for direct infusion studies, and analyte enrichments for CP-MIMS measurements using the PIM system relative to those utilizing a PDMS membrane and methanol acceptor.

Target Analyte	PIM System Detection Limit[a] ng/L	Rel. Signal Intensity[b]	Rel. Response Time[c]	Rel. IE[d]	Rel. Enrichment[e]
Gemfibrozil	4.3	3.5 ± 0.3	2.7 ± 0.5	0.99 ± 0.05	7.1 ± 0.4
Nonylphenol	120	1.5 ± 0.3	5.2 ± 0.6	1.6 ± 0.1	2.5 ± 0.4
2,4,6-Trichlorophenol	90	3.5 ± 0.2	1.4 ± 0.2	1.3 ± 0.1	9.8 ± 0.2
Triclosan	230	0.9 ± 0.2	3.4 ± 0.5	0.96 ± 0.03	2.4 ± 0.3

[a] S/N = 3

[b] Signal intensities obtained for the PIM system relative to a PDMS membrane and methanol acceptor.

[c] Ratio of $t_{10-90\%}$ response times for a PDMS membrane and pure methanol acceptor to those obtained for the PIM system (0.046 mole fraction heptane in methanol).

[d] Ratio of direct infusion calibration slopes generated from a combined standard (0 to 35 µg/L) in 0.046 mole fraction heptane in methanol relative to those obtained in pure methanol. Uncertainties obtained using the method of least squares.

[e] Enrichment for the PIM system relative to a PDMS membrane and methanol acceptor, obtained for CP-MIMS measurements of a 6 µg/L aqueous combined standard.

2.3.2 Sensitivity Studies

The target analyte signal intensities observed for various heptane cosolvent compositions studied are illustrated in Figure 2.4. The greatest analytical sensitivity for most analytes is observed at a 0.046 mole fraction heptane in the methanol acceptor. As observed in Figure 2.4, the sensitivity of the PIM system actually decreases for higher heptane cosolvent compositions (mole fraction in methanol greater that 0.065). This decrease is likely a combined effect of the limited heptane solubility in methanol affecting ESI droplet formation and also decreasing ionization efficiency due to organic partitioning effects within the electrospray droplets.[32-33] On the basis of these results, a cosolvent acceptor system of 0.046 mole fraction heptane in methanol was used for all subsequent studies, referred to as the PIM system.

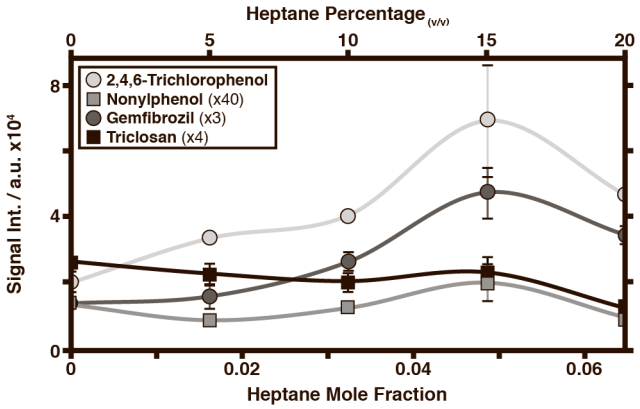

Figure 2.4: Effect of increasing acceptor phase heptane composition upon CP-MIMS signal intensities. Identical samples (6 µg/L each of gemfibrozil, nonylphenol, 2,4,6-trichlorophenol, and triclosan in DI, pH < 4) were used to generate each data point. Data is scaled, as noted, for clarity.

Table 2.2 summarizes detection limits for steady-state measurements obtained with the PIM system, as well as a comparison of performance characteristics for CP-MIMS with heptane in the acceptor phase relative to those without it. The PIM system demonstrates detection limits in the low parts per trillion (ng/L) range for direct, online measurements of the target analytes studied. The improvement in the relative response times alone (which we attribute to greater diffusivity in the PIM system), would contribute to increased membrane permeability, and therefore be expected to give rise to a greater signal intensity. This is particularly so for nonylphenol, gemfibrozil, and triclosan, which exhibited significant reductions in their $t_{10-90\%}$ response times. However, Figure 2.4 illustrates marked signal increases for trichlorophenol and gemfibrozil, a modest increase for nonylphenol, and a slight decrease for triclosan on going from pure methanol to a 0.046 mole fraction heptane in a methanol acceptor. The fact that the signal enhancements do not map the concurrent changes in diffusivities strongly suggests that other

factors affecting mass transport and/or ionization efficiency are influencing the signal intensity (Table 2.2). This is most clearly demonstrated for trichlorophenol, which experiences essentially no change in diffusivity but a greater than 3 fold increase in signal intensity. One explanation is that the partitioning into the membrane (K_{m-s}) becomes more favorable for this analyte in a heptane-infused PDMS membrane. Adding a heptane cosolvent to PDMS would be expected to increase the hydrophobic character of the PDMS, thus favoring the mass transport of hydrophobic analytes such as those studied here. Therefore, analytes that exhibit high organic partitioning behaviors as reported by log K_{ow} values ranging from 3.7 to 5.8 (Table 2.1) exhibit increased sensitivity when the PIM system is used instead of a PDMS membrane with a methanol acceptor.

To evaluate the origin of sensitivity improvements observed when using the PIM system with CP-MIMS, it is useful to evaluate contributions at both the membrane transport and ESI levels. Since it is known that ionization efficiency in ESI can be affected by solvent composition,[33] a series of direct infusion experiments were conducted to explore the influence of the heptane cosolvent. A calibration series using a combined standard of the target analytes was obtained in pure methanol and 0.046 mole fraction heptane in methanol (Table 2.5.1). The results of these experiments are summarized in Table 2.2, which reports the relative ionization efficiency as the ratio of the calibration slope in heptane/methanol to the calibration slope in pure methanol. While there was no observed effect of the heptane cosolvent on the ionization efficiency for gemfibrozil and triclosan, trichlorophenol and nonylphenol exhibit modest enhancements 30 and 60% (respectively) in the presence of the heptane cosolvent. These results suggest that overall, ionization efficiency is not responsible for the majority of signal enhancement as shown in Figure 2.4.

The level of analyte enrichment in the CP-MIMS acceptor phases relative to the sample concentration can be probed further by using calibration curves from direct infusion experiments. The relative enrichments presented in Table 2.2 are based on the concentrations derived from the observed signals in the CP-MIMS experiments with and without the PIM system. Enrichment was calculated by dividing the steady-state concentration of analyte in the acceptor by the known concentration in the aqueous sample. Relative enrichments were calculated by dividing the enrichment observed for measurements made with the PIM system by those obtained with a PDMS membrane and pure methanol acceptor. All relative enrichments presented are greater than one, indicating that mass transport is favored when using the PIM system. While further correlations of the observed trends and improvements to analyte physicochemical properties may be done, we believe such discussions are better explored more comprehensively elsewhere.

2.3.3 Non-Steady-State Measurements

Frequently, for calibration and measurements with CP-MIMS, analyte signals are allowed to reach their maximum, steady-state levels.[6-8, 29, 34-36] For analytes with longer $t_{10-90\%}$ responses, this increases the analytical duty cycle. As an alternative strategy to reduce measurement times,

the membrane interface can be exposed to the sample for fixed, short periods, removing it from the sample before steady-state signals are achieved. The resulting measurements yield peak-shaped responses. Although the maximum signal intensities possible may not be achieved, the analytical duty cycle can be significantly shortened. These experiments are referred to as non-steady-state CP-MIMS measurements.[34]

The response time improvements arising from using the PIM (Figure 2.3) may be exploited for non-steady-state measurements, since significant analytical signal levels can be achieved for short membrane exposure times (<1 min). To investigate the potential use of this approach, calibration data was obtained for target analytes in aqueous samples (5 to 110 μg/L), using both pure methanol and 0.046 mole fraction heptane in methanol acceptors, exposing the sample to the membrane for both 10 and 30 s intervals. For all of the target analytes, satisfactory linear calibrations were achieved (Table 2.5.2). Figure 2.5 illustrates typical calibration curves for the target analytes, obtained for 10 s sample exposures using the PIM system, along with representative analytical signals obtained for triplicate aqueous gemfibrozil measurements. Table 2.3 summarizes the observed calibration sensitivity improvements for the PIM system based CP-MIMS measurements obtained using the non-steady-state approach, as well as corresponding detection limits. Calibration sensitivity improvement factors are derived from the ratio of the calibration slopes obtained for the PIM system relative to those for PDMS with a pure methanol acceptor (Table 2.3). This improvement is universal for all analytes studied because of the faster (and uniform) response times achieved using the PIM and, consequently, its ability to achieve greater signal levels (and ng/L−μg/L detection limits) for the short measurement times.

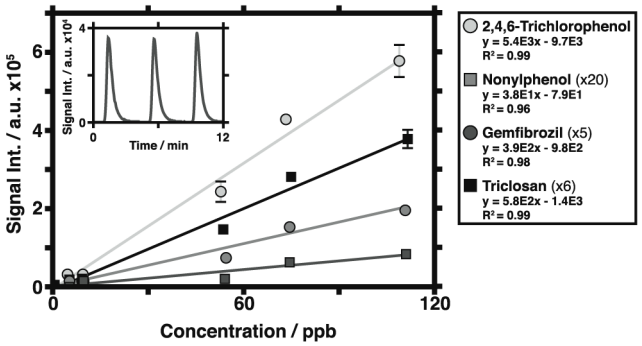

Figure 2.5: Non-steady-state CP-MIMS measurement calibration data (10 s membrane exposure times) of aqueous DI samples obtained using the PIM system. Data is scaled as noted for clarity. The inset illustrates the analytical signals obtained for the direct measurement of 74 μg/L aqueous gemfibrozil using 10 s membrane exposure times.

Table 2.3: Calibration sensitivity improvement and detection limits observed for PIM based CP-MIMS using the non steady-state measurement approach.

Target Analyte	Calibration Sensitivity Improvement Factor[a]		Non-Steady-State Detection Limits µg/L[b]	
	10 s Sample Exposure	30 s Sample Exposure	10 s Sample Exposure	30 s Sample Exposure
Gemfibrozil	10 ± 1	5.9 ± 0.7	1.4	0.51
Nonylphenol	7.5 ± 0.8	4.8 ± 0.4	27	1.4
2,4,6-Trichlorophenol	5.7 ± 0.4	3.6 ± 0.3	0.68	0.51
Triclosan	8.6 ± 0.7	3.6 ± 0.3	1.8	0.55

[a] Uncertainties obtained using the method of least squares.
[b] S/N = 3.

2.3.4 Performance in Complex Matrices

Ionization suppression has consistently been a significant issue for quantitative ESI analyses with mass spectrometry.[8, 37-40] With CP-MIMS employing ESI, ionized components of complex sample matrices are rejected by the PDMS membrane but any neutral matrix component that is permeable will diffuse through the membrane and be transferred to the ion source, potentially contributing to ionization suppression effects.[8] In order to test the applicability of the presented PIM system based CP-MIMS for use with complex sample matrices, measurements made in surface water, seawater, and artificial urine were conducted. The improved response times observed in DI water samples were conserved across all analyses for a 50 µg/L spike of the target analytes prepared in each sample matrix. Sensitivity effects are presented in Table 2.4 as "signal intensity ratios" for the specific matrices, calculated as the steady-state signal in a complex matrix divided by the steady-state signal for a sample of identical concentration prepared in DI. These ratios were calculated for both a PDMS membrane using a methanol acceptor and for the PIM system. In this way, the ratios are not indicative of signal improvements from the addition of cosolvent to the acceptor phase but rather give information based solely on ionization suppression induced by the matrix (*i.e.*, a ratio below 1 is indicative of ionization suppression). As can be seen in Table 2.4, the signal intensity ratios observed are essentially the same across various sample matrices for both CP-MIMS variants, suggesting that any ionization suppression effects from complex matrices are equal for the PIM system. In previous work, we have shown that improvement in direct quantitation across different matrices may be achieved using internal standard strategies that correct for ionization suppression effects.[8]

Table 2.4: Signal intensity ratios obtained for CP-MIMS measurements made in complex matrices compared with those made in DI water.

Target Analyte	PDMS Membrane and Methanol Acceptor			PIM System		
	Surface Water	Seawater	Artificial Urine	Surface Water	Seawater	Artificial Urine
Gemfibrozil	0.67 ± 0.01	0.8 ± 0.1	0.45 ± 0.01	0.7 ± 0.1	0.69 ± 0.02	0.45 ± 0.02
Nonylphenol	0.8 ± 0.1	0.6 ± 0.2	0.4 ± 0.1	1.0 ± 0.1	0.6 ± 0.1	0.5 ± 0.1
2,4,6-Trichlorophenol	0.79 ± 0.03	0.9 ± 0.1	0.45 ± 0.01	0.83 ± 0.05	0.77 ± 0.04	0.50 ± 0.03
Triclosan	1.0 ± 0.1	1.0 ± 0.2	0.7 ± 0.1	1.0 ± 0.1	0.8 ± 0.1	0.7 ± 0.1

2.3.5 Performance with Complex Analyte Mixtures

A class of environmental analytes that has proven particularly challenging to analyze by CP-MIMS and other methods are the naphthenic acids.[7, 29, 35] Naphthenic acids (NAs) are a highly complex mixture of alkylated carboxylic acids, containing multiple degrees of unsaturation via double bonds or ring structures spanning a typical mass range from *m/z* 200−600.[41-45] Naphthenic acids containing one carboxylic acid functional group are represented by the formula $C_nH_{2n+z}O_2$, where *n* is the number of carbons and *z* is a negative integer indicating the number of degrees of unsaturation. Characterization of NAs in environmental samples and oil sands process waters continues to be a priority as these compounds are a corrosive byproduct from heavy oil extraction and processing and are associated with aquatic toxicity in the Alberta oil sands.[41, 46] We have previously shown that CP-MIMS, using pure methanol as an acceptor phase, is useful for both quantitative and qualitative NAs screening directly in "dirty" samples.[29, 35] However, some of the higher molecular weight NAs exhibit long $t_{10-90\%}$ signal response times (>10 min) because of their larger molar volumes (*i.e.*, lower diffusivities).[7]

To evaluate the use of the PIM system based CP-MIMS for NA measurements, a standard NAs mixture (Merichem) was analyzed at 141 μg/L (total concentration of all NAs species) in DI water. When using the PIM system, both $t_{10-90\%}$ signal response times and signal-to-noise ratios were improved. Table 2.5 shows that signal-to-noise ratios double, providing greater sensitivity. Response times became markedly shorter, leveling out at ~2 min across all observed NA *m/z* values. Improvements in signal response times for CP-MIMS can be achieved using a 500 nm thick PDMS membrane,[7] but the use of the PIM system is superior because of its durability and robustness (relative to a delicate, 500 nm thick membrane), and the uniform signal response times. The robustness in particular makes PIM-based CP-MIMS better suited for portable and in-field use when analyzing real-world (heterogeneous) samples *in situ*.

Table 2.5: Signal response times and signal/noise ratios for selected NA isomer classes observed using CP-MIMS for the direct measurement of 141 μg/L Merichem in aqueous solution.

m/z $[M-H]^-$	PDMS Membrane and Methanol Acceptor		PIM System	
	$t_{10-90\%}$ min	S/N	$t_{10-90\%}$ min	S/N
185	5.0	39 ± 5	2.1	77 ± 4
213	7.4	63 ± 8	1.9	138 ± 10
223	8.6	114 ± 12	1.9	177 ± 13
237	9.2	72 ± 10	2.2	137 ± 11
251	9.8	62 ± 8	2.1	123 ± 11

2.4 Conclusions

The first intentional use of a PIM-based CP-MIMS system is presented, characterized, and demonstrated for the online measurement of a range of analytes in complex sample matrices. This system demonstrates a significant reduction and leveling of analyte signal response times. For the analytes studied, sensitivity generally improved with the use of a PIM as a result of improved analyte diffusivities and analyte partitioning. Future work includes scaling down the size of the presented CP-MIMS system for in field applications, as well as the exploration of other PIM systems.

2.5 Supporting Information

Table 2.5.1: Calibration data for direct infusion ESI measurements obtained using pure methanol and 0.046 mole fraction heptane cosolvent systems (0 to 35 μg/L, four concentrations).

Target Analyte	Pure Methanol	0.046 Mole Fraction Heptane in Methanol
Gemfibrozil	$y = 7.6\times10^2x + 2.3\times10^2$	$y = 7.5\times10^2x - 4.0\times10^2$
	$R^2 = 0.999$	$R^2 = 0.999$
Nonylphenol	$y = 1.6\times10^1x - 4.7$	$y = 2.6\times10^1x - 2.7\times10^1$
	$R^2 = 0.999$	$R^2 = 0.998$
2,4,6-Trichlorophenol	$y = 1.5\times10^3x - 6.8\times10^2$	$y = 1.9\times10^3x - 1.6\times10^3$
	$R^2 = 0.998$	$R^2 = 0.997$
Triclosan	$y = 2.9\times10^2x + 6.0\times10^1$	$y = 2.7\times10^2x - 1.1\times10^2$
	$R^2 = 0.9996$	$R^2 = 0.9995$

Table 2.5.2: Calibration data for non-steady state CP-MIMS measurements obtained using a PDMS membrane with pure methanol and 0.046 mole fraction heptane cosolvent acceptor phases (*i.e.* the PIM system) for sample exposure times of 10 and 30 seconds (0 to 110 μg/L, six concentrations).

Target	PDMS Membrane and Methanol Acceptor		PIM System	
Analyte	10 s exposure	30 s exposure	10 s exposure	30 s exposure
Gemfibrozil	$y=3.8\times10^{1}x+3.6\times10^{1}$	$y=2.3\times10^{2}x-5.3\times10^{2}$	$y=3.9\times10^{2}x-9.8\times10^{2}$	$y=1.4\times10^{3}x+1.4\times10^{3}$
	$R^2 = 0.95$	$R^2 = 0.99$	$R^2 = 0.98$	$R^2 = 0.96$
Nonylphenol	$y=5.1x+6.1\times10^{1}$	$y=3.1\times10^{1}x+5.5\times10^{1}$	$y=3.8\times10^{1}x-7.9\times10^{1}$	$y=1.5\times10^{2}x-1.1\times10^{2}$
	$R^2 = 0.8$	$R^2 = 0.99$	$R^2 = 0.96$	$R^2 = 0.99$
2,4,6-TCP [a]	$y=9.6\times10^{2}x+3.9\times10^{2}$	$y=3.7\times10^{3}x+1.4\times10^{3}$	$y=5.4\times10^{3}x-9.7\times10^{3}$	$y=1.4\times10^{4}x-1.2\times10^{4}$
	$R^2 = 0.99$	$R^2 = 0.99$	$R^2 = 0.99$	$R^2 = 0.98$
Triclosan	$y=6.7\times10^{2}x+1.9\times10^{2}$	$y=5.7\times10^{2}x-4.9\times10^{2}$	$y=5.8\times10^{2}x-1.4\times10^{3}$	$y=2.1\times10^{3}x-2.9\times10^{3}$
	$R^2 = 0.94$	$R^2 = 0.96$	$R^2 = 0.99$	$R^2 = 0.98$

[a] Trichlorophenol

Chapter 3

Direct Analysis of Polycyclic Aromatic Hydrocarbons in Soil and Aqueous Samples Using Condensed Phase Membrane Introduction Tandem Mass Spectrometry with Low-Energy Liquid Electron Ionization

Reproduced with minor changes and permission from Vandergrift, G.W.; Monaghan, J.; Krogh, E.T.; Gill, C.G. "Direct Analysis of Polyaromatic Hydrocarbons in Soil and Aqueous Samples Using Condensed Phase Membrane Introduction Tandem Mass Spectrometry with Low-Energy Liquid Electron Ionization." *Analytical Chemistry*, **2019**, *91*, 1587-1594. G.W. Vandergrift designed the experiments and analyzed the data. G.W. Vandergrift primarily collected the data, with contributions from J. Monaghan. G.W. Vandergrift drafted the manuscript, with intellectual and editorial contributions from all authors.

3.1 Introduction

Polycyclic aromatic hydrocarbons (PAHs) are ubiquitous, non-polar compounds produced by both natural and anthropogenic sources and are classified as persistent organic pollutants (POPs). PAHs are mutagenic, carcinogenic, and bioaccumulative, and as a result are listed as priority pollutants by the United States Environmental Protection Agency (U.S. EPA).[47] While all PAHs are highly hydrophobic (log K_{ow} 3−7),[30] they are globally distributed throughout air,[48] water,[36, 49-56] sediments,[57-63] and biota.[64] The complexity of samples contaminated with PAHs often requires extensive sample preparation and cleanup prior to analysis, with procedures that differ significantly depending upon the sample matrix. While recent research has improved the rapidity, robustness, and green chemistry aspects of analytical methods for PAHs, extensive sample handling/cleanup procedures still remain as a significant impasse. PAHs have been analyzed by liquid chromatography using fluorescence and ultraviolet absorbance detection,[50-52, 57] and gas chromatography flame ionization.[61, 65] Gas chromatography mass spectrometry (GC-MS) is generally the preferred PAH measurement method.[66] However, GC-MS methods generally require time-consuming sample extraction and cleanup steps.

Despite their low water solubility, aqueous PAHs are monitored because of their mutagenic and carcinogenic effects at low concentrations.[30] Aqueous sample analyses have traditionally used liquid−liquid extraction sample preparation,[50-51] requiring significant time and quantities of hazardous solvents. Alternative aqueous extraction procedures have been developed, including solid-phase extraction,[67] solid-phase microextraction (SPME),[49] stir bar sorptive extraction,[52] molecularly imprinted polymers,[56] and membrane extraction.[36, 54-55]

Soils, sediments, and biota are often a sink for PAHs because of favorable organic partitioning behavior. Soxhlet extraction has long been employed to isolate PAHs from complex solid samples due to high extraction recovery.[58-59, 61-62] However, the time (up to 16 hr) and large solvent quantities required has led to alternative, greener techniques, including microwave,[57-58] sonication,[59-60] supercritical fluid,[61, 63] and pressurized solvent extractions.[62] While these techniques provide improvements, they still involve considerable sample pretreatment and cleanup in advance of analysis. These steps increase both the cost and time of analysis, limiting sample throughput. A rapid PAH screening approach for soils was developed by Frandsen *et al.* using field-portable, miniature mass spectrometers and a hot cell to heat the soil,[68] but as presented, this method suffers from inadequate detection limits (milligram per kilogram levels), especially for larger, less volatile PAHs.

Recent research has targeted the development of simpler analytical methods for PAHs and other similar compounds in complex matrixes. Zenobi and co-workers analyzed aqueous pesticides and POPs using online SPME coupled with photo and dielectric barrier discharge ionization sources with MS.[49, 69] The Amirav and Cappiello groups have analyzed liquids for nonpolar compounds with electron impact sources and MS, using a molecular beam interface[70] and liquid electron ionization (LEI),[36, 71-72] respectively. All are more universal with respect to the analyte, but without additional extraction techniques, they have generally been restricted to solution phase samples as presented.

CP-MIMS typically uses a hollow fiber PDMS membrane mounted on a direct sampling probe. The PDMS membrane is permeable to hydrophobic analytes, which are often transferred in an organic solvent acceptor phase to an atmospheric pressure ionization source.[17, 73] The membrane rejects charged solutes and particulate matter, while hydrophobic analytes (such as PAHs) permeate through the PDMS. Direct sampling CP-MIMS probes are applicable with a variety of different sample matrixes and can be paired with different ionization sources compatible for specific analyte classes. For PAHs, CP-MIMS may be coupled to electron ionization through the use of liquid electron ionization (LEI). In LEI, a nanoflow of liquid forms an aerosol in a heated helium stream under modest vacuum, followed by desolvation and solute (analyte) vaporization. The gas-phase analytes are then ionized in an EI source. The coupling of CP-MIMS to LEI represents an ideal pairing of online membrane extraction and ionization for hydrophobic, neutral compounds, such as PAHs. Earlier work in our group employed CP-MIMS

coupled to an early variant of LEI (termed direct EI, DEI) for the measurement of PAHs in a variety of aqueous samples.[36] The study presented here represents a significant advancement for the direct measurement of PAHs in complex heterogeneous samples (i.e., soils) with minimal sample handling.

3.2 Experimental Section

3.2.1 Standard and Sample Preparation

Aqueous PAH samples were prepared in 18 MΩ-cm deionized water (model MQ Synthesis A10, Millipore Corp., Billerica, MA, U.S.A.), seawater (unfiltered, collected from a local industrial area), and surface water (unfiltered, collected from a local river). Aqueous standards were prepared at 0.80, 5.0, 25, and 50 μg/L for pyrene and naphthalene, and at 0.80, 5.0, and 25 μg/L for anthracene. Further details are available in the Supporting Information, Section 3.5.

For prepared soil samples, clean sandy loam (Sigma-Aldrich, 5.96% organic matter by mass, PAH-free) was used. An amount of 4.0 g of soil was pre-wetted with 1500 μL of 2-propanol and spiked with PAHs to yield dry soil concentrations of 500, 1000, 1500, and 2000 μg/kg each for anthracene, pyrene, and benzo[*a*]pyrene. The prepared soil samples were left to air-dry at ambient conditions for 5 days before analysis. PAH-contaminated soil samples were obtained from the Ontario Ministry of Environment and Climate Change.

For all organic and aqueous sample measurements, the CP-MIMS probe was directly immersed into magnetically stirred (900 rpm) 38 mL samples (40 mL glass vials). Unless otherwise noted, analyte signals were allowed to reach steady-state and were background-subtracted using the signal from an appropriate matrix blank. For all soil sample measurements, samples (0.5 g) were suspended in 7 mL of 2-propanol in 8 mL glass vials and spiked with 280 μg/L internal standard (pyrene-d_{10} in 2-propanol). The slurry was then sonicated (FS140 ultrasonic bath, Fisher Scientific, 135 W) while heating at 75 °C (Precision Scientific Co. Porta Temp, Chicago, IL, U.S.A.) for 3 min. The CP-MIMS probe was then directly immersed in the 2-propanol/soil suspension for 2 min immediately after sonication, with no further sample cleanup. During measurements, soil slurries were stirred at 900 rpm. Following all measurements, the probe was rinsed in stirred 2-propanol for 2 min to return the signal to baseline levels.

3.2.2 Condensed Phase Membrane Introduction Mass Spectrometry-Liquid Electron Ionization (CP-MIMS-LEI) System

Figure 3.1 provides a schematic diagram of the CP-MIMS−LEI instrumental apparatus. A triple quadrupole mass spectrometer (Agilent Technologies Inc. 7010B GC-MS/MS, Santa Clara,

CA, U.S.A.) equipped with a high-efficiency source (HES) was used for tandem mass spectrometry (MS/MS) with a 500 ms dwell time. Analyte MS/MS parameters are presented in Table 3.1, and their respective physicochemical properties are presented in Table 3.5.1. Custom yttria-coated yttria/rhenium alloy filaments (Scientific Instrument Services Inc., Ringoes, NJ, U.S.A.) were used for all studies, operated at 20 eV with a 100 µA emission current. A source temperature of 280 °C was used.

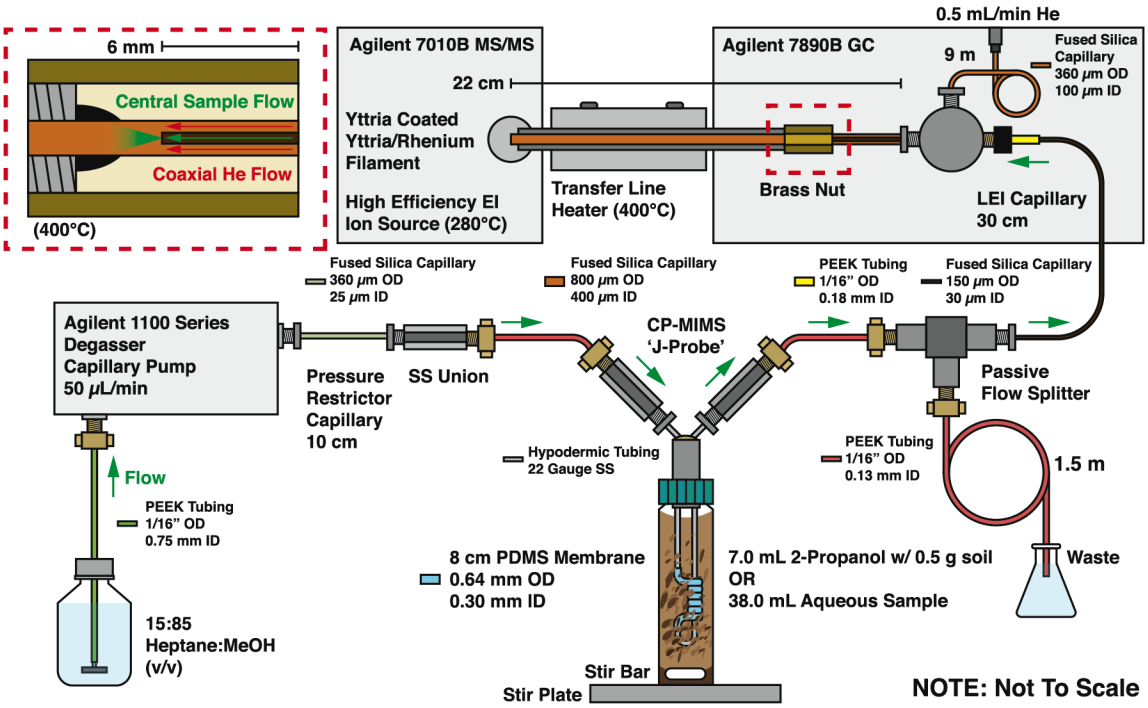

Figure 3.1: Schematic diagram of the CP-MIMS−LEI experimental apparatus.

Table 3.1: MS scan parameters.

Analyte	MS/MS Transition	Collision Energy eV
Naphthalene	128 → 102	30
Anthracene	178 → 176	34
Pyrene	202 → 200	42
Benzo[*a*]pyrene	252 → 250	42
Pyrene-d_{10}	212 → 208	42

An 8.0 cm length of 170 µm thick (0.30 mm i.d., 0.64 mm o.d.) PDMS hollow fiber membrane (Silastic brand, Dow Corning, Midland, MI) was coil-mounted on a CP-MIMS immersion "J-probe" (Figure 3.1), with construction details previously described.[7] A capillary HPLC pump and degassing module (1100 series, Agilent) was used to supply acceptor phase at

50 μL/min through the lumen of the hollow fiber membrane. To achieve stable pump flows, 10 cm of fused-silica capillary flow restrictor yielded *ca.* 50 bar operating pressures. All fused-silica capillaries for this study were polyimide-coated and not deactivated (Polymicro Technologies, Phoenix, AR, U.S.A.). Our previous studies have shown that organic cosolvents present in the acceptor phase form in situ polymer inclusion membranes with PDMS that improve membrane permeability.[9] For all presented studies, a 15:85 heptane/methanol (v/v) acceptor phase was used to increase sensitivity and shorten analyte response times. Further advantages and justifications of this solvent system are detailed in Chapter 2 of this thesis.

A zero dead volume stainless steel tee junction was used as a passive flow splitter (Figure 3.1) post-membrane, reducing the acceptor phase flow rate to ~300 nL/min for optimal signals,[72] to minimize internal pressure within the PDMS membrane. Flow rate measurements were made off-line using a Sensirion SLG-0150 flowmeter (Staf̈a, ZH, Switzerland). Both rough and high vacuum pressures were monitored as an indicator of stable LEI performance (typically 1.3×10^{-1} and 9.5×10^{-5} Torr, respectively). Neither are ideal measures for the ion source region pressure, which is more relevant for LEI performance monitoring. Thus, an in-house built stainless steel flange was mounted on the source end of the MS manifold (Figure 3.5.1) and equipped with an ion gauge (Hewlett-Packard 59864A ionization gauge and controller, Palo Alto, CA, U.S.A.). Stable LEI performance resulted from source region pressure measurements of 1.0×10^{-4} Torr.

A modern LEI interface has been described in detail by Termopoli et al.[72] In our presented system, the acceptor phase was flowed post-splitter into 30 cm of a fused-silica capillary (150 μm o.d., 30 μm i.d., referred to subsequently as the LEI capillary) toward the MS. The LEI capillary extended through a stainless steel tee into a fused-silica capillary liner (800 μm o.d., 400 μm id.). A capillary column gas chromatograph (Agilent 7890B GC) was used to supply 0.5 mL/min helium flow to the tee (Figure 3.1). In this way, helium is flowed coaxially within the capillary liner, around the liquid flow in the LEI capillary. The transfer line of the GC/MS/MS system was maintained at 400 °C for all studies. The liner capillary extended through the transfer line, and the tip of the liner capillary extended 2 mm past the end of the transfer line into the MS source. The liner capillary helps to prevent analyte degradation/loss within the heated zone by preventing analyte contact with the transfer line metal surfaces. Negligible performance degradation occurred over weeks of daily use. The LEI capillary extended 6 mm into the transfer line unless otherwise specified. A 3 cm gap between the entrance of the transfer line and the helium tee was used to separate the tee from the heated zone, preventing premature vaporization in the LEI capillary. Acceptor phase exiting the LEI capillary was subsequently nebulized, desolvated, and vaporized in the heated coaxial helium flow, pneumatically transferring neutral analytes and vaporized acceptor phase solvent to the MS source.

3.2.3 Data Analysis for CP-MIMS-LEI

All measurements were conducted in triplicate unless otherwise noted, with standard deviation error bars. The signal-to-noise ratios (S/N) presented in Table 3.5.3 and Figure 3.2 were calculated using unsmoothed data. Standard deviations for the signal-to-noise ratios were calculated using steady-state signal measurements (i.e., not baseline noise). A 7-point moving boxcar smoothing function was applied to all other presented data. Detection limits were calculated as 3 times the standard deviation of the baseline for the appropriate matrix blank, divided by the calibration curve slope, given by Equation 3.1:

Equation 3.1 $$DL = 3SD_{baseline}/slope$$

For the direct quantitation of PAHs present in soil samples, naphthalene, anthracene, pyrene, and benzo[a]pyrene response factors were calculated relative to pyrene-d_{10}, utilizing 100 µg/L PAH standards prepared in 2-propanol (six replicates, Table 3.5.2). Relative response factors were observed to be constant for up to 5 mg/L of all target PAHs in 2-propanol. Soil sample quantitation results are presented as dry soil PAH concentrations for specific isomer classes based upon precursor mass-to-charge (*m/z*) values (Table 3.1). Given that the response factors are calculated for specific PAHs (described above), PAH isomer class concentrations are represented as "equivalent concentration units" for the respective model PAHs used to generate the response factors.

3.3 Results and Discussion

3.3.1 LEI Optimization for PAHs

A parametric investigation of PAH vaporization efficiency for various LEI capillary insertion positions inside the heated transfer line was conducted (Figure 3.2A). S/N for naphthalene and anthracene, which have the highest vapor pressures of the analytes studied, were essentially independent of the LEI capillary position. However, less volatile pyrene and benzo[a]pyrene had significant sensitivity effects dependent upon capillary insertion depth. Vaporization is likely aided for these less volatile analytes because of the higher temperatures and reduced pressures experienced with deeper insertion into the heated zone.[72] An optimum LEI capillary insertion depth of 6 mm was determined for the PAHs examined and used for all subsequent studies.

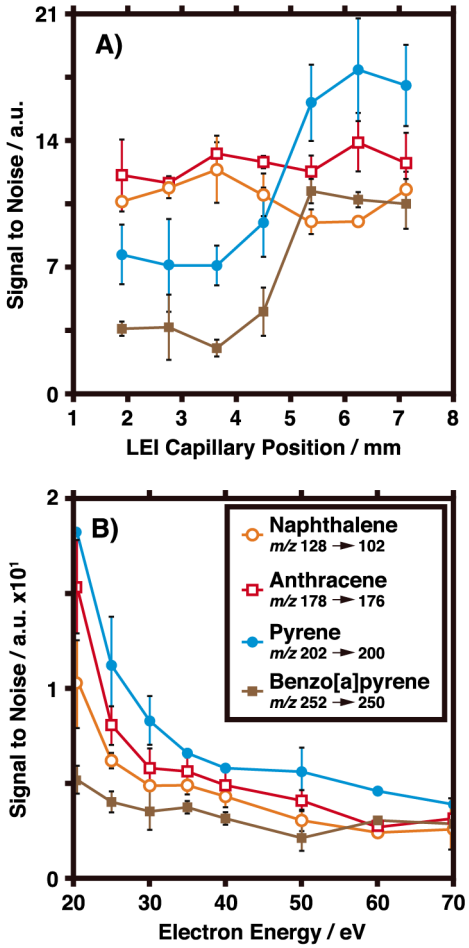

Figure 3.2: CP-MIMS−LEI system optimization. (A) Optimization of capillary position in the transfer line for select PAHs. (B) Electron energy optimization for select PAHs with LEI source.

Historically, 70 eV electron energy has been used for most EI experiments, as electron ionization cross section for many analytes is maximized at 70 eV.[4] Lower electron energies may be desirable to limit fragmentation and preserve the molecular ion for tandem mass spectrometry (MS/MS). The HES used for these studies allowed the examination of lower electron energy use. In Figure 3.2B, electron energy was varied from 20 to 70 eV, demonstrating optimal S/N for all the PAH MS/MS transitions at 20 eV. Less extensive fragmentation at 20 eV resulted in greater precursor ion abundance, and consequently signal improvements. The HES design uses an extended electron collision zone, coaxial with the analyzer ion beam path, and is further compressed by concentric magnetic fields to increase efficiency.[74] This is unlike the typical Nier-type EI source design used in most EI systems,[4] which has the electron beam perpendicular to the ion beam and a truncated electron collision volume. The trends observed in Figure 3.2B are of particular interest with regard to PAHs, which typically do not display extensive EI fragmentation at 70 eV. Although beyond the scope of this study, we speculate the observed trend should be more pronounced for compound classes experiencing increased fragmentation at

higher electron energies. An alternative contribution to the observed trend in Figure 3.2B may also relate to the reduced ionization efficiency for the acceptor solvent at lower electron energies, resulting in reduced intra-ion source space charge effects.[75]

While the analytical benefits of 20 eV operation are apparent, there were initial challenges with respect to the filament material. Commercially available rhenium filaments were found to erode and eventually fail after prolonged use, likely due to the high acceptor phase solvent vapor levels present in the ion source. By utilizing custom yttria/rhenium alloy filaments with an yttria oxide coating that allowed filament operation at lowered temperatures, effective 20 eV operation was possible for months of daily use. Images of both rhenium and yttria-coated filaments after 50+ hours of CP-MIMS−LEI operation are given in Figure 3.3. Therefore, yttria-coated filaments were used for all presented studies.

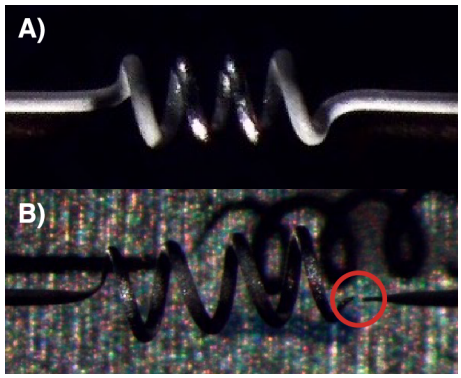

Figure 3.3: Image comparing EI filaments operated for 50+ hours of CP-MIMS−LEI measurements. (A) Custom yttria-coated yttria/ rhenium alloy filament operated at 20 eV. (B) Yttria/rhenium alloy filament operated at 70 eV. The red circle in panel B represents a filament failure.

3.3.2 Aqueous PAH Calibration Studies

Aqueous calibration curves for naphthalene, anthracene, and pyrene were obtained at low microgram per liter levels in deionized water, seawater, and river water. All PAHs examined demonstrated good linearity ($R^2 > 0.996$), low nanogram per liter detection limits, and fast $t_{10-90\%}$ signal response times (≤1.6 min.) for these aqueous sample matrixes (Table 3.2). These results represent over an order of magnitude sensitivity improvement and significantly shorter response times than presented in our earlier studies.[36] Faster response times are attributed to greater analyte permeability, facilitated by the heptane/methanol acceptor phase, consistent with earlier work.[9] The sensitivity improvements are due to both the greater permeability and ion source optimization. Interestingly, the PAH calibration slopes presented in Table 3.2 for river water and seawater are comparable to that of deionized water, despite the significant differences in matrix composition. The results presented are consistent with other findings, which suggest that matrix effects in LEI are significantly reduced when compared to other liquid−mass

spectrometry couplings,[71] particularly electrospray ionization (ESI).[37, 40] While the PDMS membrane rejects salts, ionized species, and particulate matter from the sample, co-permeating compounds have still been observed to cause significant ionization suppression in ESI-based CP-MIMS measurements presented in earlier studies.[8] The low nanogram per liter aqueous detection limits demonstrated by this study may prompt future studies on expanding aqueous analyses to larger, less water-soluble PAHs.

Table 3.2: Calibration data, detection limits, and response times for PAHs in aqueous matrices.

Analyte	Matrix	Equation of line	R^2	Detection Limit[a] ng/L	$t_{10\text{-}90\%}$ min
Naphthalene	De-ionized water	y = 41.5x + 21.2	0.9991	330	1.3
	Seawater	y = 40.7x + 20.5	0.9988	330	1.3
	River water	y = 49.3x + 15.0	0.9995	270	1.1
Anthracene	De-ionized water	y = 44.5x + 6.7	0.9997	83	1.4
	Seawater	y = 45.3x + 5.0	0.9996	85	1.4
	River water	y = 51.7x + 5.9	0.9995	70	1.3
Pyrene	De-ionized water	y = 68.1x + 16.4	0.9996	70	1.6
	Seawater	y = 62.7x + 52.3	0.9963	76	1.5
	River water	y = 78.9x + 44.3	0.9977	61	1.5

[a] Estimated using Equation 3.1

3.3.3 Solvent Selection for Direct Soil PAH Measurements

A series of common organic solvents (acetonitrile, dichloromethane, ethanol, ethyl acetate, N,N-dimethylformamide, methanol, and 2-propanol) were evaluated for their compatibility with PDMS membranes and their suitability as an analysis solvent for direct soil PAH measurements. The solvent choice must sufficiently aid PAH solubility and extraction from solid sample matrixes, but not excessively swell the PDMS membrane. If the solvent-PDMS solubility is too large, a soft, less robust membrane results, which is more prone to physical damage. Table 3.5.3 summarizes the observed S/N ratios for the direct analysis of representative PAHs (100 µg/L each) utilizing various sampling solvents. Dichloromethane, a common PAH extraction solvent,[50-51] demonstrated poor analytical performance with CP-MIMS-LEI and excessively swelled the PDMS membranes. Hexane, another common PAH extraction solvent,[51] was not investigated, since it similarly causes excessive PDMS swelling. Ethyl acetate and 2-propanol demonstrated the best analytical performance for the solvents studied, with 2-propanol exhibiting the best overall performance (Table 3.5.3).

The differences in sensitivity for the tested sampling solvents may be evaluated by examining factors influencing membrane transport. For a given analyte concentration and membrane thickness, the steady-state signal intensity in a CP-MIMS experiment is directly

related to the membrane permeability (P), which can be expressed as the product of a partitioning term and a diffusivity term as given in Equation 3.2:

Equation 3.2 $$P = K_{m-s}D_m$$

where D_m is the analyte diffusivity in the membrane and $K_{m\text{-}s}$ is the relative solubility of the analyte in the membrane and sample (a partition constant). Sample solvent can therefore affect P (and consequently sensitivity) by affecting either or both $K_{m\text{-}s}$ or D_m. In part, increased solvent solubility in the membrane may cause the membrane to swell, making the membrane more permeable due to an increase in analyte diffusivity through the membrane (D_m).[9, 25] In addition to the degree of swelling, solubility parameters (e.g., Hansen, Hildebrand; derived from cohesive energy densities) may be used to predict solvent-polymer membrane solubility and D_m, as phases with similar solubility parameters are generally more soluble with each other.[28] Solubility parameters (in $MPa^{1/2}$) for the sampling solvents examined here are given in Table 3.5.4. The parameter for ethyl acetate (18.2) is reasonably close to that of PDMS (14.9), consistent with an increased PAH diffusivity in the swelled PDMS, and therefore a greater permeability.

2-Propanol (solubility parameter of 23.5) is not excessively soluble in PDMS, indicated by solubility parameter comparisons and minimal membrane swelling. The optimal PAH performance observed must therefore come from an effect on $K_{m\text{-}s}$. This is supported by lower PAH solubilities in 2-propanol than ethyl acetate (Table 3.5.5), suggesting a higher activity of PAHs in 2-propanol compared to ethyl acetate when present at equimolar concentrations. Consequently, we attribute the improved sensitivity of PAHs in 2-propanol solution compared to ethyl acetate to an increased $K_{m\text{-}s}$, leading to a larger concentration gradient in the membrane, and subsequently greater mass transport. It should be noted that PAH solubility in 2-propanol is still sufficiently high to justify using 2-propanol as a sampling solvent for PAHs present in soil samples ($[\text{pyrene}]_{sat} = 7.69\times10^3$ mg/L, $[\text{anthracene}]_{sat} = 9.60\times10^2$ mg/L). Therefore, 2-propanol was chosen as the optimal sampling solvent for direct soil measurements. Furthermore, 2-propanol is now recommended as a green solvent alternative, a significant advantage over conventional PAH sample extraction solvents such as hexane or dichloromethane.[76]

Figure 3.4 demonstrates an evaluation of 2-propanol suitability as a sampling solvent for the direct measurement of PAHs in soil samples. Panel A gives the signal chronograms of four representative PAHs (100 μg/L each) spiked together into 2-propanol at t = 3 min. Signals were allowed to rise to steady-state levels, and at t = 7 min, 1.0 g of clean, sandy loam was added directly to the continuously stirred sample. Despite the high organic content of the soil (5.96 wt %), no significant change to the steady-state signal was observed, indicating that the PAHs remained free in solution rather than being sorbed by the soil. This behavior is in stark contrast to a similar experiment conducted in deionized water (panel B), where the MS signals for the solution phase concentration of naphthalene, anthracene, and pyrene decrease dramatically

within 5 min of adding soil to the stirred water sample. The data suggests nearly complete PAH sorption on the soil when present in aqueous suspensions. Benzo[*a*]pyrene was not used in the deionized water study because of its limited water solubility. Upon the basis of these sorption studies, 2-propanol demonstrated promise as an effective sampling solvent for direct soil measurements of the PAHs examined.

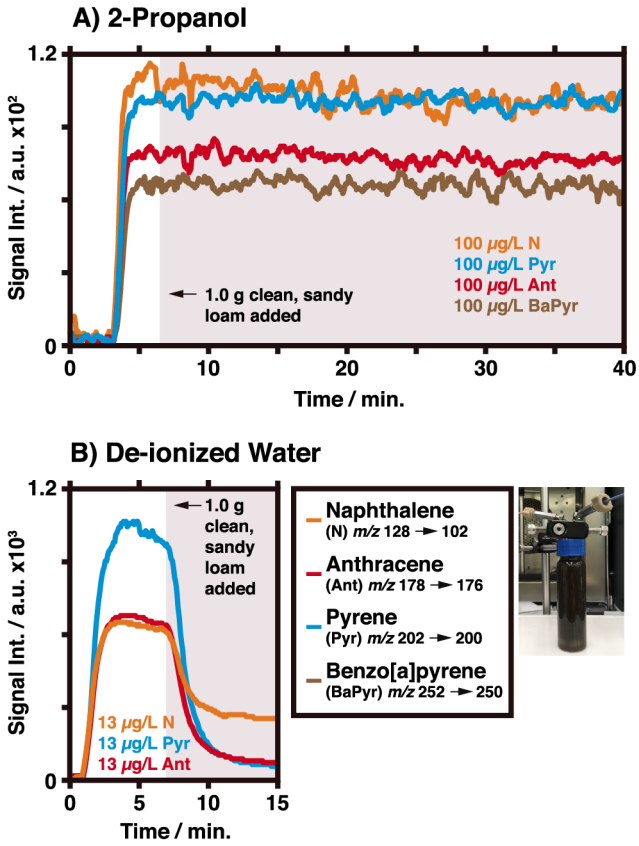

Figure 3.4: Comparison of signal chronograms for target PAHs in (A) 2-propanol and (B) deionized water (both 38.0 mL) with the addition of clean, sandy loam using CP-MIMS-LEI. Inset picture is of the aqueous sample after the addition of the clean, sandy loam.

3.3.4 Prepared Soil Measurements

Prepared PAH soil samples (500−2000 µg/kg) were analyzed by CP-MIMS-LEI. The masses of PAHs extracted into 2-propanol were plotted against the masses of PAHs loaded, as shown in Figure 3.5. Linear relationships are observed ($R^2 \geq 0.992$), demonstrating that different PAH loadings correlate with their measured concentrations. Percent recoveries (represented by the slopes in Figure 3.5) for anthracene, benzo[*a*]pyrene, and pyrene were 62%, 76%, and 76% respectively (average of 71%), with corresponding detection limits of 120, 70, and 60 µg/kg (Figure 3.5.2). Although the short, 3 min sonicated extraction in hot 2-propanol is not exhaustive

for soil PAHs, we believe the simplicity of the CP-MIMS-LEI work flow presented, bypassing any sample cleanup, provides significant advantages as a semi-quantitative rapid-screening method.

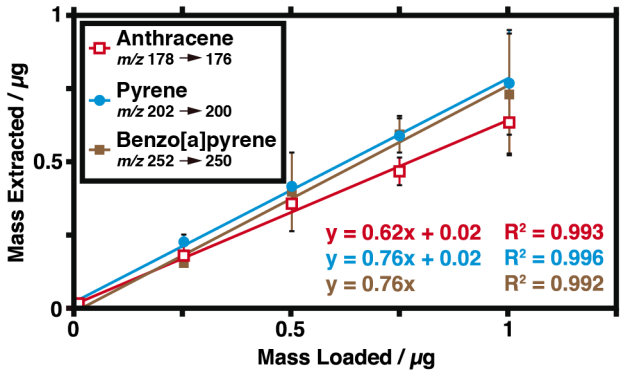

Figure 3.5: Investigation of PAH recoveries for direct CP-MIMS-LEI measurements of prepared soil samples.

3.3.5 Contaminated Soil Measurements

To examine the potential for direct PAH measurements in contaminated soil samples, three real-world samples were analyzed by CP-MIMS-LEI. A suite of 21 individual PAHs were also previously measured in these samples by an independent laboratory using accelerated solvent extraction in dichloromethane, workup, and isotope dilution GC/MS.[77] For the CP-MIMS-LEI measurements, concentrations of PAHs in 2-propanol were quantified via predetermined response factors (Table 3.5.2) and reported as mass ratios in the original soil sample (Table 3.3). Because PAH structural isomers are not resolved by CP-MIMS-LEI (*i.e.*, there is no chromatographic separation), quantitative results in Table 3.3 are reported for isomer classes. These are expressed as equivalent amounts of naphthalene (*m/z* 128), anthracene (*m/z* 178), pyrene (*m/z* 202), and benzo[*a*]pyrene (*m/z* 252), based upon the MS/MS transitions in Table 3.1. The internal standard signal (pyrene-d_{10}), consistently present in each sample at 280 µg/L, had a percent relative standard deviation of 5% across all CP-MIMS-LEI measurements. Percent relative standard deviations for individual PAHs ranged from 1% to 47% (three samples with three replicates each, see also Figure 3.6).

Table 3.3: Soil analysis results for PAH isomer classes by GC-MS and CP-MIMS-LEI

Sample	Isomer Class *m/z*	CP-MIMS-LEI mg/kg	GC-MS mg/kg	% Bias[a]
1	128	0.7 ± 0.4 [b]	0.97 [b]	-29
	178	5 ± 2 [c]	8.77 [d]	-44
	202	10 ± 2 [e]	14.13 [f]	-31
	252	9.7 ± 0.4 [g]	10.36 [h]	-8
2	128	0.12 ± 0.06 [b]	0.41 [b]	-72
	178	4.9 ± 0.6 [c]	5.62 [d]	-14
	202	14.0 ± 0.9 [e]	16.86 [f]	-17
	252	21.1 ± 0.3 [g]	14.54 [h]	+45
3	128	1.2 ± 0.2 [b]	2.11 [b]	-43
	178	19 ± 2 [c]	38.56 [d]	-51
	202	26 ± 2 [e]	57.08 [f]	-54
	252	19 ± 1 [g]	34.08 [h]	-43

[a] % bias = (CP-MIMS-LEI result – GC-MS result)/GC-MS result ×100%.
[b] Concentration of naphthalene.
[c] Reported as equivalent amount of anthracene.
[d] Summed concentration of anthracene and phenanthrene.
[e] Reported as equivalent amount of pyrene.
[f] Summed concentration of fluoranthene and pyrene.
[g] Reported as equivalent amount of benzo[*a*]pyrene.
[h] Summed concentration of benzo[*a*]pyrene, benzo[*b*]fluoranthene, benzo[*e*]pyrene, benzo[*k*]fluoranthene, and perylene.

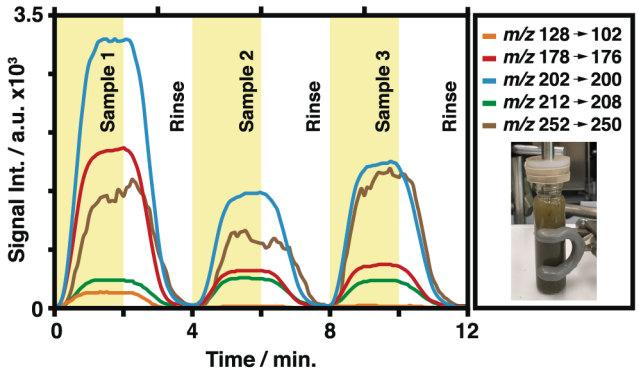

Figure 3.6: Representative signal chronograms for three soil sample analyses by CP-MIMS-LEI, illustrating rapid sample throughput. Inset picture is that of a representative sample.

Soil PAH concentrations observed by 2-propanol sonicated sampling followed by CP-MIMS-LEI measurements were generally less than those reported by accelerated solvent extraction GC-MS (Table 3.3). The average percent bias of CP-MIMS-LEI relative to GC-MS was −30%, where individual biases ranged from −72% to +45% (negative in 11 out of 12 cases).

These results are consistent with the recoveries observed for the prepared soil samples in Figure 3.5 (*i.e.*, non-exhaustive extraction, −29% average bias). Quantitation results from GC-MS, which were for individual PAHs, were similarly summed according to isomer classes for purposes of comparison to CP-MIMS-LEI data, as presented in Table 3.3.

As presented, the complete analytical duty cycle for direct PAH determinations in soil using CP-MIMS-LEI is *ca.* 15 soil samples/hr, representing a significant improvement over existing analytical strategies, such as GC-MS. Although not examined, it is anticipated that the use of previously demonstrated, non-steady-state CP-MIMS measurement approaches would further reduce the analysis times.[9]

In spite of the fact that the lack of chromatography in CP-MIMS-LEI does not allow for the quantitation of individual PAH isomers, given the simplified green chemistry workflow, rapidity, reproducibility, and sensitivity of CP-MIMS-LEI, we propose this technique as a rapid-screening tool for high-throughput applications. Although beyond the scope of this study, we are actively exploring liquid reagent chemical ionization (CI) strategies for direct PAH isomer differentiation with our approach. Mosi *et al.* demonstrated the use of halocarbon cations as CI reagents for PAH isomer differentiation.[78] CP-MIMS-LEI can be readily adapted for use with a variety of liquids as sources for reagent ions, either by using a suitable liquid acceptor phase itself or by admixing suitable dopants. Further, adapting the presented methodology for use with small MS systems may allow for onsite applications (e.g., contaminated site remediation, critical incident response, etc.), where obtaining reliable semi-quantitative information can be used to support decisions in the field and inform adaptive sampling strategies for complementary lab-based analytical determinations. Importantly, CP-MIMS-LEI measurements are time-resolved and may be used to monitor online processes, such as the adsorption and desorption phenomena presented herein. Ongoing work is being conducted to improve PAH extraction efficiency from soils and to further increase sample throughput.

3.4 Conclusions

CP-MIMS-LEI represents a novel, sensitive, and direct rapid-screening technique for PAHs from both aqueous and soil samples without any instrumental or sampling modifications. The rapid detection of PAHs in environmental samples has potential applications for protection of the environment and human health. Furthermore, this study represents novel soil analyses that completely obviate sample cleanup, allowing for significantly simpler sample handling and faster sample throughput.

3.5 Supporting Information

3.5.1 Standards and Solvents

Anthracene (99%) was obtained from Alfa Aesar (Ward Hill, MA, USA). Benzo[*a*]pyrene (≥96%), naphthalene (99%), pyrene (98%) and pyrene-d_{10} (98 atom % D) were obtained from Sigma Aldrich (Oakville, ON, Canada). 2-Propanol, methanol, acetonitrile (HPLC grade) and ethyl acetate (99.9%) were obtained from VWR International (Edmonton, AB, Canada). Reagent alcohol (90% ethanol, 5% 2-propanol, 4.5% methanol, HPLC grade) and N,N-dimethylformamide (99.9%) were obtained from Fisher Scientific (Ottawa, ON, Canada). Reagent alcohol is subsequently referred to as ethanol for the purposes of this study. Heptane (HPLC grade) and dichloromethane (≥99.5%) were obtained from Sigma Aldrich. For eventual analysis in aqueous solutions, PAH stock and sub-stock solutions were prepared in methanol. For eventual analysis in organic solutions, PAH stock solutions were prepared in dichloromethane, and sub-stock solutions were prepared in 2-propanol. Aqueous solutions were prepared volumetrically such that the final methanol concentration was below 0.25% by volume. Organic solutions were also prepared volumetrically such that the final dichloromethane concentration was below 0.5% by volume.

3.5.2 Microscopic Images

Microscopic images were obtained using a dissection microscope (Model MDG 17, Wild Heerbrugg, Switzerland) equipped with a digital camera imaging system (Model MD500, Amscope, Irvine, CA, USA).

Table 3.5.1: Analyte physicochemical properties[a]

	Molar Mass g/mol	Vapour Pressure mmHg	logK_{ow}	Water Solubility mg/L
Naphthalene	128.18	8.5×10^{-2}	3.3	31
Anthracene	178.24	6.53×10^{-6}	4.45	0.0434
Pyrene	202.26	4.5×10^{-6}	4.88	0.135
Benzo[*a*]pyrene	252.32	5.49×10^{-9}	6.13	0.00162

[a] From SRC database [30]

Table 3.5.2: PAH response factors relative to pyrene-d_{10} in isopropanol.

	Response Factor[a]
Naphthalene	1.5 ± 0.1
Anthracene	1.22 ± 0.05
Pyrene	1.66 ± 0.05
Benzo[*a*]pyrene	1.01 ± 0.04

Calculated for all analytes at 100 µg/L

[a] RF = ($Signal_{PAH}$ / [PAH]) / ($Signal_{Pyrene\text{-}d10}$ / [Pyrene-d_{10}])

Table 3.5.3: Signal to noise ratios for PAHs in various organic solvents monitored by CP-MIMS-LEI.

Solvent	Naphthalene	Anthracene	Pyrene	Benzo[*a*]pyrene
Acetonitrile	3 ± 2	5 ± 2	7 ± 1	4.0 ± 0.2
Dichloromethane	2 ± 1	3 ± 2	5 ± 2	4.6 ± 0.9
Ethanol	5 ± 2	8 ± 2	13 ± 1	6.2 ± 0.7
Ethyl acetate	8 ± 2	9 ± 1	14 ± 3	11 ± 2
Methanol	6 ± 2	8 ± 1	11 ± 3	3.6 ± 0.3
2-Propanol	11 ± 2	14 ± 3	17 ± 6	11 ± 3

All analytes present at 100 µg/L each

No appreciable signals were observed for PAHs in N,N-dimethylformamide

Table 3.5.4: Solubility parameters, and boiling points for select organic solvents and polydimethylsiloxane.

Solvent/Polymer	Solubility Parameter $Mpa^{1/2}$	Boiling Point[c] °C
Acetonitrile	24.6 [a]	82
Dichloromethane	20.3 [a]	39.6
N,N-Dimethylformamide	22.7 [a]	153
Ethanol	26.0 [b]	78.4
Ethyl acetate	18.2 [a]	77.1
Methanol	29.7 [a]	64.7
2-Propanol	23.5 [a]	82.6
Polydimethylsiloxane	14.9 [b]	-

[a] Hansen solubility parameter, From Zeng *et al.* [28]

[b] Hildebrand solubility parameter, from Zeng *et al.* [28]

[c] From SRC database [30]

Table 3.5.5: PAH solubilities in ethyl acetate and 2-propanol.

Analyte	Ethyl Acetate Solubility		2-Propanol Solubility	
	χ	mg/L	χ	mg/L
Anthracene [a]	0.00484	8.87×10^{3}	0.000411	9.60×10^{2}
Pyrene [b]	0.04251	9.19×10^{4}	0.00290	7.69×10^{3}

Solubilities of naphthalene and benzo[*a*]pyrene in these solvents are not readily available, although similar solubility trends are expected.

[a] Data for 25°C, from Powell *et al.* [79]

[b] Data for 26°C, from Roy *et al.* [80]

Figure 3.5.1: In-house built stainless steel flange was mounted on MS source with Hewlett Packard 59864A Ionization Gauge Controller.

Chapter 4

Mass Spectrometry Based Approach for Organic Synthesis Monitoring

Reproduced with minor changes and permission from Termopoli, V.; Torrisi, E.; Famiglini, G.; Palma, P.; Zappia, G.; Cappiello, A.; Vandergrift, G.W.; Zvekic, M.; Krogh, E.T.; Gill, C.G. "Mass Spectrometry Based Approach for Organic Synthesis Monitoring." *Analytical Chemistry*, **2019**, *91*, 11916-11922. Two author lists were published for this manuscript, with V. Termopoli as lead author for the first list of authors, and G.W. Vandergrift as the lead author for the second list of authors. C.G. Gill, G.W. Vandergrift, and V. Termopoli designed the experiments. G.W. Vandergrift, C.G. Gill, and V. Termopoli primarily collected the data, with contributions from M. Zvekic. E. Torrisi synthesized and characterized the alkyl glycinate standards. G.W. Vandergrift primarily analyzed the data, with contributions from V. Termopoli. G.W. Vandergrift drafted the manuscript, with intellectual and editorial contributions from all authors.

4.1 Introduction

The synthesis of organic compounds on an industrial scale is of enormous economic importance. Understanding optimum reaction conditions is key to maximizing the yields of desired products, as well as simultaneously reducing the production of inadvertent side products, which lower yields, may be harmful, and require additional separation steps. Synthetic chemists have a wide variety of analytical methodologies at their disposal to investigate and optimize reaction conditions for industrial applications. These include spectroscopic methods (e.g., FT-IR, UV−vis, fluorescence, NMR, etc.)[81-83] as well as mass spectrometry (MS).[84] However, many of these techniques are carried out off-line, requiring subsample collection and rapid analysis, frequently with some form of quenching. This is because the reaction will continue in the subsamples until the time of measurement, potentially compromising any information obtained. Online dilutions of subsampled reaction mixtures are also frequently employed to make satisfactory measurements, reducing sensitivity for trace analytes. Kinetic data obtained in this manner is laborious and often intermittent. A number of spectroscopic techniques have been adapted for continuous online monitoring,[85-86] but these tend to lack specificity for target analytes and the sensitivity for quantitation of trace components.

To increase both sensitivity and selectivity for quantitative online reaction monitoring, chemists have largely turned to MS based approaches, as resolution by *m/z* ratios is more selective and reliable when compared to other chemical analysis strategies (*i.e.*, monitoring chromophores). Atmospheric pressure ionization sources, particularly ESI, have been used extensively for coupling reactions to MS. As a recent example, the Cooks group has demonstrated an online, multiplexed MS reaction monitoring system based on direct sampling ESI-MS, simultaneously monitoring up to six reaction types without sample carryover.[87] The McIndoe group has also been exploring the use of online ESI-MS monitoring to investigate catalytic reactions.[88-90] Many other variants of ESI-MS have been used for reaction monitoring, including desorption ESI (DESI), extractive ESI (EESI), ESI assisted laser desorption ionization (ELDI), and paper spray (PS-MS).[84] However, for many ESI-based techniques, care must be taken to ensure that clogging of fine sampling capillaries does not occur. This may preclude their use in complicated, heterogeneous reaction slurries or for small reaction volumes, as the monitoring itself consumes a portion of the reacting mixture.

While the Cooks group has bypassed many practical challenges of this strategy by using inductive ESI,[91-92] perhaps the most significant obstacle associated with ESI-related monitoring techniques is the requirement that the chemical species being monitored must be satisfactorily ionized by ESI (e.g., easily charged species). ESI sensitivity is further confounded by high salt concentrations and varying solvent compositions,[33, 37] excluding the use of these techniques from many reaction monitoring applications because of analyte and reaction mixture incompatibility. Other ambient ionization techniques, such as direct analysis in real-time (DART),[93] have been used to bypass ESI ionization complications encountered in reaction monitoring in principle. In a particularly intriguing application of DART-MS/MS, the Volmer group monitored micro-reactions in acoustically levitated droplets.[94] However, DART-based MS methods often lack reliable quantitative information and are predominantly restricted to offline, snapshot measurements.[84]

As an alternative sample introduction strategy for online reaction monitoring, the method of membrane introduction mass spectrometry (MIMS) may offer a suitable solution to the identified deficiencies. There are several reviews of MIMS that explain the methodology, as well as its suitability for direct, online monitoring in complex sample mixtures.[17, 73] Simply described, MIMS utilizes a semipermeable membrane, often PDMS (silicone), to nonexhaustively extract and directly transfer analytes (as a mixture) to a mass spectrometer, where they are resolved by their *m/z* ratios, by selective ionization, and by tandem mass spectrometry (MS/MS). The membrane rejects particulate materials and is hydrophobic, with perm-selectivity characteristics favoring mass transfer of nonpolar analytes, rejecting highly polar and charged components, making MIMS ideally suited for the online extraction of neutral compounds from a complex reaction mixture.[17, 73]

There is some precedent in the literature for the use of MIMS for reaction monitoring utilizing EI. As a few examples, in early work, the Cooks group used a silicone membrane interface to transfer permeating analytes directly into a high vacuum EI triple quadrupole MS. While effective, the membrane interface design was also prone to memory effects and slow signal response times.[95] The Cooks group also demonstrated MIMS use for the online monitoring of the reactions of epichlorohydrin in water using a polyphenyl ether liquid membrane and a quadrupole ion trap.[96] Our group has used a flow cell interface MIMS system to follow the oxidative degradation kinetics for trace gasoline contaminants in aqueous samples[97] and also the reductive dehalogenation kinetics of organic contaminants in natural waters.[98] A commonality with these early MIMS reaction-monitoring studies was the use of a gaseous acceptor (or high vacuum) to desorb permeating analytes from the membrane, and frequently from aqueous reaction systems. While effective for smaller analytes of higher volatility, these strategies were ineffective for larger, less volatile analytes. Alternatively, permeating analytes in a MIMS measurement can be transferred from the membrane by a continuously flowed liquid (condensed) phase and then coupled with a variety of atmospheric pressure ionization strategies. This approach has been termed condensed phase MIMS (CP-MIMS) and has been described in several reviews.[17, 73]

The use of CP-MIMS has allowed researchers to utilize a variety of MS ionization strategies, including ESI, atmospheric pressure chemical ionization (APCI)[6-8, 29, 34-35] and liquid electron ionization (LEI),[10, 36, 72] to extend the application of MIMS to larger, significantly less volatile analytes. In early work, Clinton *et al.* demonstrated the use of a CP-MIMS type interface system with a hydrophobic polyvinylidene fluoride microporous sheet membrane coupled with APCI to follow the course of a synthetic reaction, implemented by sampling reaction aliquots as a function of time.[99] Additionally, we have presented the real-time monitoring of aqueous chlorination reactions,[6, 34] as well as the photo-oxidative degradation[7] and adsorption of naphthenic acids in aqueous solutions[73] by CP-MIMS using ESI. The coupling of LEI with CP-MIMS is of particular interest for reaction monitoring, as it is a more universal ion source and overcomes a limitation with ESI, which typically requires polar functional group(s) to carry a charge. Thus, CP-MIMS paired with LEI represents an ideal monitoring strategy for synthetic organic reactions, especially for measuring neutral hydrophobic analytes that exhibit poor performance with ESI.

The LEI concept has been discussed in recent publications.[10, 72] It represents a new approach for efficiently addressing the difficult conversion of a liquid-phase into a gas-phase for EI, using a nanoscale flow rate, generating library searchable spectra. Since ionization occurs in the gas phase, LEI strongly mitigates suppression effects from co-eluting reaction components permeating through the membrane, offering reliable quantitative reaction data.

We present the newer variant of LEI[100] paired with CP-MIMS, as a strategy for quantitative online monitoring, directly in organic solvent reaction mixtures. Permeating neutral analytes are effectively vaporized and ionized directly by LEI, where the vaporization and ionization steps are spatially decoupled. As previously mentioned, LEI is effective for ionizing analytes with poor ESI performance, and as presented with CP-MIMS, addresses a significant gap in currently available online quantitative reaction monitoring approaches, providing complementary results to those obtained using ESI based strategies. This manuscript presents the first use of CP-MIMS coupled with LEI for quantitative online monitoring of non-aqueous synthetic organic reactions. The resulting system is robust and facilitates direct, quantitative measurements of neutral reactant and product species in complex, highly acidic, and heterogeneous organic solvent reaction mixtures.

4.2 Experimental Section

4.2.1 Standards and Solvents

Details regarding solvent and standard sources and their preparation and the characterization of the alkyl glycinate standards are reported in the Supporting Information, Section 4.5. All standard and reaction measurements were made in magnetically stirred 20 or 40 mL glass vials with Teflon faced septum seals (EPA/VOA Type, Scientific Specialties Inc., Hanover, MD, U.S.A.) at ambient conditions (ca. 25 °C, 101 kPa), unless otherwise noted.

4.2.2 Instrumentation

Two EI-MS systems were employed for these studies, including a single quadrupole system (Model 5975, Agilent Technologies, Santa Clara, CA, U.S.A.) operated in selected ion monitoring mode (SIM), and a triple quadrupole tandem mass spectrometry (MS/MS) system (Model 7010, Agilent Technologies, Santa Clara, CA, U.S.A.) operated in a multiple reaction monitoring mode (MRM). Both MS systems were equipped with identical CP-MIMS, hollow fiber polydimethylsiloxane membranes (5.0 mm long, 0.30 mm i.d., 0.64 mm o.d., 170 μm thick, and LEI configurations (Figure 4.1). Details of the SIM and MRM conditions used for all analytes are given in Supporting Information, Section 4.5 (Table 4.5.1). In addition, for the MS/MS system, concomitant changes in the UV-vis absorbance of post membrane permeant was also continuously monitored by diverting the splitter waste flow through a capillary UV-vis detector (Spectra 100, Spectra Physics Inc., Santa Clara, CA). MS tuning parameters were checked periodically and remained constant for the studies shown here, demonstrating robustness and ease of use.

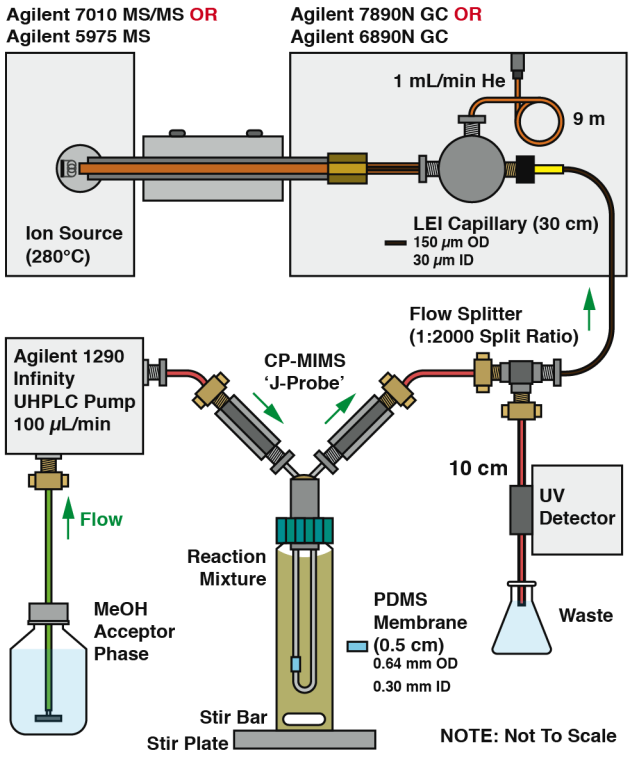

Figure 4.1: Schematic diagram of the modified CP-MIMS-LEI system.

4.2.3 Oxidation of Phenylacetylene Reaction

Phenylacetylene undergoes acid-catalyzed hydrolysis, and the reaction rate is greatly increased in the presence of a chloroauric acid ($HAuCl_4$) catalyst. 90 mM phenylacetylene was added to the 20 mL of reaction mixture (95:4:1 methanol/deionized water/sulfuric acid v/v, 4 mM $HAuCl_4$) with gentle heating (~50 °C) and magnetic stirring. This procedure is described elsewhere.

4.2.3 Alkyl Glycinate Reaction

To initiate the reaction, 1.0 mL of ethylbromoacetate (yielding an initial concentration of 330 mM) was added to a magnetically stirred mixture containing 330 mM triethylamine and 300 mM α-methyl benzylamine in 24 mL of dry acetonitrile.

4.2.4 Alkyl Glycinate Standard Synthesis

To a mixture of (R)-α-methyl benzylamine (0.92 mL, 7.27 mmol) and triethylamine (1.11 mL, 7.99 mmol) in dry acetonitrile (20 mL), 0.89 mL of ethyl bromoacetate (7.99 mmol) was added in one portion. The solution was maintained under stirring at room temperature until the disappearance of (*R*)-*α*-methyl benzylamine, concentrating the reaction mixture under reduced pressure. The residue was dissolved in ethyl acetate (50 mL) and washed with H_2O (15 mL), saturated NaCl brine (15 mL), dried over Na_2SO_4, filtered, and concentrated under reduced

pressure. The residue was purified by flash chromatography on silica gel, eluting with cyclohexane/ethyl acetate (20:80%, v/v) to give first the dialkyl product, diethyl (*R*)-2,2′-((1-phenylethyl)-azanediyl)-diacetate [minor product] (0.176 g, 0.6 mmol, 8%), as an oil, followed by the monoalkyl product, ethyl (*R*)-(1-phenylethyl)glycinate [major product] (1.18 g, 5.7 mmol, 78%), as an oil.

4.3 Results and Discussion

4.3.1 CP-MIMS-LEI Instrumentation

The CP-MIMS-LEI experimental system has been described elsewhere.[10] A schematic diagram of the specific configuration used for synthetic reaction monitoring is given in Figure 4.1. Several modifications were necessary to reduce the analyte flux transferred to the MS ion source, allowing successful monitoring of high concentrations present in synthetic reaction mixtures. These included a shorter membrane, an increased methanol acceptor phase flow rate through the membrane lumen (100 μL/min), and drastically reduced acceptor phase flow rate to the LEI interface (*ca.* 50 nL/min, split ratio 1:2000), all of which act to reduce the mass transfer of analyte to the MS. The sensitivity of the presented system is highly tunable, and may be adjusted according to the requirements of a given online reaction monitoring application.

4.3.2 Solvent-Membrane Compatibility Investigations

To date, the majority of CP-MIMS type measurements have been made in aqueous samples.[8, 10, 29, 36] It is known that solvent-membrane solubility can significantly influence membrane permeability.[9, 25, 27] We have begun to exploit acceptor phase cosolvents with CP-MIMS by forming *in situ* polymer inclusion membranes, which improve both the sensitivity and measurement duty cycle.[9-10] In addition, recent developments utilizing modified donor phases (e.g., mixed organic sample solvents) with CP-MIMS have shown promise for making direct measurements of fatty acids.[101] However, because synthetic reactions are most often conducted in non-aqueous solvents, the analytical performance of PDMS membranes in a variety of non-aqueous sample solvents was investigated.

A series of individual standards containing biphenyl or chlorobenzene in the 10 to 50 mM range were prepared in a wide range of common protic and aprotic solvents that could potentially be used for organic syntheses (acetonitrile, dichloromethane, N,N-dimethylformamide, ethanol, methanol). Analyte signals for CP-MIMS-LEI measurements for each standard were allowed to reach steady state, and were background-subtracted using the signal from the appropriate solvent blank (Tables 4.5.2 and 4.5.3). In all cases, calibrations showed satisfactory linearity ($R^2 \geq 0.98$), suggesting broad applicability of CP-MIMS-LEI for quantitative reaction monitoring in different solvent/reaction systems. The order of the relative sensitivities for both analytes (*i.e.*, calibration slopes) in the different solvents was conserved, and faster $t_{10-90\%}$ signal response times also correlated with greater sensitivities. These trends may be understood by considering the intrinsic

factors governing membrane transport. For a given analyte, the steady-state signal intensity for a CP-MIMS measurement is related to membrane permeability (P), which can be expressed as the product of analyte diffusivity through the membrane (D_m) and the partitioning constant of the analyte between the membrane and the sample ($K_{m\text{-}s}$, Equation 4.1):[18]

Equation 4.1 $$P = K_{m-s}D_m$$

The time required for an analyte signal to reach steady-state can be expressed as the $t_{10-90\%}$ response time and is inversely proportional to D_m (Equation 4.2).[20]

Equation 4.2 $$t_{10-90\%} \propto \frac{l^2}{D_m}$$

The differing analyte response times in different solvents indicate changes in the corresponding diffusivities (D_m), as these solvents swell membranes to varying extents and change their permeation characteristics. However, it is clear that the permeability is also affected by concomitant changes in the partitioning behavior ($K_{m\text{-}s}$) in different solvent systems.

4.3.3 Simultaneous Time Resolved MS and UV-Vis Detection

Because a large fraction of the (post membrane) acceptor phase is diverted from the CP-MIMS-LEI combination via the passive flow splitter (Figure 4.1), this stream can also be analyzed by other continuous analyzers to provide orthogonal data sets. To demonstrate this, the diverted acceptor phase waste was passed through a capillary UV−vis detector. Figure 4.2 illustrates an example of an orthogonal time series data set obtained from MS and UV−vis detection of a 25 mM chlorobenzene standard prepared in methanol (original MS and UV−vis recorded traces are given in the Supporting Information, Section 4.5, Figure 4.5.1). As expected, the data illustrates identical time-resolved signals, with superior signal-to-noise for the MS trace (due to the lower sensitivity of UV−vis absorbance measurements). The time constant associated with the rise to steady-state signal is correlated with membrane transport kinetics and depends on a variety of factors including the membrane thickness, the size of the permeant and the presence of solvent co-permeants. The $t_{10-90\%}$ signal rise time for chlorobenzene under these conditions is 0.33 min, typical for the compounds studied here. The technique is therefore well suited for monitoring reactions that take place on the time scale of minutes to hours, applicable for a wide range of synthetic organic reactions. While spectroscopic methods can be utilized to characterize a number of reactions based upon changes in their optical properties, they are inherently less selective than MS, and may therefore be challenging in complex reaction mixtures with overlapping chromophores. This highlights the advantages of MS based reaction monitoring strategies.

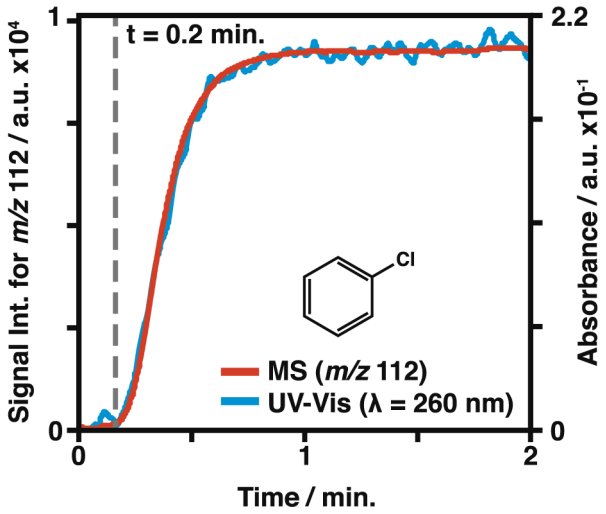

Figure 4.2: Comparison of simultaneous online monitoring data measured by CP-MIMS-LEI (*m/z* 112) and parallel UV−vis spectrophotometry detection (λ = 260 nm) for 25 mM chlorobenzene in methanol (spiked at t = 0.2 min).

4.3.4 Online Synthetic Reaction Monitoring Examples

As a first demonstration of CP-MIMS-LEI for *in situ*, continuous reaction monitoring, the catalytic oxidation of phenylacetylene to acetophenone in highly acidic methanol solvent was examined (Figure 4.3) using a single quadrupole MS system (SIM mode). As shown in Figure 4.3, phenylacetylene (*m/z* 102) undergoes rapid catalytic conversion to the Markovnikov-favored addition product, acetophenone (*m/z* 105, 100% yield). Concentrations were determined using direct calibrations made with methanol standards, and the $t_{10-90\%}$ signal rise times were ≤0.4 min (Table 4.5.4), whereas the reaction occurred over about 30 min. The presence of acetophenone was monitored by *m/z* 105 ($[M\text{-}CH_3]^+$), chosen since it is free of isobaric interference from phenylacetaldehyde, a possible non-Markovnikov product. No substantial amount of phenylacetaldehyde was formed under the given reaction conditions, indicated by the stoichiometric mass balance illustrated in Figure 4.3.

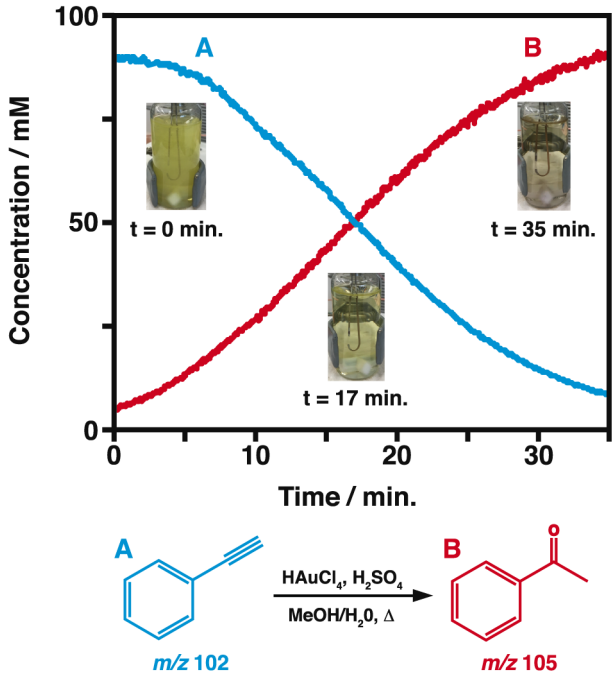

Figure 4.3: CP-MIMS-LEI online monitoring of the catalytic oxidation of phenylacetylene (A) to acetophenone (B) under highly acidic conditions.

The online reaction monitoring of phenylacetylene oxidation to acetophenone illustrates the significance of CP-MIMS-LEI pairing, as both the reactant and product are incompatible with ESI based monitoring systems. As shown by the photo insets in Figure 4.3, the reaction is occurring in a heterogeneous (cloudy) system, which would pose serious problems if direct capillary sampling strategies (e.g., ESI) were employed.

The PDMS membrane provides an online "cleanup" that effectively removes particulates, and charged corrosive components (e.g., sulfuric acid, chloroauric acid catalyst), while allowing hydrophobic molecules to permeate for continuous mass spectrometric analysis. While some oxidative damage was observed for the PDMS membrane near the completion of the reaction (due to the high concentration of sulfuric acid, ~1% v/v in methanol, larger images in Figure 4.5.2), the membrane and probe assembly are both inexpensive and easily replaced within minutes, without the need to vent the MS. The LEI interface required no maintenance during the experiments here, but the LEI capillary may also be simply replaced as needed without venting the MS.

To further demonstrate the utility of CP-MIMS-LEI for online reaction monitoring, the synthesis of alkyl glycinates in an aprotic solvent was examined. Alkyl glycinates have been used as intermediates for the preparation of α-amino acids,[102] as well as building blocks in the

preparation of peptidomimetics.[103] A synthesis strategy is presented in the reaction scheme given in Figure 4.4. While advantageous because of the mild reaction conditions, this reaction can be plagued by overalkylation products, reducing the yield of a desired product.[104] In this context, simultaneous monitoring of the formation of various alkylation products is of significant synthetic interest.

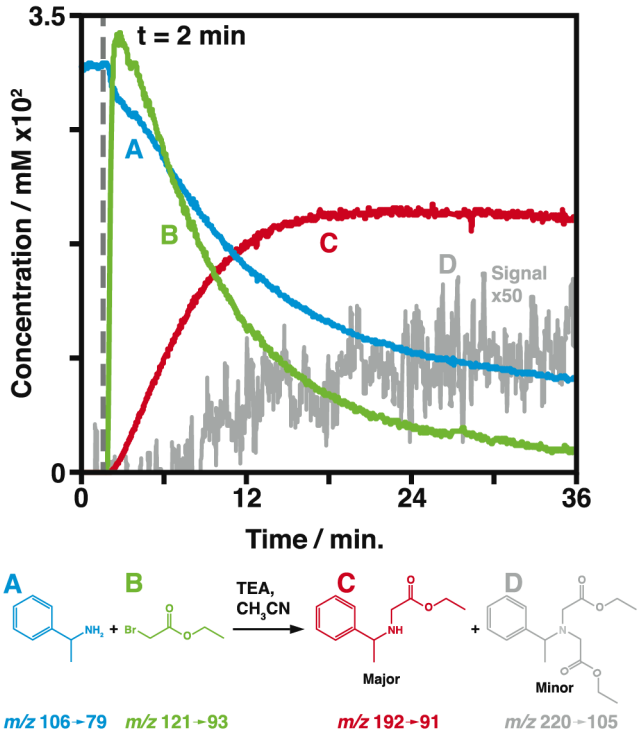

Figure 4.4: CP-MIMS-LEI demonstration of the quantitative online monitoring of an alkyl glycinate synthesis in dry acetonitrile with triethylamine (TEA) catalyst: (A) (*R*)-*α*-methyl benzylamine; (B) ethyl bromoacetate; (C) ethyl (*R*)-(1-phenylethyl)glycinate; (D) diethyl (*R*)-2,2′-((1-phenylethyl)-azanediyl)-diacetate.

For this demonstration, the MS/MS system was employed. To initiate the reaction, ethylbromoacetate was added to reaction mixture at t = 2 min. Production of both monoalkylated (major product, 70% yield) and dialkylated (minor product, 0.7% yield) species was observed (Figure 4.4). The synthesis was conducted in acetonitrile with a basic catalyst, yielding an alkaline reaction mixture. Under these conditions, both the reactants and products are neutral, and successfully monitored by CP-MIMS-LEI. If attempted, direct sampling ESI reaction monitoring would not be satisfactory, as it would require post-sampling pH adjustments to protonate the analytes, as well as dilution steps. Figure 4.4 also illustrates that the ethylbromoacetate alkylation reagent is consumed at a faster rate than *α*-methyl benzylamine. This is likely due to formation of the dialkylated product and the presence of trace moisture in

the reaction system, possibly present in the triethylamine catalyst used. Information such as that shown in Figure 4.4 may be used for rapid, online reaction optimization, as the real-time data allows for continuous assessment of reagent purity, consumption, and production of possible side-products.

All reagents and products for this study demonstrated linear direct calibrations over the concentration ranges presented, and the $t_{10-90\%}$ signal rise times were significantly faster than the observed reaction rates (Table 4.5.5). Even for reactions where product crystallization occurred over the course of a measurement (Figure 4.5), free solution concentration changes for reactants and products were still observable in these heterogeneous slurries, further demonstrating the robustness of the CP-MIMS-LEI synthesis monitoring strategy.

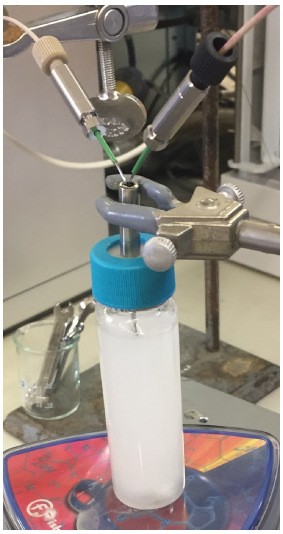

Figure 4.5: Photograph of an alkylation reaction mixture with CP-MIMS-LEI probe in place illustrating crystallized product formation.

4.4 Conclusions

We demonstrate the use of an *in situ* mass spectrometry based reaction monitoring technique compatible with complex, non-aqueous solutions. This approach yields real-time feedback for the optimization of synthetic reaction conditions and important mechanistic insight. The coupling of CP-MIMS and LEI exploits advantages of both methodologies, resulting in a robust system that allows the direct measurements of neutral organic analytes in complex, heterogeneous and corrosive reaction mixtures. CP-MIMS and LEI are ideally paired to suit the online measurement of a variety of synthetic reactants and products. Further, CP-MIMS-LEI quantitatively measures molecules that are not amenable to other online reaction monitoring strategies, such as direct sampling ESI approaches, providing a complementary strategy that addresses a significant gap in current synthetic reaction monitoring methodology using mass

spectrometry. The quality of online quantitative data is ensured by both membrane selectivity and LEI's capacity to operate in the presence of co-permeating reagents, with concentrations varying in time, and by employing analytical calibrations obtained in the same solvents used for a given reaction. Although beyond the scope of the presented work, in future studies, the membrane may be replaced with one made from a different material (such as Nafion) for more polar compound applications. Future work includes the use of online CP-MIMS monitoring simultaneously employing both LEI-MS and ESI-MS to enable the simultaneous online measurement of both charged and neutral species in synthetic reactions.

4.5 Supporting Information

4.5.1 Synthesis of Alkyl Glycinate Standards

To a mixture of *(R)*-*α*-methyl benzylamine (0.92 mL, 7.27 mmol) and triethylamine (1.11 mL, 7.99 mmol) in dry acetonitrile (20 ml), 0.89 mL of ethyl bromoacetate (7.99 mmol) was added in one portion. The solution was maintained under stirring at room temperature until the disappearance of *(R)*-*α*-methyl benzylamine, concentrating the reaction mixture under reduced pressure. The residue was dissolved in ethyl acetate (50 ml) and washed with H_2O (15 ml), saturated NaCl brine (15 ml), dried over Na_2SO_4, filtered and concentrated under reduced pressure. The residue was purified by flash chromatography on silica gel, eluting with cyclohexane/ethyl acetate (20:80%, v/v) to give first the dialkyl product: diethyl (*R*)-2,2'-((1-phenylethyl)-azanediyl)-diacetate [Minor product] (0.176 g, 0.6 mmol, 8%) as an oil, followed by the monoalkyl product: ethyl (*R*)-(1-phenylethyl)glycinate [Major product] (1.18 g, 5.7 mmol, 78%) as an oil.

TLC (Cyclohexane:AcOEt, 60:40 v/v): $R_f = 0.72$;
$[\alpha]_D = +33.56$ (c = 0.015 M in $CHCl_3$)
[Minor product Spectroscopic Characterization]:
^{1}H NMR (400 MHz, $CDCl_3$): δ 7.44 – 7.20 (m, 5H), 4.20 (q, *J* = 6.9 Hz, 1H), 4.13 (q, *J* = 7.1 Hz, 4H), 3.57 (s, 4H), 1.35 (d, *J* = 6.7 Hz, 3H), 1.24 (t, *J* = 7.1 Hz, 6H); ^{13}C NMR (125 MHz, $CDCl_3$): δ 171.528, 144.100, 128.460, 127.493, 127.284, 77.355, 77.038, 76.720, 60.957, 60.410, 52.400, 20.937, 14.189; MS (*m/z*): 293

TLC (Cyclohexane:AcOEt, 60:40 v/v): $R_f = 0.50$;
$[\alpha]_D = +70.62$ (c = 0.026 M in $CHCl_3$); Literature value for (S)-enantiomer = - 64.4 (c = 2.27 g/mL in $CHCl_3$)[105];
[Major product Spectroscopic Characterization]:
^{1}H NMR (400 MHz, $CDCl_3$): δ 7.36 – 7.21 (m, 5H, Ar), 4.16 (q, *J* = 7.1 Hz, 2H), 3.80 (q, *J* = 6.6 Hz, 1H), 3.35 – 3.16 (m, 2H), 1.99 (s, 1H), 1.39 (d, *J* = 6.6 Hz, 3H), 1.25 (t, *J* = 7.2 Hz, 3H), ^{13}C NMR (125 MHz, $CDCl_3$): δ 172.548, 144.581, 128.496, 127.153, 126.742, 77.354, 77.039, 76.719, 60.687, 57.735, 48.863, 24.207, 14.18; MS (*m/z*): 207

Table 4.5.1: MS scan parameters.

Analyte	MW g/mol	Scan Type[a]	*m/z*	Collision Energy eV
Acetophenone	120.15	SIM	105	-
Biphenyl	154.21	SIM	154	-
Chlorobenzene	112.56	SIM	112	-
Phenylacetylene	102.13	SIM	102	-
Ethyl bromoacetate	167.01	MRM (Quant)	121→93	10
		MRM (Qual)	138→120	5
α-Methylbenzylamine	121.18	MRM (Quant)	106→79	10
		MRM (Qual)	106→77	10
Mono-alkylated product	207.26	MRM (Quant)	192→91	10
		MRM (Qual)	192→118	10
Dialkylated product	293.34	MRM (Quant)	220→105	10
		MRM (Qual)	278→107	5

[a] Quant = quantitation transition, Qual = qualifying transition

Table 4.5.2: Biphenyl calibrations and response times for 10-50 mM solute concentrations in various organic solvents.

Solvent	Equation	R^2	$t_{10\text{-}90\%}$ min
Acetonitrile	y = 1.13x + 0.83	0.990	0.67
Dichloromethane	y = 5.39x – 4.36	0.999	0.41
N,N-Dimethylformamide	y = 0.50x + 1.70	0.983	0.63
Ethanol	y = 4.23x – 0.68	0.998	1.1
Methanol	y = 2.41x + 3.89	0.994	0.68

Triplicate measurements (intraday)
Risetimes calculated for 50 mM sample

Table 4.5.3: Chlorobenzene calibrations and response times for 10-50 mM solute concentrations in various organic solvents.

Solvent	Equation	R^2	$t_{10\text{-}90\%}$ min
Acetonitrile	y = 1.78x – 2.79	0.996	0.48
Dichloromethane	y = 5.24x + 2.83	1.000	0.33
N,N-Dimethylformamide	y = 1.62x – 2.27	0.996	0.43
Ethanol	y = 2.78x – 4.27	0.998	0.69
Methanol	y = 2.57x – 2.42	0.999	0.46

Triplicate measurements (intraday)
Risetimes calculated for 50 mM sample

Table 4.5.4: Reactant and product calibrations and response times for oxidation reaction in methanol.

Analyte	Equation	R^2	$t_{10\text{-}90\%}$ min
Phenylacetylene	y = 16.8x – 29.7	0.999	0.35
Acetophenone	y = 5.33x – 1.79	1.000	0.40

Single Measurements in 95:4:1 methanol:de-ionized water:sulfuric acid v/v, 4 mM $HAuCl_4$ with gentle heating (~50°C); 5-200 mM; Risetimes calculated for 90 mM sample

Table 4.5.5: Reactant and product calibrations and response times for alkylation reaction in acetonitrile.

Analyte	Equation	R^2	$t_{10\text{-}90\%}$ min
Ethyl bromoacetate [a]	y = 19.1x + 82.3	0.999	0.23
α-Methylbenzylamine [a]	y = 59.6x + 243	0.999	0.42
Mono alkylated product[b]	y = 16.1x + 68.3	0.999	0.60
Dialkylated product[c]	y = 4.85x + 1.36	1.000	1.2

[a] Triplicate measurements (interday); 1-500 mM; Risetimes calculated for 250 mM sample

[b] Duplicate measurements (interday); 1-250 mM; Risetime calculated for 250 mM sample

[c] Single measurements; 10-75 mM; Risetime calculated for 75 mM sample

Chapter 5

Condensed Phase Membrane Introduction Mass Spectrometry with *In Situ* Liquid Reagent Chemical Ionization in a Liquid Electron Ionization Source (CP-MIMS-LEI/CI)

Reproduced with minor changes and permission from Vandergrift, G.W.; Lattanzio-Battle, W.; Krogh, E.T.; Gill, C.G. "Condensed Phase Membrane Introduction Mass Spectrometry with In Situ Liquid Reagent Chemical Ionization in a Liquid Electron Ionization Source (CP-MIMS-LEI/CI)." *Journal of the American Society for Mass Spectrometry*, **2020**, *31*, 908-916. G.W. Vandergrift designed the experiments and analyzed the data. G.W. Vandergrift primarily collected the data, with contributions from W. Lattanzio-Battle. G.W. Vandergrift drafted the manuscript, with intellectual and editorial contributions from E.T. Krogh and C.G. Gill. This article was selected for the front cover of *Journal of the American Society for Mass Spectrometry*.

5.1 Introduction

The field of direct mass spectrometry (DMS) has grown rapidly because of its applicability for a wide range of sample types, ease of analysis, and potential for high sample throughput.[3-5] DMS typically eliminates extensive sample workup and chromatographic separations, which are often associated with conventional sample analyses. As a result, DMS strategies often tend to require less consumable products, fulfill many green chemistry principles, and may allow for portability, providing timely information to support real-time and in field decisions. DMS strategies do not need to replace conventional (*i.e.*, chromatographic) methods, but rather may be used in advance of or in combination with conventional techniques to provide rapid, initial sample information. However, DMS may only provide useful information if the sample introduction step does not compromise analytical performance (*i.e.*, sensitivity and selectivity), and the targeted analytes can be sufficiently resolved by selectivity at the sample introduction, ionization, and mass spectrometry level.

An example analyte class for which DMS methods have been applied is phthalates. Phthalates, widely used as plasticizers, are ubiquitous pollutants that contaminate air, foods, cosmetics, and waters, among other matrices.[106] Because phthalates are known endocrine disruptors and potential carcinogens, there is a need for sensitive, robust, and effective analysis techniques.[107-109] Conventional phthalate analysis typically consists of an extraction step (e.g., solid phase micro extraction, ultrasonic extraction, etc.) in advance of GC-MS, and there is also advancement toward hyphenated analytical techniques (e.g., SPE-LC-MS/MS).[110] However, as referred to earlier, these methods may be undesirable with respect to sample cleanup, time, cost, and waste. Several ambient ionization techniques coupled with mass spectrometry have alternatively been used for direct phthalate analysis. These include direct analysis in real time,[111-113] desorption electrospray ionization,[114] spray-inlet microwave plasma torch ionization,[115] and thermal desorption electrospray ionization[116] among others. While generally rapid, these ambient methods may be susceptible to ionization suppression and/or have inadequate sensitivity/selectivity. Furthermore, they may not be universally suitable for a wide range of sample types (*i.e.*, waters, soils, materials, etc.).

Many of the complications associated with DMS measurements of phthalates are inherently related to the nature of the ambient ionization mechanism based techniques used.[37-38, 40] To mitigate these disadvantages, a chemical ionization (CI) approach may be a viable alternative. CI strategies may allow for protonation and/or adduction formation in the gas phase as a result of increased reagent pressure at the ionization source, which generates increased analyte and reagent collisions/ reactions.[4] Positive ion CI with EI-based techniques (*i.e.*, GC-MS) has been demonstrated as an effective strategy to minimize molecular ion fragmentation resulting in improvements in analytical sensitivity/selectivity. For example, Bergh *et al.* used an isobutane reagent gas and tandem mass spectrometry for phthalates in the analyses of house dust samples.[117] Similarly, Jeilani *et al.* and Harvan *et al.* used a methane reagent for increased protonated molecular ion intensities.[118-119] While the aforementioned studies involved GC-MS, CI strategies can also be used in combination with DMS to improve selectivity. The need for improved selectivity is particularly true for phthalates, which exhibit common fragmentation patterns in EI; a dominant, characteristic ion at *m/z* 149 (protonated phthalic anhydride) occurs in most cases.

An alternative DMS strategy, condensed phase membrane introduction mass spectrometry liquid electron ionization with *in situ* liquid reagent chemical ionization (CP-MIMS-LEI/CI), is presented here. In CP-MIMS, a liquid (acceptor phase) is continuously flowed through the lumen of a hollow fiber membrane, typically PDMS. The membrane is mounted on a probe and directly immersed into a complex sample (donor phase). Neutral analytes that are free in solution are transported across the membrane under a concentration gradient, where membrane permeability is a function of both analyte partitioning into and analyte diffusivity through the membrane interface. Charged and particulate matrix components are rejected by the

membrane and consequently do not interfere with ionization or mass resolution.[8-10, 101] The liquid acceptor phase dissolves analytes that permeate the membrane, eliminating the volatility limitations associated with GC-MS applications. The analytes are then entrained to an EI interfaced mass spectrometer. Here, a nanoflow of liquid is directly infused into a heated transfer line, where it forms an aerosol assisted by vacuum and a coaxial helium flow. This is rapidly followed by heated desolvation, vaporization, and finally electron ionization, referred to as liquid electron ionization (LEI).[10, 72, 100] Variants of LEI, termed direct electron ionization (DEI), were published as early as 2002 by Cappiello *et al.*[120-122] These studies emphasized the technique's robustness, minimal matrix effects, and ability to produce library searchable EI mass spectra, while also noting that CI behavior (*i.e.*, protonation) may occur in an LEI type source, depending upon the solvent composition.[72] Other work in the literature with direct liquid ionization has been demonstrated by the Amirav group, who coupled LC to EI via supersonic molecular beams.[70, 123] As an alternative DMS strategy, Amirav *et al.* also developed the "Open Probe" analytical strategy, which allows for direct sampling by ambient sample vaporization and fast GC separation (~30 s) in advance of EI.[124-125]

We have previously presented CP-MIMS with LEI as a direct analysis strategy for polycyclic aromatic hydrocarbons (PAHs) from both aqueous and soil samples. For soil samples, this method obviated sample cleanup, resulting in remarkably high throughput (15 soil samples per hour) combined with sensitive detection (70 μg/kg detection limit for benzo[*a*]pyrene from soil).[10] We also have previously used MIMS for phthalate quantitation using enzyme-derivatized PDMS,[126] and for the study of phthalate-particulate interactions.[127] The study presented here demonstrates the use of CP-MIMS for phthalate analysis and extends the capabilities of the technique with respect to both selectivity and sensitivity. We present the use of acetonitrile and diethyl ether as a CP-MIMS acceptor phase and source of *in situ* liquid CI reagents, and demonstrate their applicability with the direct analysis of phthalates in house dust. CP-MIMS-LEI/CI uses the acceptor phase solvent system to improve analyte permeation through the sampling membrane[9] and simultaneously provide suitable CI reagent ions via gas phase autoprotonation reactions.

5.2 Experimental Section

5.2.1 Liquid Reagent and Sample Preparation

Bis(2-ethyl-hexyl) phthalate (DEHP; analytical standard), dibutyl phthalate (DBP; 99%), and diethyl phthalate (DEP; 99.5%) were obtained from Sigma-Aldrich (Oakville, ON, Canada). For eventual analyses by CP-MIMS-LEI/CI, samples were prepared volumetrically in 18.4 MΩ-cm deionized water (Facility Scale Reverse Osmosis/Ion Exchange Water Purification System, Applied Membranes Inc., Vista CA, USA), 2-propanol (ACS grade, VWR International), or acetonitrile (≥99.9%, VWR International). Acceptor phase/ CI reagent systems were prepared

volumetrically from mixtures of acetonitrile, acetonitrile-d_3 (99.8% atom % D, Sigma- Aldrich), diethyl ether (ACS grade, Fisher Chemical, Ottawa, ON, Canada), and diethyl ether-d_{10} (99 atom % D, Sigma- Aldrich) as further described in the Results and Discussion.

5.2.2 Condensed Phase Membrane Introduction Mass Spectrometry-Liquid Electron Ionization with *In Situ* Liquid Reagent Chemical Ionization (CP-MIMS-LEI/CI) System

The base CP-MIMS-LEI/CI system used has been described elsewhere.[10, 72, 100] Briefly, a triple quadrupole mass spectrometer (Agilent Technologies Inc. 7010B GC/MS/MS, Santa Clara, CA, USA) equipped with an open geometry, high- efficiency EI source (190 °C) was used for full scan (profile data: Q1, *m/z* 30−200, 0.1 amu step size, 150 ms scan time; centroid: Q1, *m/z* 145−400, 0.1 amu step size, 3000 ms scan time, 150 threshold) and tandem mass spectrometry (MS/MS, 350 ms dwell time per SRM) experiments. All experiments were conducted using 70 eV electron ionization. Analyte SRMs and relevant physicochemical properties are presented in Tables 5.1 and 5.5.1, respectively.

Table 5.1: Tandem mass spectrometry parameters for phthalates.

Phthalate	SRM Transition	Collision energy eV
Bis(2-ethylhexyl)	391 → 149	5
Dibutyl	279 → 149	5
Diethyl	223 → 149	5

The CP-MIMS immersion probe utilized 8 cm of PDMS hollow fiber membrane (0.30 mm i.d., 0.64 mm o.d.; Silastic brand, Dow Corning, Midland, MI) loosely coiled around the probe tip. Construction and further details of the probe have been previously described.[10, 100] The CP-MIMS probe was connected to a manually actuated six-port valve (Rheodyne Model 7010, Sigma-Aldrich), allowing analyte measurements to be made using steady-state signals or via a "stopped-flow" sampling method. Figure 5.5.1 gives a simplified flow path schematic for the system. "Steady-state" CP-MIMS measurements involve direct immersion of the probe into the sample, allowing sufficient time for the analyte signals to achieve their maximum, steady-state levels while continuously flowing liquid acceptor through the hollow fiber membrane lumen. Conversely, "stopped-flow" sampling involves halting the flow of acceptor phase solvent through the membrane while the CP-MIMS probe is immersed in a sample by actuating the six-port valve for a fixed period. This allows for the concentration of analyte to increase in a slug of acceptor phase within the membrane lumen. The valve is then actuated again after a fixed period of time, yielding a signal peak (visually similar to that of a chromatographic peak). For both steady-state and "stopped-flow" modes, the resulting data are collected as ion chronograms. Both steady-state and "stopped-flow" type CP-MIMS measurements have been previously reported.[6-8]

For individual measurements, the CP-MIMS immersion probe was directly immersed into magnetically stirred (900 rpm) liquid samples in 40 mL glass vials at ambient temperatures and pressures. Following each measurement, the CP-MIMS immersion probe was rinsed in 40 mL of magnetically stirred clean methanol to return signals to baseline levels in advance of the next sample measurement.

A syringe pump (Harvard Apparatus 11 Elite, Holliston, MA, USA; 10 mL gastight syringe, Hamilton Company, Reno, NV, USA) was used to deliver solvent at 50 μL/min through the membrane lumen. Postmembrane, the flow into the LEI/ CI interface was reduced to ~500 nL/min using a passive flow splitter (Figure 5.5.1). This flow rate was measured offline using a nano flow-meter (Sensirion SLG-0150, Staf̈a, ZH, Switzerland) and calibrated using the acceptor phase solvent systems used. Vacuum pressure measurements were used to monitor the stability of liquid flow into the MS source using an ion gauge (Hewlett-Packard 59864A ionization gauge and controller, Palo Alto, CA, U.S.A.) mounted on a custom- made flange attached to the source end of the MS manifold. Stable LEI/CI performance resulted in source region pressures of 1.2×10^{-4} Torr. The mass spectrometer was tuned on a daily basis using the instrument's internal FC-43 (Perfluorotributylamine) calibration standard, and the CP-MIMS-LEI/CI system exhibited stable analytical performance over weeks of daily use. Construction details of the ion gauge flange and additional details regarding flow splitting, signal stability, and monitoring have also been discussed elsewhere.[10]

5.2.3 House Dust Sample Preparation and Analysis

House dust samples were collected from three different residential homes (Nanaimo, BC, Canada) and mechanically sieved (150 μm) prior to measurements. For analysis, 0.5 g of house dust was suspended in 7 mL of 2-propanol in an 8 mL glass vial and ultrasonically extracted (Fisher Scientific FS140 ultrasonic bath, 135 W) for 5 min at ambient temperatures and pressures. Immediately following extraction, the CP-MIMS probe was directly immersed in the vial and analyzed via "stopped-flow" mode (5 min), with magnetic stirring. Previous work has demonstrated that, for polycyclic aromatic hydrocarbons, 2-propanol is an effective solvent for both analyte extraction and direct CP-MIMS-LEI analyses.[10]

For standard addition experiments, samples were measured as described above, then subsequently spiked with 6 mg/L DEHP from a 2-propanol standard, and reanalyzed. For direct calibration experiments, 2-propanol DEHP standards (0.5, 9, 25, 35 mg/L) were analyzed via "stopped-flow" mode. All house dust sample measurements were conducted in triplicate. Representative measurements for "stopped-flow" measurements of 9 mg/L DEHP from 2-propanol are given in Figure 5.5.2.

5.2.4 Data Analysis

Analyte signal risetimes were calculated as the time required for a steady-state signal to rise from 10% to 90% relative intensity ($t_{10-90\%}$). "Steady-state" data were smoothed with a 7-

point moving boxcar (Microsoft Excel), and signal intensity was evaluated using height. Error bars for steady-state data are representative of the standard deviation of a steady-state signal. "Stopped-flow" data were smoothed with a 15-point Savitzky-Golay function (MassHunter Qualitative Analysis Navigator, version B.08.00, Agilent Technologies Inc.), and signal intensity was evaluated as peak areas. Error bars for "stopped-flow" data are representative of the standard deviation of triplicate measurements. DEHP detection limits were calculated as 3 times the standard deviation of measurements for a 0.5 mg/L DEHP in 2-propanol sample divided by the calibration slope.[10]

5.3 Results and Discussion

5.3.1 Acetonitrile Reagent System

Figure 5.1 displays the full scan mass spectrum obtained for the direct infusion of acetonitrile at 500 nL/min into the LEI/CI source. While the molecular ion (*m/z* 41) is present, the dominant peak in the spectrum appears to be the protonated molecular ion at *m/z* 42. This is in stark contrast to the acetonitrile NIST library EI spectrum,[128] for which the molecular ion is the dominant peak and *m/z* 42 is largely absent. To confirm the origin of the protonation, acetonitrile-d_3 was analyzed in the same manner, producing the deuterated molecular ion at *m/z* 46 as the dominant peak (Figure 5.1). Therefore, an autoprotonation reaction is occurring within the LEI/CI source.[4] Moneti *et al.* previously observed and confirmed this effect for acetonitrile, although their studies were not conducted via continuous liquid infusion. Furthermore, they used a quadrupole ion trap mass spectrometer, with significantly longer reaction times[129] when compared to that occurring in the open geometry EI source presented here. The abundance of chemical ionization behavior is particularly noteworthy, given that a standard, open EI source has no restrictions to intentionally increase reagent gas partial pressure, as is typically done with "tight" CI source geometries.[4] Also shown in Figure 5.1 is the appearance of a chemical species at *m/z* 54 from acetonitrile, which is also confirmed to be the result of in-source reactions by the acetonitrile-d_3 infusion experiment. This species ($C_3H_4N^+$) has been noted by Moneti *et al.* and similarly confirmed to originate from acetonitrile. Its presence in this study is further evidence of the potential CI capabilities afforded by using an open geometry EI source with direct liquid introduction.

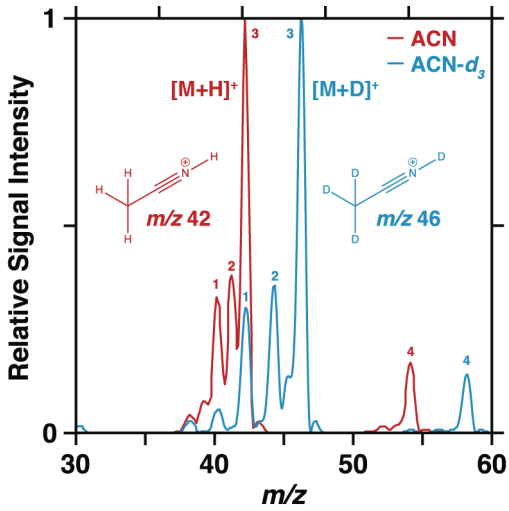

Figure 5.1: Full scan mass spectra of ACN and ACN-d_3 with LEI/CI-quadrupole mass spectrometry. List of major peaks with proposed molecular formulas (for non-deuterated species): (1) *m/z* 40 $[CH_2CN]^+$; (2) *m/z* 41 $[CH_3CN]^{\bullet+}$; (3) *m/z* 42 $[CH_3CN\text{-}H]^+$; (4) *m/z* 54 $[C_3H_4N]^+$. The deuterated species have analogous formulas.

The abundance of protonated acetonitrile molecular ions suggests they could be used as potential proton transfer CI reagent ions, provided that the proton affinity for acetonitrile is less than that of the analyte.[4] While proton affinity data for dialkyl phthalates are not readily available, the proton affinity of methyl benzoate (850.5 kJ/mol) is higher than that of acetonitrile (779 kJ/mol), suggesting acetonitrile could potentially be an effective dialkyl phthalate proton transfer reagent (Table 5.5.2). Furthermore, in combination with its potential use for CI, acetonitrile has previously been used as an acceptor phase with CP-MIMS style experiments.[99] Based upon these results, full scan mass spectra for the direct analyses of DEP, DBP, and DEHP by CP-MIMS-LEI/CI using acetonitrile as an acceptor phase were generated. The results are compared with NIST EI spectra[128] in Figure 5.2, and further described in Table 5.2. Representative full scan mass spectra from CP-MIMS-LEI/CI obtained for steady-state measurements are shown (Figure 5.2). The presence of protonated molecular ions ($[M+H]^+$) demonstrates that acetonitrile is functioning as a proton transfer reagent for dialkyl phthalates. This is in clear contrast to the NIST EI spectral data,[128] where the molecular ions are nearly absent because of extensive fragmentation. The CI behavior in the CP-MIMS-LEI/CI experiments is especially pronounced for DEP, where the peak for the loss of an alkoxy group from the protonated molecular ion (*m/z* 177)[118] is the base peak instead of the protonated phthalic anhydride ion (*m/z* 149). The data in Table 5.2 involve phthalate measurements conducted in three sample (donor) solvent systems, deionized water (6 mg/L each), 2-propanol (300 mg/L each), and acetonitrile (3000 mg/L each). Because of its low aqueous solubility,[30] DEHP was not analyzed in deionized water for these studies.

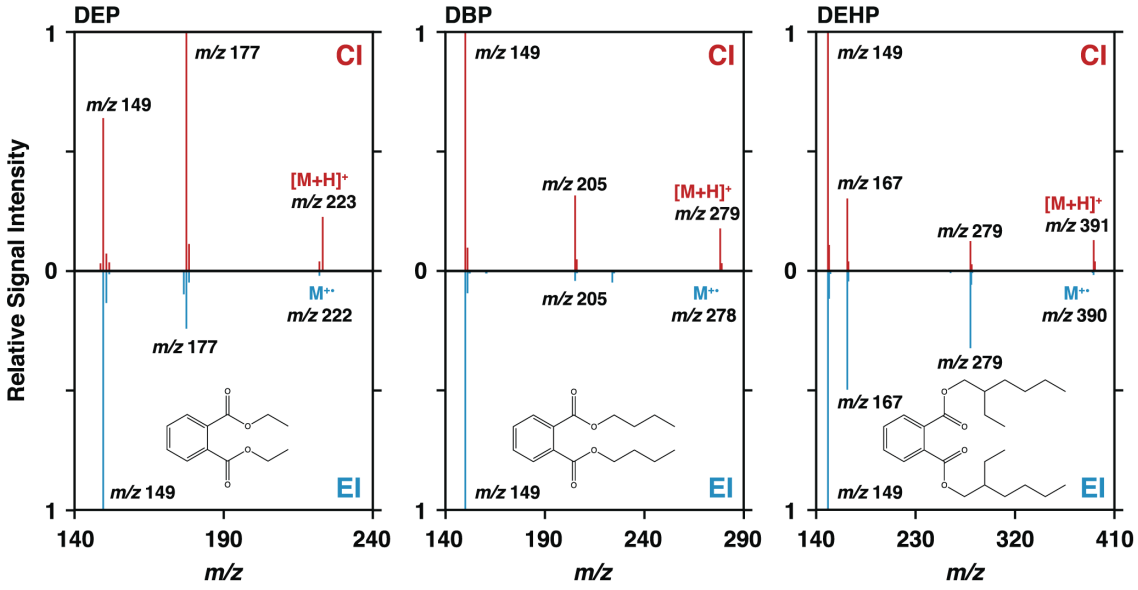

Figure 5.2: Comparison of full scan MS spectra for DEP, DBP, and DEHP from CP-MIMS-LEI/CI (ACN reagent) (CI, top three panels) to that of the NIST library (EI, lower three reflected panels). For the spectra shown here, DEP and DBP (6 mg/L each) were measured in deionized water, and DEHP (3000 mg/L) was measured in ACN.

Table 5.2: Full scan MS spectra major *m/z* ions for DEP, DBP, and DEHP from CP-MIMS-LEI/CI, comparing different sample (donor) solvents (ACN liquid CI reagent).

			Sample (Donor) Solvents		
Phthalate	*m/z*	Formulae	Acetonitrile[a]	2-Propanol[b]	De-ionized Water[c]
			Rel. Signal	Rel. Signal	Rel. Signal
DEP	149	$[C_8H_5O_3]^+$	0.657	0.650	0.640
	177	$[C_{10}H_9O_3]^+$	1	1	1
	223[d]	$[C_{12}H_{15}O_4]^+$	0.241	0.252	0.225
DBP	149	$[C_8H_5O_3]^+$	1	1	1
	205	$[C_{12}H_{13}O_3]^+$	0.302	0.299	0.317
	279[d]	$[C_{16}H_{23}O_4]^+$	0.179	0.199	0.179
DEHP	149	$[C_8H_5O_3]^+$	1	1	-
	167	$[C_8H_7O_4]^+$	0.305	0.337	-
	279	$[C_{16}H_{23}O_4]^+$	0.123	0.147	-
	391[d]	$[C_{24}H_{39}O_4]^+$	0.130	0.120	-

[a] 3000 mg/L sample concentration for each phthalate
[b] 300 mg/L sample concentration for each phthalate
[c] 6 mg/L sample concentration for each phthalate
[d] Protonated molecular ion ($[M+H]^+$)

Analysis of the data presented in Table 5.2 demonstrates that the CI behavior observed during CP-MIMS-LEI/CI measurements is essentially independent of the sample (donor) phase. For DEP, this is indicated by similar relative signal intensities for the protonated molecular ion across three different sample phases examined (5.7% relative standard deviation (RSD) for DEP $[M+H]^+$ signal intensities across acetonitrile, 2-propanol, and deionized water donor phases). DBP shows a similar result (6.2% RSD), as does DEHP (8.0% difference). Therefore, the differing membrane permeants from the sample solvent matrix do not appear to appreciably alter the observed CI behavior, suggesting minimal matrix effects for the tested solvent donor systems, and potentially broader applicability for a wider variety of sample types. Table 5.2 also illustrates that an isobaric interference exists between DBP and DEHP: both phthalates produce an ion at *m/z* 279 through either protonation (DBP) or fragmentation (DEHP). While this may seem to complicate the potential direct measurement of complex mixtures, it is important to note that all three phthalates analyzed here exhibit multiple, predictable ion signals. This would therefore allow phthalate quantitation using multiple tandem mass spectrometry transitions with predictable relative intensities. In support of this strategy, Mosi *et al.* successfully demonstrated data deconvolution strategies to differentiate polycyclic aromatic hydrocarbon isomer mixtures using difluoroethane as a reagent gas for CI.[78, 130] In summary, the use of acetonitrile as a CI reagent ion source with CP-MIMS-LEI/CI represents an improvement relative to EI with respect to selectivity (*i.e.*, presence of protonated molecular ions). Because the CP-MIMS acceptor phase composition can be easily modified, we tested the addition of other cosolvents (with CI potential) to determine whether further analytical improvements could be observed.

5.3.2 Acetonitrile and Diethyl Ether Reagent System Optimization

In earlier work, we observed that alkane cosolvents admixed in a methanolic CP-MIMS acceptor phase (coupled with electrospray ionization) resulted in improved membrane permeability for model compounds.[9] This was due to the alkane cosolvent solubility in PDMS membranes, resulting in greater analyte sensitivity and faster membrane transport (*i.e.*, reduced analyte risetimes).[9-10] Detailed discussions regarding membrane cosolvent permeability effects are available elsewhere.[9-10, 25, 28] Applying these principles, diethyl ether was selected as a cosolvent because of its solubility in both acetonitrile and PDMS.[28] Prior to determining an optimal acceptor phase composition, diethyl ether and diethyl ether-d_{10} were directly infused at 500 nL/min in separate experiments into the LEI/CI source, with the resulting full scan mass spectra given in Figure 5.3. Interestingly, the results are analogous to that observed for acetonitrile, again in stark contrast to the NIST Library EI spectrum; the dominant peak for diethyl ether is the protonated molecular ion (*m/z* 75), also confirmed by the diethyl ether-d_{10} experiment to be the result of autoprotonation.[4] This result was significant and suggested diethyl ether might also be used as a proton transfer reagent for phthalates, since the proton affinity for methyl benzoate (850.5 kJ/mol) is also greater than that of diethyl ether (828.4 kJ/mol).[128] Furthermore, the EI fragmentation of diethyl ether (Figure 5.5.3) in the LEI/CI source results in the serendipitous creation of additional potential proton transfer reagent ions, including

protonated acetaldehyde (768.5 kJ/mol, *m/z* 45) and formaldehyde (712.9 kJ/mol, *m/z* 31).[128] All of these ions have proton affinities lower than that of methyl benzoate.

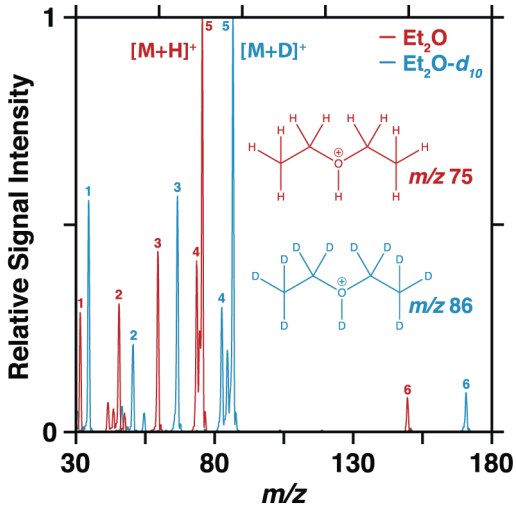

Figure 5.3: Full scan mass spectra of Et_2O and Et_2O-d_{10} with LEI/CI-quadrupole mass spectrometry. List of major peaks with proposed molecular formulas (for the nondeuterated species): (1) *m/z* 31 $[CH_2O\text{-}H]^+$; (2) *m/z* 45 $[C_2H_4O\text{-}H]^+$; (3) *m/z* 59 $[(CH_2)O(C_2H_5)]^+$; (4) *m/z* 73 $[(C_2H_5)O(C_2H_4)]^+$; (5) *m/z* 75 $[(C_2H_5)_2O\text{-}H]^+$; (6) *m/z* 149 $[((C_2H_5)_2O)_2\text{-}H]^+$. The deuterated species have analogous formulas.

To optimize acceptor phase composition, mixtures of diethyl ether (0−50% v/v) and acetonitrile were used as acceptor phase/reagent systems for the direct analysis of phthalates. For each acceptor phase system, DEP and DBP were measured in deionized water (at 125 µg/L each), and DEHP was measured in 2-propanol (100 mg/L). Tandem mass spectrometry was used to monitor the SRM from the protonated molecular ion to *m/z* 149 for each dialkyl phthalate (Table 5.1) via "steady-state" measurements. Figure 5.4 summarizes the results, depicting the signal-to-noise ratio (*i.e.*, sensitivity) on the left axis (solid lines) and signal rise time ($t_{10-90\%}$; minutes) on the right axis (dashed lines). Figure 5.4 illustrates that, for all phthalates examined, the sensitivity is maximized for a 70:30 ACN/Et_2O v/v acceptor phase system. One source of the sensitivity improvement is due to the solubility of diethyl ether in PDMS, which thereby improves the permeation of analyte through the membrane via the formation of a polymer inclusion membrane.[9-10, 25] However, it was noted that, with increasing diethyl ether composition, the signal noise also increased; this is likely due to rapid and more sporadic evaporation of the acceptor phase in the LEI/CI source, resulting from the lower boiling point of diethyl ether (34.6 °C) compared to that of acetonitrile (81.6 °C).[30] This contributes to the lower phthalate sensitivities above 30% v/v diethyl ether in the acceptor phase. A further benefit of the diethyl ether solubility in the PDMS is increased analyte diffusivity through the membrane, evidenced

by the reduction in the analyte signal risetimes. Based upon these results, an acceptor phase composition of 70:30 ACN/Et_2O v/v was chosen for its combination of improved sensitivity and concomitant improved membrane transport characteristics.

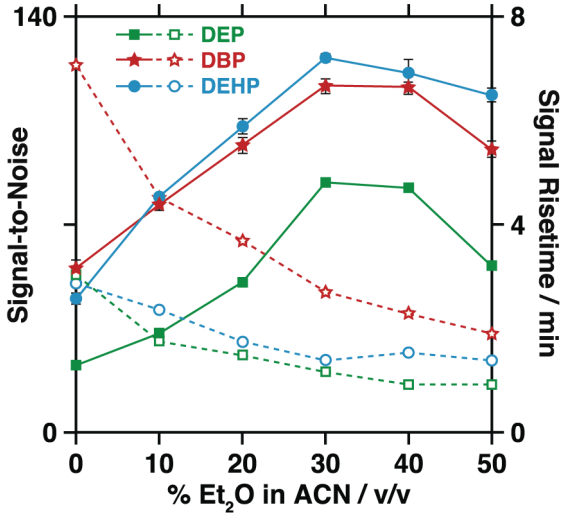

Figure 5.4: Optimization of an ACN and Et_2O (0−50% v/v) acceptor phase/reagent system for CP-MIMS-LEI/CI tandem mass spectrometry analyses of DEP (125 µg/L in deionized water), DBP (125 µg/L in deionized water), and DEHP (100 mg/L in 2-propanol; data scaled ×1/5) with respect to steady-state signal-to-noise (plotted on primary axis; solid lines with filled data symbols) and analyte rise time (plotted on secondary axis; dashed lines with open data symbols).

Aside from improving phthalate membrane permeability, the sensitivity improvement from diethyl ether cosolvent use may also be due to increased gas-phase phthalate protonation, facilitated by the presence of the additional reagent ions it produces (Figure 5.3). Figure 5.5.4 gives the full scan mass spectrum for the direct 500 nL/min infusion of the 70:30 ACN/Et_2O v/v reagent into the LEI/CI source, indicating the presence of multiple potential proton transfer CI reagents generated by both diethyl ether (*m/z* 31, 45, 75) and acetonitrile (*m/z* 42). To investigate the possibility of proton transfer from diethyl ether related reagent ions in addition to those from acetonitrile, deuterium-labeled reagents were used. Using CP-MIMS-LEI/CI, 6 mg/L DBP was sampled from deionized water using a variety of acceptor phase/reagent systems (Figure 5.5): 70:30 ACN/Et_2O v/v (panel a), 70:30 ACN-d_3/Et_2O v/v (panel b), 70:30 ACN/Et_2O-d_{10} v/v (panel c), and 70:30 ACN-d_3/Et_2O-d_{10} v/v (panel d). In panel (a), the relative intensity of the molecular ion (versus *m/z* 205) is increased by a factor of 1.5 when compared to that of DBP in Figure 5.2, which used only acetonitrile as the reagent. In panels (b) and (c), the presence of both deuterated and protonated phthalate molecular ions ([M+D]+ and [M+H]+, respectively) suggests that both acetonitrile and diethyl ether, after autoprotonation, are working simultaneously as proton transfer reagents. While we do not have explicit knowledge as to which

specific chemical species/fragment is the dominant proton donor, these studies do confirm that the phthalate protonation originates from the liquid acceptor phase/reagent. Panel (d) further confirms that sample matrix co-permeants do not appreciably affect CI behavior, indicated by the lack of protonated species, and the sole presence of a deuterated, molecular ion signal for DBP. The presence of *m/z* 223, which originates from a McLafferty rearrangement of the unprotonated phthalate molecular ion,[4] suggests that the resulting CI spectra generated from CP-MIMS-LEI/CI are a composite of both EI and CI behavior. The fragmentation/protonation origins for DBP ions are shown in Figure 5.5, which are consistent with the proposed fragmentation pathways for protonated phthalates by Jeilani *et al.*[118]

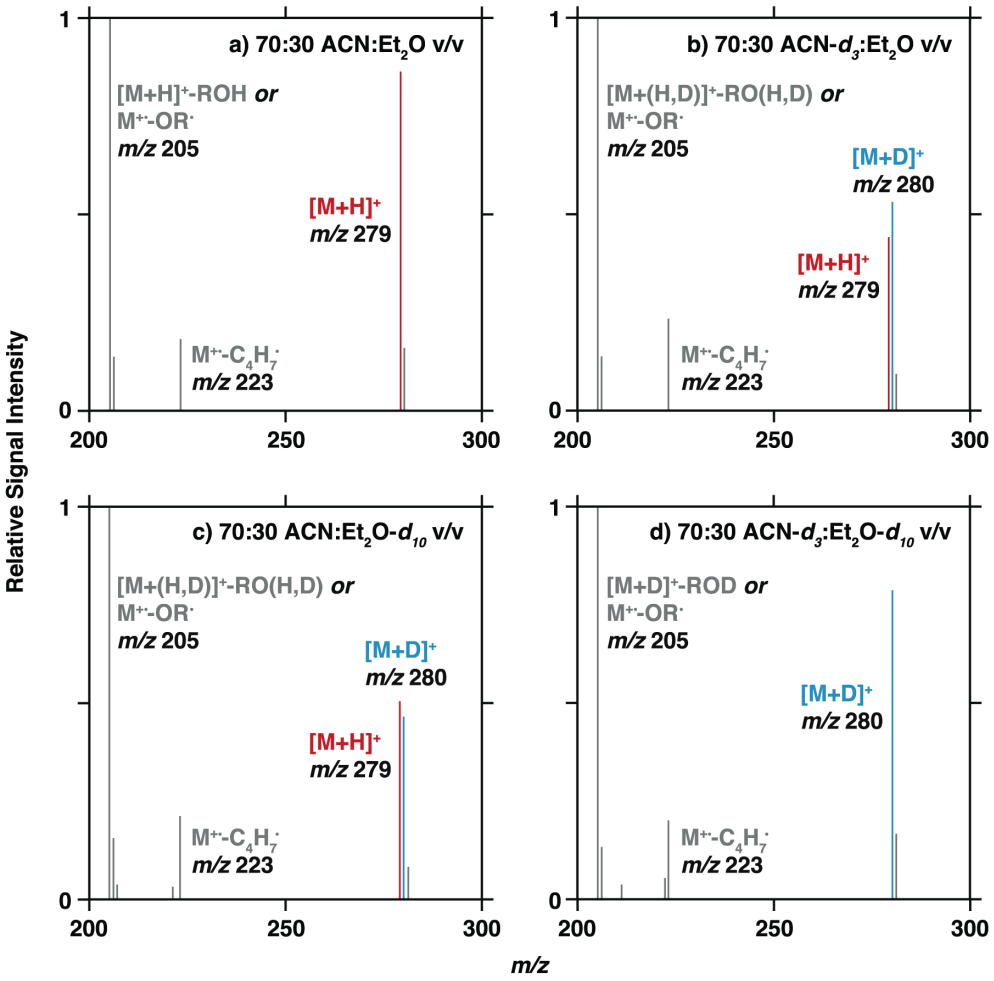

Figure 5.5: Full scan mass spectra of DBP (6 mg/L) sampled from deionized water with four different acceptor phase/reagent systems: (a) 70:30 ACN/Et_2O v/v; (b) 70:30 ACN-d_3/Et_2O v/v; (c) 70:30 ACN/Et_2O-d_{10} v/v; (d) 70:30 ACN-d_3/Et_2O-d_{10} v/v. Support for proposed fragmentation pathways may be found elsewhere.[4, 118]

5.3.3 House Dust Analysis

As a final demonstration, CP-MIMS-LEI/CI was used for the analysis of DEHP in house dust. DEHP was analyzed as a means to assess the performance of CP-MIMS-LEI/CI with a complex sample, and not to provide full characterization of all phthalates in house dust. DEHP was chosen as a representative analyte, as it is a commonly used phthalate plasticizer, and additionally is a potential carcinogen and known endocrine disruptor.[107, 109] As detailed in the Experimental Section, 0.5 g house dust samples was suspended in 2-propanol and sonicated for 5 min. The CP-MIMS probe was immediately and directly immersed in the stirred sample slurry and analyzed using stopped-flow mode. Extracted DEHP concentrations were determined in triplicate by both standard addition (6 mg/L DEHP spike) and direct calibration (Peak Area = 496 mg^{-1} L [DEHP] + 338, R^2 = 0.995; Figure 5.5.5). Both quantitation strategies demonstrate comparable results (Figure 5.6). The detection limit for DEHP in 2-propanol using this approach is 0.45 mg/L, as described in the Experimental Section. Assuming exhaustive extraction, we estimate a detection limit for DEHP in house dust of 6 mg/kg. This level of sensitivity is comparable to that achieved by Abb *et al.*, who reported a detection limit of 4.0 mg/kg DEHP from house dust using ultrasonic extraction followed by liquid chromatography electrospray tandem mass spectrometry.[106] While the short extraction time (5 min) used herein may not be exhaustive, the simple procedure presented is reproducible, obviates sample cleanup, bypasses chromatography, and suggests that CP-MIMS-LEI/CI may effectively be used for semi-quantitative and sensitive rapid-screening in advance of or in combination with conventional analyses. In addition, the sample throughout using the stopped flow CP-MIMS-LEI/CI technique described here is 10 min per sample (6 per hour).

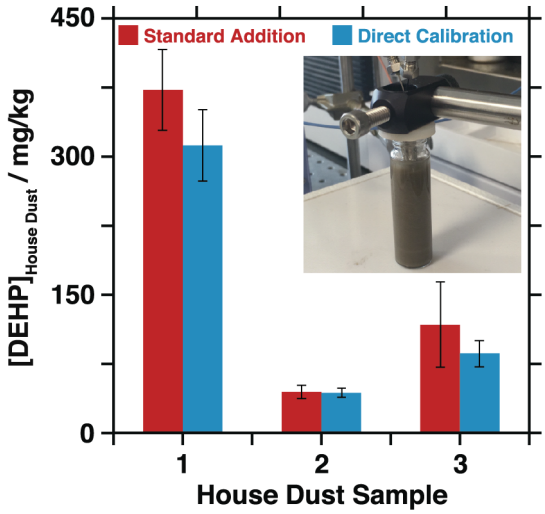

Figure 5.6: Analyses of DEHP from three different house dust samples, quantitated in triplicate by both standard addition and direct calibration methods. Inset picture was taken during the analysis of a representative house dust sample slurry.

5.4 Conclusions

The use of liquid-EI in CI mode with condensed phase membrane introduction mass spectrometry is a significant step forward for this direct mass spectrometry method. CI reagent ions formed from acetonitrile and diethyl ether were generated *in situ* with electron ionization directly from the liquid acceptor phase. These experiments were conducted using an open geometry, electron ionization source. Both acetonitrile and diethyl ether produced proton-donating reagent ion species that worked in concert to ionize dialkyl phthalates, and were not influenced by the sample (donor) matrices tested, suggesting applicability for a wide variety of sample types. While the use of CI does not allow for the NIST library identification facilitated by EI, the advantages of using mixed CP-MIMS-LEI/CI acceptor solvent systems are twofold, simultaneously improving both membrane transport and ionization selectivity. The method was demonstrated for the rapid and sensitive direct quantitation of phthalates from house dust (6 mg/kg detection limit for DEHP); the use of LEI/CI generated protonated phthalate molecular ions, enabling increased selectivity via tandem mass spectrometry experiments. In summary, CP-MIMS-LEI/CI represents a useful direct mass spectrometry strategy, as shown here through the determination of phthalates in house dust. Future developments will include further method validation and application of the technique to other analyte classes that exhibit a high degree of fragmentation with EI. CP-MIMS-LEI/CI may also be used for adaptive, high sample throughput phthalate screening of a variety of complex matrices, in combination with conventional analyses where appropriate, as well as extending the technique to other classes of CI amenable analytes.

5.5 Supporting Information

Table 5.5.1: Analyte physicochemical properties[30]

Phthalate	Molar mass g/mol	Water solubility mg/L	Vapor pressure mmHg
Bis(2-ethylhexyl)	390.57	0.27	0.000000142
Diethyl	222.24	1080	0.0021
Dibutyl	278.35	11.2	0.0000201

Table 5.5.2: Proton affinity data for that of the neutral molecule[131]

	Proton affinity kJ/mol
Acetonitrile	779.2
Acetaldehyde	768.5
Ethyl Ether	828.4
Formaldehyde	712.9
Methyl Benzoate	850.5

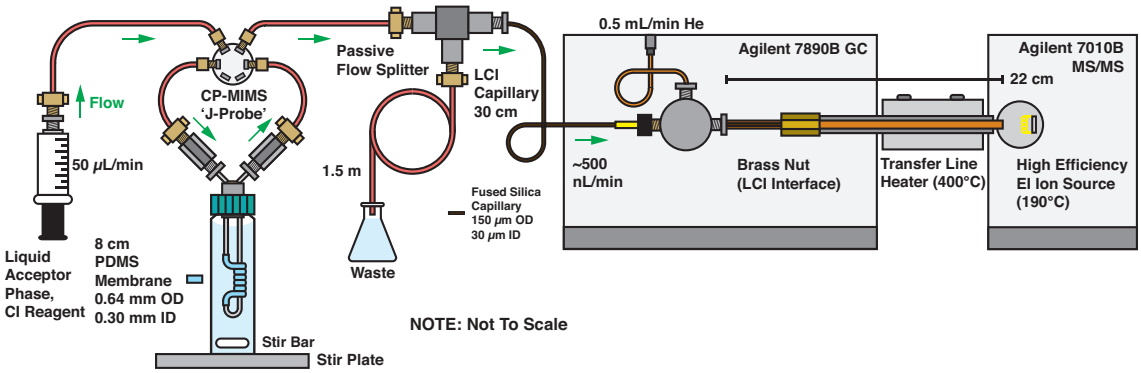

Figure 5.5.1: Experimental schematic for condensed phase membrane introduction mass spectrometry coupled to liquid electron ionization with *in situ* liquid reagent chemical ionization (CP-MIMS-LEI/CI).

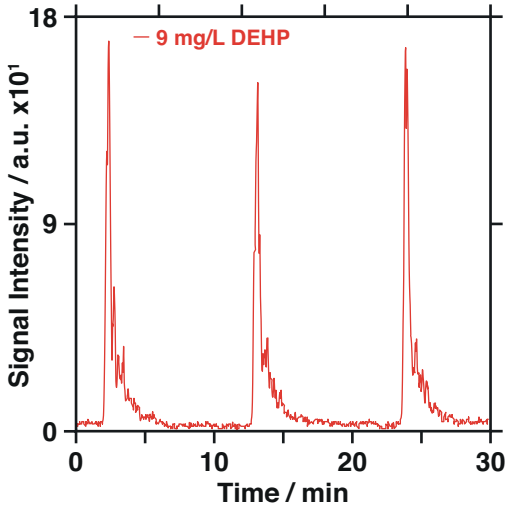

Figure 5.5.2: Triplicate measurements of 9 mg/L DEHP from 2-propanol by CP-MIMS-LEI/CI using 'stopped-flow' mode.

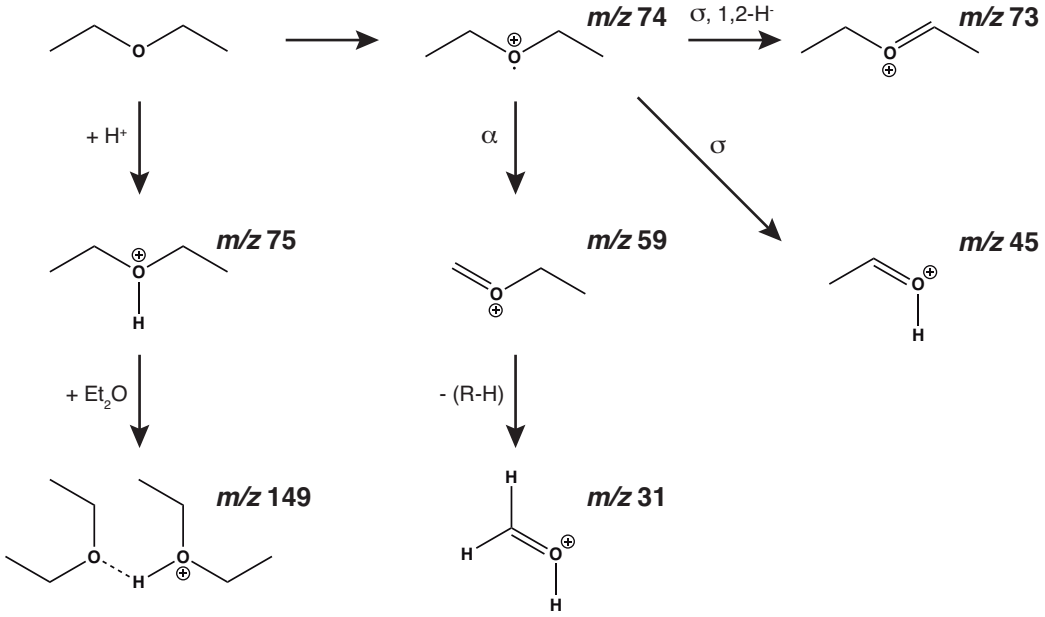

Figure 5.5.3: Fragmentation and chemical ionization of ethyl ether.

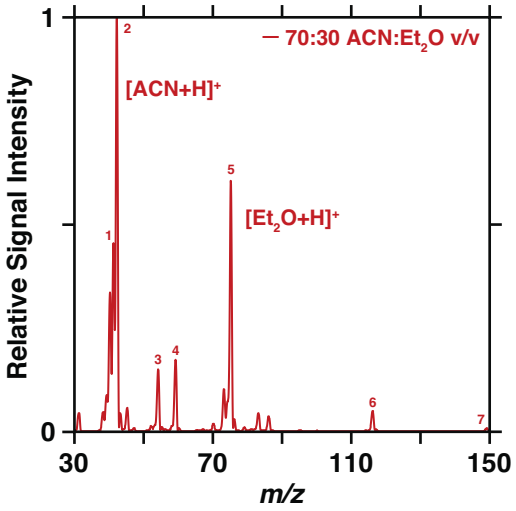

Figure 5.5.4: Full scan mass spectra of 70:30 acetonitrile:ethyl ether v/v with LEI/CI quadrupole mass spectrometry. List of major peaks with proposed molecular formulae: 1) *m/z* 41 $[CH_3CN]^{\bullet+}$; 2) *m/z* 42 $[CH_3CN\text{-}H]^+$; 3) *m/z* 54 $[C_3H_4N]^+$; 4) *m/z* 59 $[(CH_2)O(C_2H_5)]^+$; 5) *m/z* 75 $[(C_2H_5)_2O\text{-}H]^+$; 6) *m/z* 116 $[((C_2H_5)_2O)(CH_3CN)\text{-}H]^+$; 7) *m/z* 149 $[((C_2H_5)_2O)_2\text{-}H]^+$

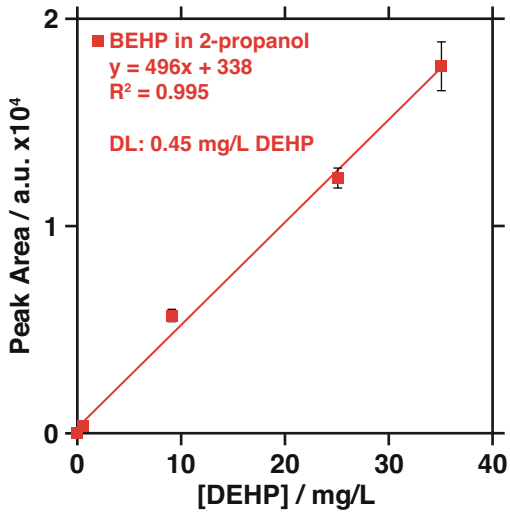

Figure 5.5.5: Bis(2-ethylhexyl) phthalate (DEHP) calibration in 2-propanol (0.5, 9, 25, 35 mg/L) using 5 minute 'stopped-flow' analyses. Error bars represent the standard deviations of triplicate measurements.

Chapter 6

Direct, Isomer-Specific Quantitation of Polycyclic Aromatic Hydrocarbons Using Membrane Introduction Mass Spectrometry and Chemical Ionization

Reproduced with minor changes and permission from Vandergrift, G.W.; Krogh, E.T.; Gill, C.G. "Direct, isomer-specific quantitation of polycyclic aromatic hydrocarbons in soils using membrane introduction mass spectrometry and chemical ionization." *Analytical Chemistry*, **2020**, In Press. G.W. Vandergrift designed the experiments, collected the data, and analyzed the data. G.W. Vandergrift drafted the manuscript, with intellectual and editorial contributions from all authors. This article was selected for the front cover of *Analytical Chemistry*.

6.1 Introduction

Polycyclic aromatic hydrocarbons (PAHs), a class of ubiquitous environmental contaminants, are carcinogenic, mutagenic and bioaccumulative.[132-133] PAHs are therefore regulated and routinely tested for in a variety of sample matrices. For PAHs in soils, GC-MS with initial sample extraction, cleanup, and concentration steps is frequently used.[134] While effective, GC-MS and the accompanying sample preparation methods may be disadvantageous with respect to cost and time. Direct mass spectrometry (DMS) methods, which involve the elimination of sample cleanup, preparation, and chromatographic steps, may therefore be advantageous in place of or in combination with conventional (*i.e.*, GC-MS) techniques because of their rapid and simple workflow, ease of use, "real-time" measurement capabilities, reduced consumable needs, and lower costs.

The challenge of directly measuring PAHs in soils should not be understated, and obtaining isomer specific, quantitative information is particularly difficult. Nonetheless, a variety of techniques have been used for DMS measurement of PAHs in soils, including laser desorption,[135-136] aerosol-MS,[137] membrane introduction MS,[68] and atmospheric pressure chemical ionization (APCI).[138] Despite any advantages afforded by DMS approaches, the absence of chromatography generally eliminates PAH structural isomer resolution. Because

some PAH isomers are significantly more toxic than others, there is a need for quantitation of individual PAH isomers, which is a common shortcoming of DMS. Castellanos *et al.* have demonstrated isomer-specific PAH measurements using ion mobility in advance of mass spectrometry, but did not use DMS or present quantitative information.[139]

Some isomer resolution strategies for PAH isomers have been developed to complement chromatographic separations using chemical ionization (CI). Generally, these studies demonstrated that PAHs and select reagents either form distinct adduct species, or form similar adduct species with differing relative intensities. Such studies have used methane,[140-141] silver cations,[142] dimethyl ether,[143] and halocarbon chemistry,[78, 130, 144] where the resolution provided by CI occurs in real time. This is very important in the context of DMS, as the chromatographic step is eliminated. In support of pairing CI-based resolution with DMS, Eftekhari *et al.* used silver ion-PAH chemistry in combination with desorption electrospray ionization (DESI) for isomer-specific PAH measurements from a paper surface.[145] While not applied to soil measurements, this strategy helps demonstrate the potential of such an analytical pairing for soil samples. However, ambient-based techniques (such as DESI) may still not be ideal for quantitative measurement of complex environmental samples because of potentially confounding matrix effects.[146-147]

A technique that may address the aforementioned challenges for direct measurement of PAHs in soils is condensed phase membrane introduction mass spectrometry with liquid electron ionization/chemical ionization (CP-MIMS-LEI/CI).[12] In CP-MIMS, a hollow-fiber polydimethylsiloxane membrane is mounted on a probe, and directly immersed into a sample to make measurements. Solution phase hydrophobic analytes permeate the PDMS membrane, while charged and particulate matrix components are rejected and remain in the sample. Permeants are then dissolved in a flowing solvent acceptor phase within the membrane lumen and subsequently transported to a LEI ion source.[7, 9, 17, 37, 73] For LEI, a technique pioneered by the Cappiello group, a liquid nanoflow is directly infused into the entrance of a mass spectrometer transfer line. Assisted by a coaxial flow of helium, the liquid nanoflow is sequentially nebulized and vaporized within a silica capillary inside the heated transfer line, and finally ionized in an electron ionization source.[72, 100, 122] The use of LEI mitigates the significant matrix effects that are commonly observed in ambient ionization techniques,[71] and furthermore may allow for NIST library matching of mixture components. The coupling of CP-MIMS-LEI has previously been demonstrated for the direct, quantitative measurement of PAH isomer classes in soils.[10] We have subsequently demonstrated that the acceptor phase solvent, present at the ion source can be used to provide chemical ionization reagent species in the direct analysis of dialkyl phthalates (*i.e.*, CP-MIMS-LEI/CI).[12] Here we present CP-MIMS-LEI/CI as a DMS technique for PAHs in soils, using *in situ* CI (with a CI source) to directly resolve PAH isomers.

6.2 Experimental Section

6.2.1 Standards and Solvents

See the Supporting Information, Section 6.5, for source, purity and physicochemical properties of selected PAHs studied. Abbreviations used in this manuscript for inclusion in tables and figures are as follows: anthracene (Ant), benz[*a*]anthracene (BaAnt), benzo[*a*]pyrene (BaPyr), benzo[*b*]fluoranthene (BbFl), chrysene (Chr), fluoranthene (Fl), naphthalene (N), perylene (Per), phenanthrene (P) and pyrene (Pyr).

6.2.2 Condensed Phase Membrane Introduction Mass Spectrometry – Liquid Electron Ionization with *In Situ* Chemical Ionization

Variations of the CP-MIMS-LEI/CI system have been previously described.[10, 12] Briefly, a triple quadrupole mass spectrometer (Agilent Technologies Inc. 7010B GC-MS/MS, Santa Clara, CA, USA) with a high efficiency, axial chemical ionization source assembly (Agilent Technologies Inc., part number G7250-65404, 200 °C) was used in both full scan (profile data; Q1: *m/z* 125−385 for naphthalene, *m/z* 150-400 for all other PAHs; 0.1 amu step size; 1000 ms scan time) and tandem mass spectrometry (MS/MS, 200 ms dwell time per transition) modes. MS/MS parameters and physicochemical properties for PAHs are shown in Table 6.1 and Table 6.5.1, respectively. Development of the MS/MS transitions is discussed in detail in the Results and Discussion section. The mass spectrometer was tuned in EI mode using the high efficiency EI source and an internal FC-43 (perfluorotributylamine) calibration standard. After tuning, the CI source was substituted without additional changes. The software (MassHunter, version B.07.06) was operated in EI mode (*i.e.*, as if an EI source was inserted). The CI source was equipped with an on-axis, coiled filament (Agilent Technologies Inc., part number G3859-60021, extractor plate removed). All experiments were conducted with 70 eV ionization energy and 50 μA filament emission current. An experimental schematic is shown in Figure 6.1.

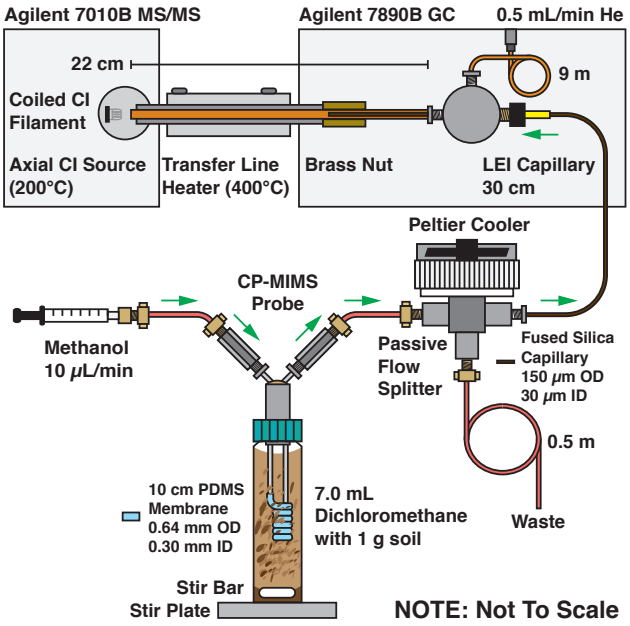

Figure 6.1: Instrumental schematic for CP-MIMS-LEI/CI.

Table 6.1: Tandem mass spectrometry parameters.

PAH Class amu	PAH	MS/MS Transition *m/z*
128	Naphthalene	175 → 139 (40)
178	Anthracene	223 → 191 (5)
	Phenanthrene	225 → 189 (40)
202	Fluoranthene	249 → 213 (40)
	Pyrene	247 → 215 (5)
228	Benz[*a*]anthracene	273 → 241 (5)
	Chrysene	275 → 239 (40)
252	Benzo[*a*]pyrene	297 → 265 (5)
	Benzo[*b*]fluoranthene	299 → 263 (40)

Collisions energies in eV are given in brackets.

A CP-MIMS direct immersion probe was constructed by mounting 10 cm of PDMS hollow fiber membrane (0.30 mm i.d., 0.64 mm o.d.; Silastic brand, Dow Corning, Midland, MI) on stainless steel hypodermic tubing (0.33 mm i.d.; 0.64 mm o.d.). To minimize the membrane lumen volume (allowing decreased acceptor phase flow rates and increased membrane robustness), coaxially inserted stainless steel wire (0.20 mm o.d.) was used. The use of reduced acceptor flow rates resulted in less dilution of membrane permeants over that used in earlier works,[10, 12] further enhancing sensitivity. Additional details regarding similar CP-MIMS probe construction are available elsewhere.[7] A syringe pump (Harvard Apparatus Pump 11 Elite,

Holliston, MA, USA) and a 1 mL gastight syringe (Hamilton Company, Reno, NV, USA) were used to continuously flow methanol acceptor phase through the membrane lumen at 10 µL/min. Post-membrane, a zero dead volume stainless steel tee junction splitter was used to reduce the flowrate to ~200 nL/min (measured using a Sensirion flow meter, model SLG-0150; Stäfa, ZH, Switzerland) before transferring to the LEI/CI source. The flow splitter was Peltier cooled (CUI Devices, Lake Oswego, OR, USA, model CP85438) to prevent premature acceptor phase vaporization prior to the LEI/CI source (Figure 6.5.1). A source pressure of 1.5×10^{-4} Torr, measured by a custom source-end pressure gauge, was used to verify stable LEI/CI performance.[12]

For analyses of PAHs in dichloromethane and chloroform standards, the CP-MIMS probe was directly immersed into 8 mL vials containing 7.0 mL of standard. For soil sample analyses, soil (1 g) and dichloromethane (7 mL) were placed into an 8 mL glass vial and sonicated for 3 min (FS140 ultrasonic bath, Fisher Scientific, 135 W). Immediately after sonication, the CP-MIMS probe was immersed into the solvent/soil slurry. Unless otherwise stated, the probe was immersed into the soil sample for 2 min, such that signals reached "steady-state". Following all measurements, the probe was immersed in clean dichloromethane for 2 min to clean the membrane, allowing signals to return to baseline levels in advance of the next sample. All measurements used magnetic stirring (900 rpm), and were conducted at ambient temperatures and pressures. An image depicting a representative soil sample analysis and an enlarged view of the CP-MIMS probe/membrane are shown in Figure 6.2.

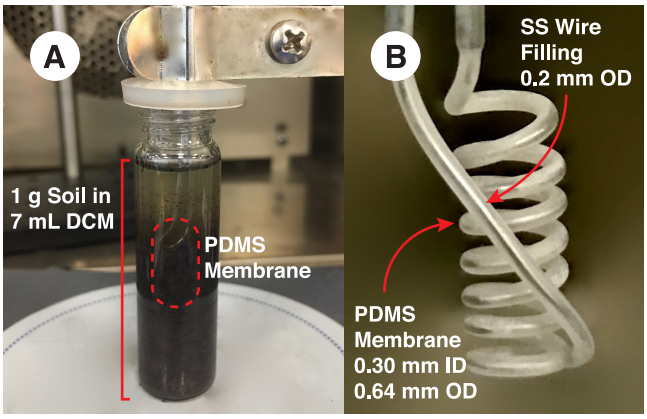

Figure 6.2: (A) Image of direct soil analysis using a CP-MIMS probe by the described methodology. (B) Enlarged image of the CP-MIMS direct immersion probe/membrane.

Both dichloromethane and chloroform readily permeate PDMS membranes because of their solubility characteristics. Consequently, in the presented measurements, the eventual acceptor phase flow introduced to the LEI/CI source is composed of methanol, sample solvent (dichloromethane or chloroform), and hydrophobic analytes (Figure 6.5.2). For the described conditions, the final volumetric compositions of the solvents infused into the LEI/CI were 77:23

dichloromethane:methanol v/v for the analyses of dichloromethane standards, and 87:13 chloroform:methanol v/v for the analyses of chloroform standards. Acceptor phase compositions were determined by gravimetric analysis of acceptor phase aliquots that were collected post-membrane (Table 6.5.2).

6.2.3 Data Analysis

Sample signals were background-subtracted using the signal from a clean, blank standard. Signals from tandem mass spectrometry experiments were smoothed using a 10-point moving boxcar function (Microsoft Excel, Redmond, WA, USA). Signal intensities were evaluated as heights. PAH signal risetimes were calculated as the time required for a "steady-state" signal to rise from 10 to 90% relative intensity ($t_{10\text{-}90\%}$), where the presented uncertainty is the standard deviation of triplicate measurements (measured for 0.5 mg/L standards of individual PAHs in dichloromethane). PAH detection limits were calculated as 3 times the standard deviation of a "steady-state" signal for 0.75 mg/L PAH in a dichloromethane standard divided by the calibration curve slope. The resulting detection limit in dichloromethane was converted to a detection limit for soil samples (1 gram soil in 7 mL dichloromethane).

6.3 Results and Discussion

6.3.1 *In Situ* Chemical Ionization of Polycyclic Aromatic Hydrocarbons

Figure 6.3 overlays the full scan mass spectra obtained for the CP-MIMS-LEI/CI direct measurement of anthracene and phenanthrene (measured separately) from dichloromethane standards (150 mg/L each), illustrating multiple adduct ions present for each PAH. Similar to results obtained by Mosi *et al*., where dichloromethane was used as a CI reagent in a quadrupole ion trap for GC-MS analyses of PAHs, we observe significant differences in the relative intensities of mass spectral peaks.[78] In a quadrupole ion trap, both selection of a desired CI reagent species and its subsequent CI reaction time can be optimized. However, in tight CI sources such as the one used here, the reagent species generated are controlled in part by source pressure and CI reagents added, with significantly shorter CI reaction times (e.g. μsec vs. msec) that cannot be easily optimized.[4] Given this, the CI behaviour in this study is particularly noteworthy, as it arises in a tight CI source equipped triple quadrupole mass spectrometer rather than in a quadrupole ion trap. As illustrated in Figure 6.3, the appearance of a diagnostic M+45 CI adduct peak for anthracene is completely absent in the mass spectra for phenanthrene, and conversely, phenanthrene exhibits a diagnostic adduct peak at M+47, which is completely absent for anthracene. Mosi *et. al* reported similar adducts, but did not observe a chemical species at M+45. Overall, the CI behaviour demonstrated here in Figure 6.3 is isomer-specific for the two PAH isomers in the $C_{14}H_{10}$ class.

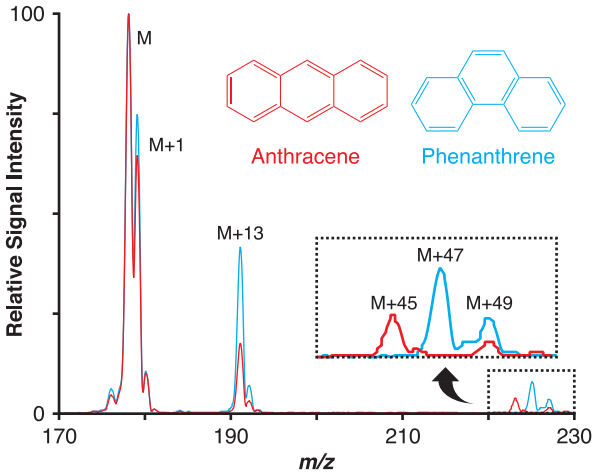

Figure 6.3: Full scan mass spectra from the individual, direct measurements of anthracene and phenanthrene (150 mg/L each in dichloromethane) by CP-MIMS-LEI/CI. Signal intensities in each spectrum are normalized for 100% $M^{+\bullet}$ abundance.

The liquid infused into the LEI/CI source is a mixture of methanol, dichloromethane, and the entrained PAH analytes. It appears that the methanol and/or dichloromethane are producing CI reagent ions in the source, evidenced by the observed adduct species (Figure 6.3). A comprehensive series of deuterium labeling studies were used to ascertain the origins of the reagent ions and ionization reactions responsible for the observed anthracene and phenanthrene CI adduct ions, notably for the diagnostic adduct ions present at M+45 (anthracene) and M+47 (phenanthrene). Full scan and tandem mass spectrometry experiments were conducted as summarized in Table 6.5.3.

It is well established that when using 70 eV electron ionization, dichloromethane forms CH_2Cl^+ and $CHCl_2^+$ reagent ions.[78] For the diagnostic M+47 adduct ion from phenanthrene, labeling studies suggest a $CHCl_2^+$ addition (generated from dichloromethane) and subsequent HCl elimination (*i.e.*, M+47 = $[M+CHCl_2\text{-}HCl]^+$), where the eliminated proton originates from phenanthrene (consistent with that proposed by Mosi *et al*).[78] For the novel, diagnostic M+45 adduct ion produced by anthracene, labeling studies suggest an addition of CH_2Cl^+ (generated from dichloromethane) and reaction with neutral methanol (Table 6.5.3). HCl is similarly eliminated, with the exception that the hydrogen eliminated originates from the exchangeable methanolic proton (*i.e.*, M+45 = $[M+CH_2Cl+CH_3OH\text{-}HCl]^+$), suggesting a subsequent or simultaneous nucleophilic attack from methanol prior to the HCl elimination. To the best of our knowledge, an adduct ion of this nature (M+45) for PAHs has not been previously reported.

Chloroform was used instead of dichloromethane as the sample phase to evaluate adduct ion formations in the absence of CH_2Cl^+ reagent ions. The M+45 adduct ion was not observed for these experiments as shown in Figure 6.5.3, which is consistent with the proposed ionization

reactions. Furthermore, for unlabeled anthracene, the use of dichloromethane-d_2 and methanol result in an M+47 adduct ion (*i.e.*, M+47 = $[M+CD_2Cl^+ + CH_3OH\text{-}HCl]^+$), dichloromethane and methanol-d_4 result in an M+48 adduct ion (*i.e.*, M+48 = $[M+CH_2Cl^+ + CD_3OD\text{-}DCl]^+$), and dichloromethane and methanol-d_1 (CH_3OD) result in an M+45 adduct ion (*i.e.*, M+45 = $[M+CH_2Cl^+ + CH_3OD\text{-}DCl]^+$). A loss of methanol from the M+45 adduct ion was confirmed for tandem mass spectrometry experiments, where the exchangeable proton on methanol originates from anthracene. In further support of the proposed reaction, an M+45 adduct ion is formed when anthracene-d_{10}, dichloromethane and methanol are used (*i.e.*, M+45 = $[M+CH_2Cl^+ + CH_3OH\text{-}HCl]^+$), while a loss of 33 occurs in tandem mass spectrometry (*i.e.*, loss of CH_3OD).

Table 6.2: Full scan mass spectra from the individual, direct measurements of PAHs (150 mg/L each in dichloromethane) by CP-MIMS-LEI/CI.

PAH	M $M^{+\bullet}$	M+1 $[M+H]^+$	M+13 $[M+CH_2Cl\text{-}HCl]^+$	M+45 $[M+CH_2Cl\text{-}HCl\text{-}CH_3OH]^+$	M+47 $[M+CHCl_2\text{-}HCl]^+$	M+49 $[M+CH_2Cl]^+$	M+83 $[M+CHCl_2]^+$
N	128	129 (77)	141 (44)	173 (0)	175 (16)	177 (5)	211 (0)
Ant	178	179 (65)	191 (17)	223 (4)	225 (0)	227 (1)	261 (0)
P	178	179 (75)	191 (42)	223 (0)	225 (7)	227 (3)	261 (1)
Fl	202	203 (79)	215 (44)	247 (0)	249 (8)	251 (4)	285 (2)
Pyr	202	203 (68)	215 (24)	247 (3)	249 (0)	251 (2)	285 (0)
BaAnt	228	229 (70)	241 (18)	273 (5)	275 (0)	277 (2)	311 (0)
Chr	228	229 (76)	241 (29)	273 (0)	275 (2)	277 (2)	311 (0)
BaPyr	252	253 (66)	265 (7)	297 (11)	299 (0)	301 (1)	335 (0)
BbFl	252	253 (64)	265 (26)	297 (0)	299 (3)	301 (3)	335 (2)
Per	252	253 (66)	265 (5)	297 (12)	299 (0)	301 (1)	335 (0)

Signal intensities scaled relative to that of the nominal mass ($M^{+\bullet}$ abundance assigned as 100%) are shown in brackets.

To determine if comparable CI behaviour was observed for other PAHs, full scan mass spectral data was collected for 10 different individual PAHs as summarized in Table 6.2 using a methanol acceptor phase and dichloromethane sample phase. Similar non-diagnostic (M, M+1, M+13, M+49, and M+83) and diagnostic (M+45 or M+47) peaks were observed for all PAHs studied, where the compositions of M+1 ($[M+H]^+$), M+13 ($[M+CH_2Cl\text{-}HCl]^+$), M+49 ($[M+CH_2Cl]^+$), and M+83 ($[M+CHCl_2]^+$) adduct ions were similarly inferred via deuterium labeling studies (Table 6.5.4). These results strongly suggest the potential for PAH-specific quantitation of whole samples without prior chromatographic separation.

To further investigate the proposed ionization schemes, the full scan signal intensities for M+13, M+45 and M+47 adduct ions scaled relative to the $M^{+\bullet}$ peak signal intensities (Table 6.2) were plotted against experimentally determined PAH first ionization energies (IEs)[128, 148] as shown in Figure 6.4. Both the M+13 ($[M+CH_2Cl\text{-}HCl]^+$) and M+47 ($[M+CHCl_2\text{-}HCl]^+$) adduct ions are linearly correlated with the IE of the PAH, with M+13 adduct ions appearing for PAHs with IEs > 6.9 eV, and M+47 adduct ions appearing for PAHs with IEs > 7.5 eV. For PAHs with

lower IEs, charge exchange with CH_2Cl^+ or $CHCl_2^+$ reagent ions may be more favourable than adduct ion formation. Therefore, increased adduct ion formation may occur as charge exchange becomes less favourable (*i.e.*, as the IE of the PAH increases), which is consistent with the data shown in Figure 6.4. The appearance of M+47 adduct ions ($[M+CHCl_2\text{-}HCl]^+$) at IE values that are ~0.6 eV greater than the IEs of PAHs forming M+13 adduct ions ($[M+CH_2Cl\text{-}HCl]^+$) as shown in Figure 6.4 is also consistent with the difference in recombination energies for CH_2Cl^+ and $CHCl_2^+$ reagent ions (8.6 eV and 8.1 eV respectively, ~0.5 eV difference)[78]. The relative intensity of M+45 adduct ions ($[M+CH_2Cl+CH_3OH\text{-}HCl]^+$) are inversely correlated with IE for PAHs with IE values of < 7.6 eV, at which point this adduct ion is no longer observed. This trend may be explained in part by examining the initial electrophilic addition of CH_2Cl^+ to a PAH, which results in a M+49 ($[M+CH_2Cl]^+$) adduct ion. For PAHs with higher IEs (*i.e.*, less favourable formation of a positively charged species), the M+49 adduct ion may be increasingly unstable and importantly short-lived for the given experimental conditions. Therefore, the nucleophilic attack by methanol (eventually resulting in an M+45 adduct ion) illustrated in Figure 6.4 may provide a kinetic rationale for the decreasing abundance of the M+45 adduct ion with increasing PAH IEs.

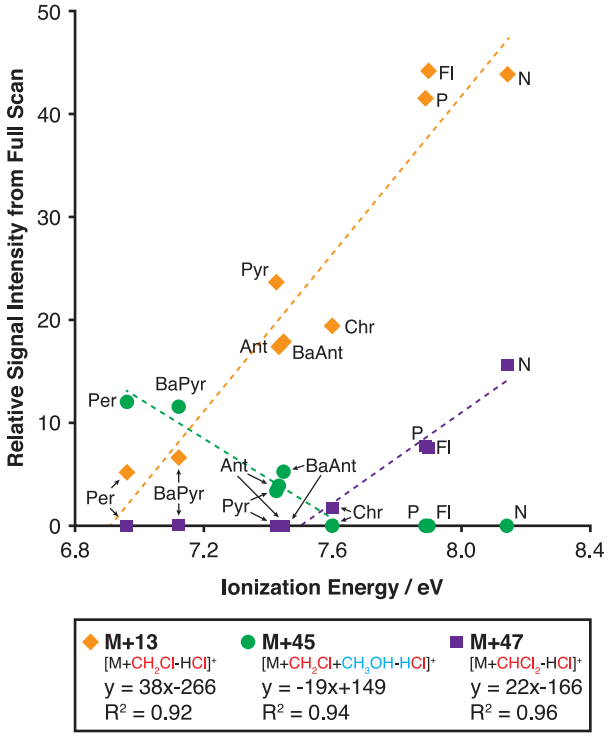

Figure 6.4: Correlations of PAH first ionization potentials with relative signal intensities (scaled relative to $M^{+\bullet}$ signal intensity) from full scan mass spectra for M+13 ($[M+CH_2Cl\text{-}HCl]^+$), M+45 ($[M+CH_2Cl+CH_3OH\text{-}HCl]^+$) and M+47 ($[M+CHCl_2\text{-}HCl]^+$) adduct formation.

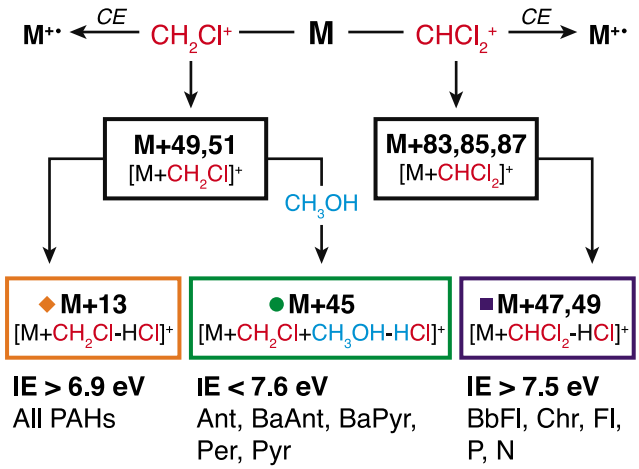

Figure 6.5: Proposed ionization schemes for PAHs (represented as "M") in the presence of dichloromethane (CH_2Cl^+, $CHCl_2^+$ ions) and methanol (CH_3OH) reagents for the described CP-MIMS-LEI/CI conditions.

Figure 6.5 presents a summary of the proposed CI behaviour for PAHs in the presence of methanol and dichloromethane reagents for the given experimental conditions (CP-MIMS-LEI/CI). Importantly, no PAH studied here simultaneously forms both M+45 and M+47 adduct ions (Table 6.2 and Figure 6.4). While we cannot ignore the possibility of alternative reaction schemes, those presented here are consistent with our experimental data. We are confident in the chemical composition of the discussed adduct ion species based upon our isotopic labeling studies. This work successfully lays the foundation for future studies regarding the dependence of novel CI behaviour upon intrinsic physical properties. A detailed description of the mechanistic pathways of adduct formation is not presented in this manuscript, but we feel that a more comprehensive delineation of the CI mechanisms is warranted for future studies, and will be well informed by computational methods. In summary, the ion-molecule chemistry discussed here provides the basis for the direct, isomer-specific measurement of PAHs in soils using tandem mass spectrometry.

6.3.2 MS/MS Method Development for Direct Measurement of PAHs in Soils

Isomer-specific MS/MS transitions based upon the diagnostic adduct ions formed at M+45 and M+47 were developed for each PAH analyzed in this study (Table 6.1). This result is significant for DMS applications as discussed earlier, and may provide the necessary resolution that is otherwise limited for DMS techniques. Naphthalene (M+47), anthracene (M+45), phenanthrene (M+47), fluoranthene (M+47), pyrene (M+45), benz[*a*]anthracene (M+45), and chrysene (M+47) may all be individually quantified by CP-MIMS-LEI/CI using MS/MS transitions that are specific to one of the aforementioned PAHs. The $C_{20}H_{12}$ PAH isomer class (*m/z* 252) presents a more complex MS/MS quantitation challenge because of the increased number of relevant members. For the purposes of this study, the bulk $C_{20}H_{12}$ isomer class is

assumed to be represented by benzo[*a*]pyrene, benzo[*e*]pyrene, benzo[*b*]fluoranthene, benzo[*k*]fluoranthene and perylene. Benzo[*b*]fluoranthene may be individually quantified, as it is the only PAH from the previous list which forms, or that would be expected to form, a M+47 adduct based upon the experimental data trends established in Figure 4 and available ionization potential data from Table 6.5.1 (IE > 7.5). Conversely, benzo[*a*]pyrene (IE = 7.12), benzo[*e*]pyrene (IE = 7.41 eV), benzo[*k*]fluoranthene (IE = 7.47 eV), and perylene (IE = 6.96 eV), all have IEs < 7.6 eV. These four PAHs therefore form or would be expected to form M+45 adducts as similarly inferred from Figure 6.4 and Table 6.5.1. As a result, the remaining four PAHs in the $C_{20}H_{12}$ PAH isomer class (*m/z* 252) are subsequently aggregated and referred to here as $BaPyr_{max}$ (*i.e.*, reported as an equivalent amount of benzo[*a*]pyrene). Given the toxicity and regulatory importance of this PAH, this approach will provide an upper bound in its concentration. Figure 6.4 suggests that benzo[*e*]pyrene and benzo[*k*]fluoranthene are expected to be minimal contributors to this adduct ion signal compared to benzo[*a*]pyrene because of their higher ionization energies (Table 6.5.1).

Calibration data for select PAHs is shown in Table 6.5.5, where all calibrations exhibited $R^2 \geq 0.991$. Detection limits for soil measurements and signal risetimes are given in Table 6.3, where estimated detection limits range from 100 ng/g for naphthalene to 1100 ng/g for benzo[*b*]fluoranthene. The benzo[*a*]pyrene detection limit (890 ng/g) is notably below the risk-based United States Environmental Protection Agency regional screening level for outdoor workers (2340 ng/g).[149] The observed signal risetimes for all PAHs were very similar (1.1 min. ≤ $t_{10\text{-}90\%}$ ≤ 1.3 min.), attributed to dichloromethane from the sample phase forming a polymer inclusion membrane that modifies PAH permeabilities through the PDMS membrane. The concept of using co-solvents to modify PDMS for improved membrane transport in CP-MIMS experiments is discussed in detail elsewhere.[9-10, 12] As described in the Experimental Section, the CP-MIMS probe was immersed in clean DCM after each soil measurement, and the time required to re-establish baseline signal levels was on the same order as the observed signal risetimes (Table 6.3). Both the sensitivity and speed of analysis presented in Table 6.3 demonstrate that CP-MIMS-LEI/CI has the potential to provide rapid, speciated and quantitative direct analysis results for PAH screening in soil samples.

Table 6.3: Detection limits and signal risetimes for select PAHs.

PAH	Detection Limit[a] ng/g	Signal Risetime[b] min.
Naphthalene	100	1.2 ± 0.1
Anthracene	250	1.2 ± 0.1
Phenanthrene	180	1.3 ± 0.1
Fluoranthene	270	1.2 ± 0.3
Pyrene	360	1.1 ± 0.1
Benz[*a*]anthracene	540	1.3 ± 0.3
Chrysene	740	1.1 ± 0.3
Benzo[*a*]pyrene	890	1.1 ± 0.5
Benzo[*b*]fluoranthene	1100	1.3 ± 0.3

[a] Detection limits are representative for 1 gram soil samples slurried in 7 mL DCM.
[b] Signal risetimes ($t_{10\text{-}90\%}$) are an average for triplicate 500 µg/L in DCM measurements.

The presented adduct ion chemistry and MS/MS transitions will only provide meaningful quantitative data for PAHs provided that the CI behaviour of one PAH is unaffected by the presence of others. To investigate this, Figure 6.6 presents the analysis of successive, highly concentrated (5.0 mg/L) additions of PAHs to a dichloromethane standard. Figure 6.6 shows that, despite the presence of other highly concentrated PAHs, the steady-state signals for PAHs already in solution remain unperturbed. While every permutation of PAH addition and concentration was not attempted, Figure 6.6 suggests that the CI behaviour and quantitation of one PAH is unaffected by the presence of others, even at very high concentrations.

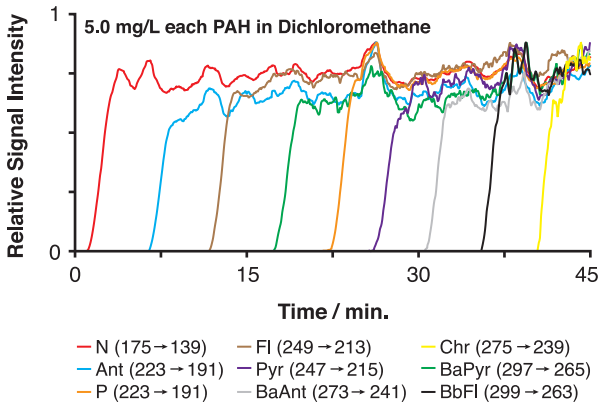

Figure 6.6: Sequential additions of high concentration PAHs (5.0 mg/L each; signals scaled relative to maximum signal intensity) to a dichloromethane standard for the demonstration of independent PAH-CI behaviour in CP-MIMS-LEI/CI.

6.3.3 Direct PAH Determination in Soil Samples

The applicability of CP-MIMS-LEI/CI for the direct analysis of soils was examined. Two PAH free soils were added to online measurements of 500 μg/L individual PAHs in dichloromethane (Figure 6.5.4). For both soils tested (organic content of 1.85 and 5.96%, respectively), the steady-state signals, and therefore free concentrations of PAHs in dichloromethane and CI behaviour, were unaffected. The results from this study suggest that dichloromethane may be used as a combination extraction/sampling solvent for CP-MIMS-LEI/CI direct analyses of PAHs in soils.

Given the success of CP-MIMS-LEI/CI for rapid, sensitive, selective and quantitative PAH analyses for analytical standards, the technique was applied to the direct measurement of PAHs in real soil samples. The analytical measurement duty cycle is 4 min per sample (2 min analysis, 2 min rinse). The CP-MIMS probe is directly immersed into dichloromethane/soil slurries immediately after sonication (3 min), and PAHs are directly analyzed from the slurry without any sample cleanup procedures or chromatography. As a result, soil sample measurement throughput for CP-MIMS-LEI/CI is 15 samples per hour, provided that sonication of one soil sample occurs during the analysis of another. This sample throughput, lack of sample carryover, and elimination of any other consumables needed for sample preparation is consistent with previous CP-MIMS based PAH measurement studies,[10] with the notable improvement of the isomer-specific resolution afforded by CI. All soil samples presented were quantified by direct calibration, for which data is summarized in Table 6.5.5.

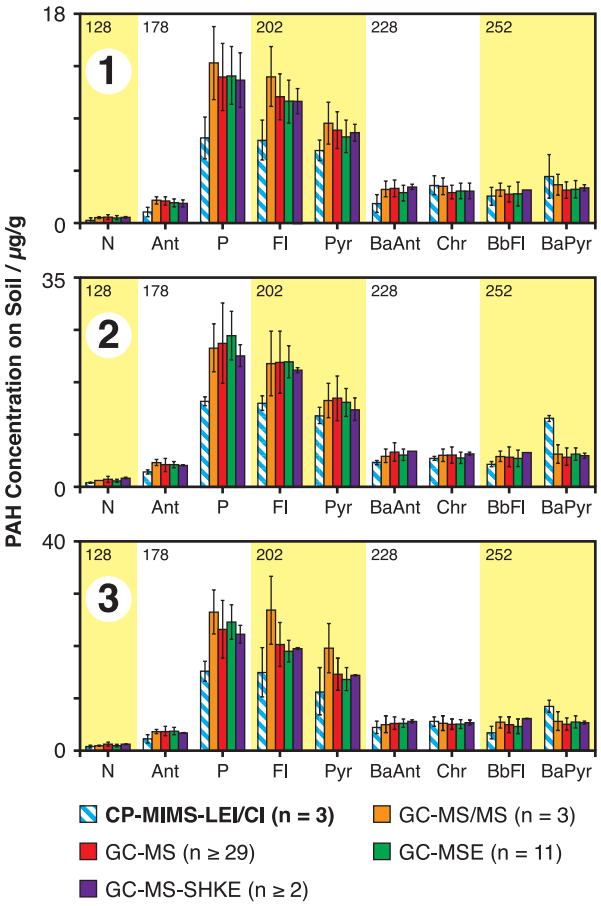

Figure 6.7: Comparison of CP-MIMS-LEI/CI to other GC-MS based techniques for the analysis of PAHs from proficiency testing soils.[150] Data bar heights are representatives of the median result, while errors bars represent the standard deviation of results. Nominal mass values for each isomer class are listed at the top of each shaded area. BaPyr results for CP-MIMS-LEI/CI are indicative of $BaPyr_{max}$.

Figure 6.7 compares the PAH analyses of three different proficiency testing soil samples by CP-MIMS-LEI/CI to the results from four other GC-MS based analyses (further details regarding the GC-MS methods are available elsewhere).[150] The relative distribution of PAHs depicted here is remarkably similar. While a negative quantitative bias is apparent for most CP-MIMS-LEI/CI PAH results, these results are anticipated given the short, non-exhaustive extraction step employed. This may be addressed in the future with more exhaustive extraction procedures, but given the remarkably short analytical duty cycle, and simple work flow, we believe that CP-MIMS-LEI/CI is well suited to a number of applications when high throughput and near 'real-time' information is needed. The results for benzo[*a*]pyrene (*i.e.*, $BaPyr_{max}$ as shown on Figure 6.7 for CP-MIMS-LEI/CI; quantified using the calibration slope for benzo[*a*]pyrene as shown in Table 6.5.5) demonstrate consistent positive biases, which is

unsurprising given that additional PAH isomers from the $C_{20}H_{12}$ isomer class forming M+45 adducts may also be contributing to the result as discussed earlier.

MS/MS was used for this study instead of simply quantifying diagnostic PAH adduct ions to mitigate any potential isobaric interferences present in complex samples. As is the case for benzo[*a*]pyrene though, the possibility that other contributions to any of the other MS/MS transitions may still exist for the direct measurement of complex, environmental samples. However, for the isomer classes studied, all members of the EPA 16 priority PAHs except for benzo[*k*]fluoranthene are specifically accounted for and, most significantly, may be directly quantified using unique CI adduct formation behaviour. The use of MS/MS on adduct ions formed through unique ion-molecule chemistry significantly limits the possibility of chemical interferents. The presented DMS analytical method provides a rapid, selective, and sensitive quantitative analysis ideally suited for quantitative pre-screening in advance of more time-consuming sample workup and analysis approaches. To this end, CP-MIMS-LEI/CI was used to analyze a set of five real environmental soil samples. These results were also compared with those obtained using GC-MS, and are presented in Figure 6.8.

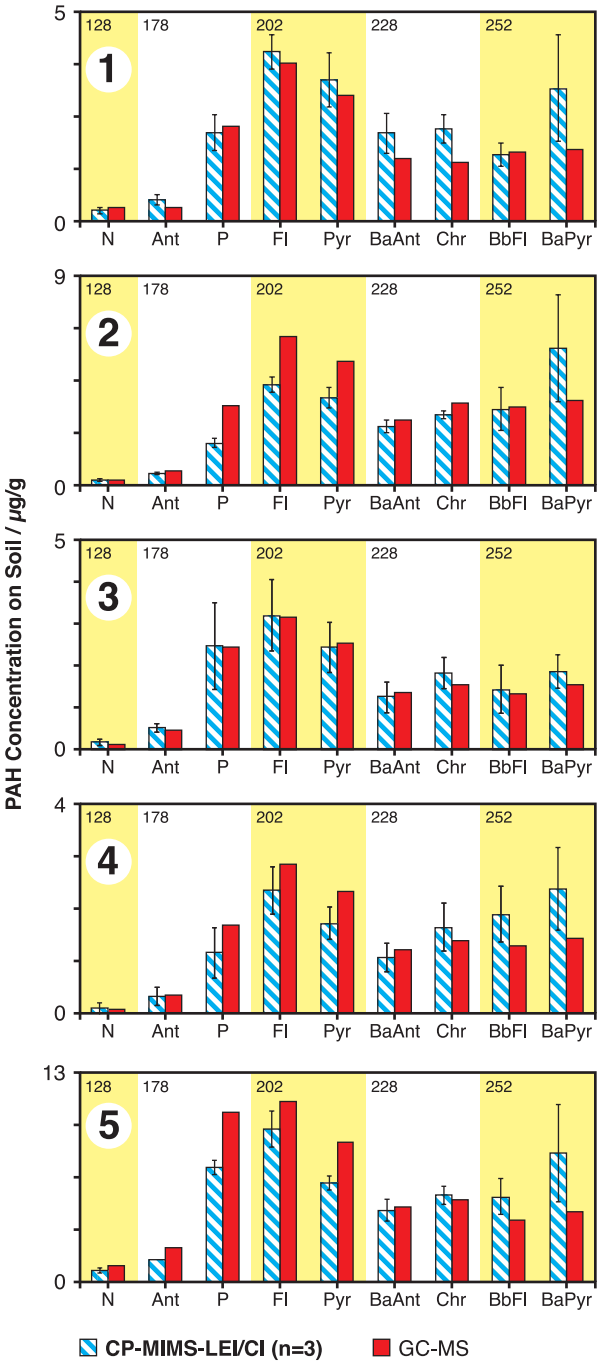

Figure 6.8: Comparison of CP-MIMS-LEI/CI to GC-MS for the analysis of PAHs present in five different environmental soils. Data bar heights are representative of the median result, while errors bars represent the standard deviation of results. Details of the GC-MS method are available elsewhere.[77] Nominal mass values for each isomer class are listed at the top of each shaded area. BaPyr results for CP-MIMS-LEI/CI are indicative of $BaPyr_{max}$.

In Figure 6.8, both CP-MIMS-LEI/CI and GC-MS techniques again provide similar PAH distributions. The predominantly positive biases observed for Sample 1 may suggest chemical interferents are present, but all the quantitative results for CP-MIMS-LEI/CI compare remarkably well to that of GC-MS, particularly given the simple and direct nature of CP-MIMS-LEI/CI measurements. For the nine PAHs quantified here, most exhibited a modest negative bias ranging from -14 to -36% across the eight soil samples measured (Table 6.5.6). The exceptions to this were chrysene (+11%), benzo[*b*]fluoranthene (0%), and benzo[*a*]pyrene (+50%). Overall, the average percent difference between CP-MIMS-LEI/CI results compared to those from GC-MS is -9 (± 23)% (Table 6.5.6). The similarity of quantitative results shown in both Figures 6.7 and 6.8 present a compelling argument for the use of CP-MIMS-LEI/CI for quantitative PAH in soil analyses in selected contexts.

6.4 Conclusions

While it is undeniable that techniques involving exhaustive extraction and chromatographic resolution can provide superior analytical performance, CP-MIMS-LEI/CI is an excellent complement to these methods. CP-MIMS-LEI/CI provides isomer-specific quantitation of PAHs in soils at ng/g quantities without time consuming and costly sample preparation/ cleanup steps, and may be used to quantitatively pre-screen samples to identify those warranting further conventional analysis. This study lays the groundwork for future experiments, with goals of miniaturization and mobilization of CP-MIMS-LEI/CI and use with other analytical platforms (*i.e.,* LC-MS, GC-MS). Eventually, CP-MIMS-LEI/CI may be used for in-field measurements, allowing for applications such as real-time monitoring, adaptive sampling, site assessment, and rapid response during a critical incident emergency or remediation effort. More broadly, the use of methanol and dichloromethane for successful isomer-specific measurements of PAHs may prompt the application of CP-MIMS-LEI/CI to other solvents/reagent ion precursors (e.g., different halogenated organics and alcohols) and analyte classes, expanding the field of DMS.

6.5 Supporting Information

6.5.1 Standards and Solvents

Anthracene (99%) was obtained from Alfa Aesar (Ward Hill, MA, USA). Anthracene-d_{10} (≥ 98 atom % D), benzo[*a*]pyrene (≥ 96%), fluoranthene (98%) naphthalene (99%), perylene (≥ 99%), phenanthrene (98%), phenanthrene-d_{10} (98 atom % D), pyrene (98%) and were obtained from Sigma Aldrich (Oakville, ON, Canada). Benz[*a*]anthracene (≥ 98.0%), benzo[*b*]fluoranthene (≥ 98.0%) and benzo[*a*]phenanthrene (*i.e.*, chrysene; ≥ 98.0%) were obtained from TCI America (Portland, OR, USA). Methanol (HPLC grade) was obtained from VWR International (Edmonton, AB, Canada). Dichloromethane and chloroform (ACS grade) were obtained from Fisher Scientific (Ottawa, ON, Canada). Deuterated methanols (CH_3OD,

99.5 atom % D; CD_3OD, ≥ 99.8 atom % D) and dichloromethane-d_2 (99.5 atom % D) were obtained from Sigma Aldrich. PAH stock and sub-stock solutions were prepared in dichloromethane.

For subsequent measurements by full scan mass spectrometry, PAH standards were volumetrically and individually prepared at 150 mg/L in dichloromethane. For tandem mass spectrometry calibration experiments, PAH standards were volumetrically and individually prepared at 0.75, 1.4, and 8.0 mg/L in dichloromethane.

6.5.2 Supporting Tables and Figures

Table 6.5.1: Polycyclic aromatic hydrocarbons physicochemical properties

PAH	Molar Mass g/mol	Vapor Pressure [a] mmHg	Experimental Ionization Energy [b] eV	Experimental Proton Affinity [b] kJ/mol
Naphthalene	128.18	8.5×10^{-2}	8.144	802.9
Anthracene	178.23	6.53×10^{-6}	7.439	877.3
Phenanthrene	178.23	1.21×10^{-4}	7.891	825.7
Fluoranthene	202.26	9.22×10^{-6}	7.9	828.6
Pyrene	202.26	4.5×10^{-6}	7.426	869.2
Benz[*a*]anthracene	228.29	2.1×10^{-7}	7.45	-
Chrysene	228.29	6.4×10^{-7}	7.60	840.9
Benzo[*a*]pyrene	252.32	5.49×10^{-9}	7.12	-
Benzo[*e*]pyrene	252.32	5.70×10^{-9}	7.41	-
Benzo[*b*]fluoranthene	252.32	5×10^{-7}	-	-
Benzo[*k*]fluoranthene	252.32	9.65×10^{-10}	7.47 [c]	-
Perylene	252.32	5.25×10^{-9}	6.960	888.6

[a] From PubChem database (data for 25°C)[151]

[b] From NIST Library database[128]

[c] Estimated value from Modelli *et al*.,[148] as experimental data not readily available.

Table 6.5.2: Acceptor phase composition determination by gravimetric analysis

Solvent Sample v/v	Mass of 50 µL Aliquot g
For **CH_2Cl_2** Donor:	
70:30 CH_2Cl_2:CH_3OH	0.05642
80:20 CH_2Cl_2:CH_3OH	0.05940
Acceptor phase aliquot [a]	0.05846
For **$CHCl_3$** Donor:	
80:20 $CHCl_3$:CH_3OH	0.06555
90:10 $CHCl_3$:CH_3OH	0.06878
Acceptor phase aliquot [b]	0.06769

Gravimetric analyses were conducted on 50 µL aliquots (measured using gas-tight syringe).
Acceptor phase aliquots for composition determination were collected into a septum sealed vial post-membrane. The LEI-CI interface was not connected during these measurements.
[a] Corresponds to composition of 77:23 CH_2Cl_2:CH_3OH v/v
[b] Corresponds to composition of 87:13 $CHCl_3$:CH_3OH v/v

Table 6.5.3: Deuterium labeling studies for anthracene (Ant), phenanthrene (P), dichloro-methane, and methanol for investigation of M+45 and M+47 adduct ions using full scan and tandem mass spectrometry.

PAH	Acceptor	Sample	Adduct *m/z*	MS/MS Loss *m/z*
For **M+45** Adduct ($[M+CH_2Cl+CH_3OH-HCl]^+$):				
Ant (178)	CH_2Cl_2	CH_3OH	223 (M+45; $[M+CH_2Cl+CH_3OH-HCl]^+$)	-32 (CH_3OH)
Ant (178)	CH_2Cl_2	CD_3OD	226 (M+48; $[M+CH_2Cl+CD_3OD-DCl]^+$)	-35 (CD_3OH)
Ant (178)	CH_2Cl_2	CH_3OD	223 (M+45; $[M+CH_2Cl+CH_3OD-DCl]^+$)	-32 (CH_3OH)
Ant (178)	CD_2Cl_2	CH_3OH	225 (M+47; $[M+CD_2Cl+CH_3OH-HCl]^+$)	-32 (CH_3OH)
Ant (178)	CD_2Cl_2	CD_3OD	228 (M+50; $[M+CD_2Cl+CD_3OD-DCl]^+$)	-35 (CD_3OH)
Ant (178)	CD_2Cl_2	CH_3OD	225 (M+47; $[M+CD_2Cl+CH_3OD-DCl]^+$)	-32 (CH_3OH)
Ant-d_{10} (188)	CH_2Cl_2	CH_3OH	233 (M+45; $[M+CH_2Cl+CH_3OH-HCl]^+$)	-33 (CH_3OD)
For **M+47** Adduct ($[M+CHCl_2-HCl]^+$):				
P (178)	CH_2Cl_2	CH_3OH	225 (M+47; $[M+CHCl_2-HCl]^+$)	-36 (-HCl)
P (178)	CD_2Cl_2	CH_3OH	226 (M+48; $[M+CDCl_2-HCl]^+$)	-36 (-HCl)
P-d_{10} (188)	CH_2Cl_2	CH_3OH	234 (M+46; $[M+CHCl_2-DCl]^+$)	-37 (-DCl)

'Acceptor' refers to solvent flowed through membrane lumen towards the LEI/CI source. 'Sample refers to the sample phase solvent. Collision energies of 5 and 40 eV were used for anthracene and phenanthrene, respectively.

Table 6.5.4: Deuterium labeling studies for anthracene (Ant), phenanthrene (P), dichloromethane, and methanol for investigation of M+1, M+13, M+49, and M+83 adduct species using full scan mass spectrometry.

PAH	Acceptor	Sample	Adduct Formed *m/z*
For **M+1** Adduct ($[M+H]^+$) [a]:			
Ant	CH_2Cl_2	CH_3OH	179 (M+1; $[M+H]^+$)
Ant	CH_2Cl_2	CD_3OD	180 (M+2; $[M+D]^+$)
Ant	CD_2Cl_2	CH_3OH	179 (M+1; $[M+H]^+$)
P	CH_2Cl_2	CH_3OH	179 (M+1; $[M+H]^+$)
P	CH_2Cl_2	CD_3OD	180 (M+2; $[M+D]^+$)
P	CD_2Cl_2	CH_3OH	179 (M+1; $[M+H]^+$)
For **M+13** Adduct ($[M+CH_2Cl\text{-}HCl]^+$) [b,c]:			
Ant	CH_2Cl_2	CH_3OH	191 (M+13; $[M+CH_2Cl\text{-}HCl]^+$)
Ant	CH_2Cl_2	CD_3OD	191 (M+13; $[M+CH_2Cl\text{-}HCl]^+$)
Ant	CD_2Cl_2	CH_3OH	193 (M+15; $[M+CD_2Cl\text{-}HCl]^+$)
Ant-d_{10}	CH_2Cl_2	CH_3OH	190 (M+12; $[M+CH_2Cl\text{-}DCl]^+$)
P	CH_2Cl_2	CH_3OH	191 (M+13; $[M+CH_2Cl\text{-}HCl]^+$)
P	CH_2Cl_2	CD_3OD	191 (M+13; $[M+CH_2Cl\text{-}HCl]^+$)
P	CD_2Cl_2	CH_3OH	193 (M+15; $[M+CD_2Cl\text{-}HCl]^+$)
P-d_{10}	CH_2Cl_2	CH_3OH	190 (M+12; $[M+CH_2Cl\text{-}DCl]^+$)
For **M+49** Adduct ($[M+CH_2Cl]^+$) [c]:			
Ant	CH_2Cl_2	CH_3OH	227 (M+49; $[M+CH_2Cl]^+$)
Ant	CH_2Cl_2	CD_3OD	227 (M+49; $[M+CH_2Cl]^+$)
Ant	CD_2Cl_2	CH_3OH	229 (M+51; $[M+CD_2Cl]^+$)
P	CH_2Cl_2	CH_3OH	227 (M+49; $[M+CH_2Cl]^+$)
P	CH_2Cl_2	CD_3OD	227 (M+49; $[M+CH_2Cl]^+$)
P	CD_2Cl_2	CH_3OH	229 (M+51; $[M+CD_2Cl]^+$)
For **M+83** Adduct ($[M+CHCl_2]^+$)			
Ant	CH_2Cl_2	CH_3OH	-
Ant	CH_2Cl_2	CD_3OD	-
Ant	CD_2Cl_2	CH_3OH	-
P	CH_2Cl_2	CH_3OH	261 (M+83; $[M+CHCl_2]^+$)
P	CH_2Cl_2	CD_3OD	261 (M+83; $[M+CHCl_2]^+$)
P	CD_2Cl_2	CH_3OH	262 (M+84; $[M+CDCl_2]^+$)

'Acceptor' refers to solvent flowed through the hollow fibre membrane lumen towards the LEI/CI source. 'Sample refers to the sample phase solvent.

[a] The gained proton is from methanol, as indicated by the M+2 peak using CD_3OH and lack of M+2 peak when using CH_2Cl_2 with CH_3OH.

[b] The eliminated proton as part of HCl is from that of the PAH, as largely indicated by the M+12 adduct ions from anthracene-d_{10} and phenanthrene-d_{10}.

[c] The proposed CI reactions for the M+13, M+49, and M+83 adduct ion formations are consistent with those proposed by Mosi *et al*.[78]

Table 6.5.5: Calibration data for polycyclic aromatic hydrocarbons in dichloromethane standards by CP-MIMS-LEI/CI (0.75, 1.4, and 8.0 mg/L).

PAH	MS/MS Transition *m/z*	Slope mg^{-1} L	y-intercept	R^2
Naphthalene	175 ⟶ 139 (M+47)	95	-1	0.9997
Anthracene	223 ⟶ 191 (M+45)	68	-1	0.9990
Phenanthrene	225 ⟶ 189 (M+47)	82	2	0.997
Fluoranthene	249 ⟶ 213 (M+47)	54	-1	0.9992
Pyrene	247 ⟶ 215 (M+45)	56	-2	0.991
Benz[*a*]anthracene	273 ⟶ 241 (M+45)	47	-1	0.996
Chrysene	275 ⟶ 239 (M+47)	24	0	0.998
Benzo[*a*]pyrene	297 ⟶ 265 (M+45)	75	2	0.997
Benzo[*b*]fluoranthene	299 ⟶ 263 (M+47)	16	0	0.997

Table 6.5.6: Percent differences between CP-MIMS-LEI/CI and GC-MS results for PAHs in soils.

Sample	N	Ant	P	Fl	Pyr	BaAnt	Chr	BbFl	BaPyr	Average
Fig. 6 - 1	-59	-64	-53	-41	-24	-54	20	-7	34	-27
Fig. 6 - 2	-68	-40	-51	-40	-22	-36	-11	-28	77	-24
Fig. 6 - 3	-45	-49	-42	-30	-25	-16	10	-38	50	-21
Fig. 7 - 1	-28	41	-7	7	11	33	44	-3	60	18
Fig. 7 - 2	-23	-21	-63	-39	-35	-10	-16	-3	47	-18
Fig. 7 - 3	29	9	0	1	-4	-8	17	8	20	8
Fig. 7 - 4	4	-4	-37	-20	-30	-13	17	38	50	1
Fig. 7 - 5	-30	-39	-39	-16	-33	-4	5	31	59	-7
Average	-27	-21	-36	-22	-20	-14	11	0	50	**-9**
Stdev	± 32	± 35	± 22	± 19	± 16	± 25	± 19	± 26	± 17	**± 23**

Percent difference calculated as [(CP-MIMS-LEI/CI) – (GC-MS)] / Average × 100%

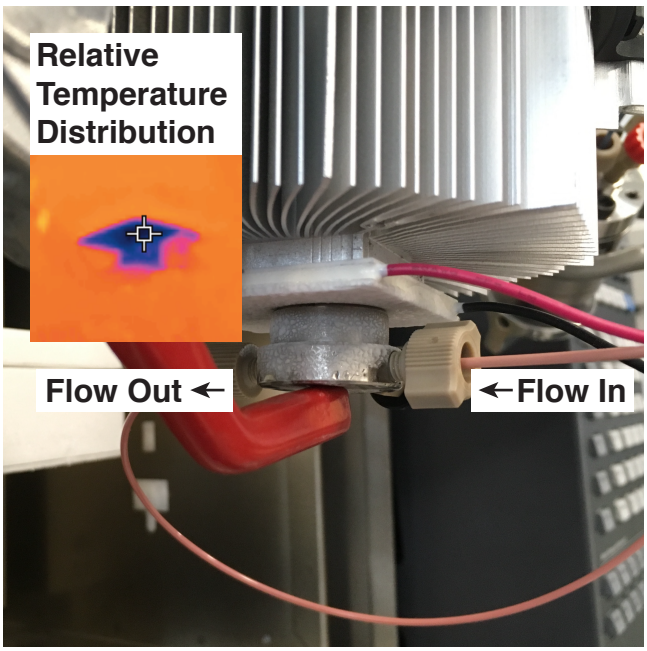

Figure 6.5.1: Picture of peltier cooler and liquid flow splitter used to reduce the liquid flow in advance of infusion into the LEI/CI source. The image depicting relative temperature distribution is from an IR camera (FLIR TG165, Wilsonville, OR, USA)

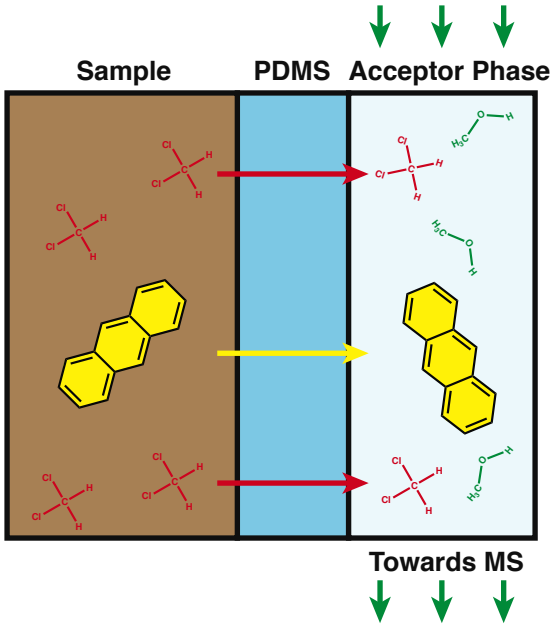

Figure 6.5.2: Schematic illustration of dichloromethane and PAH membrane permeation, such that the acceptor phase is comprised of a methanol, dichloromethane, and PAH permeant mixture that is eventually infused into the LEI/CI source.

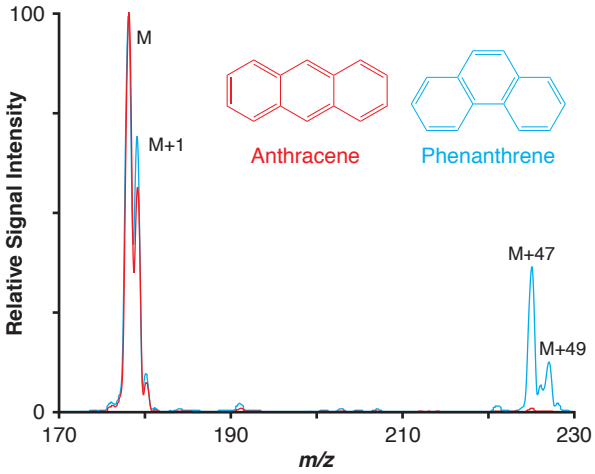

Figure 6.5.3: Full scan mass spectra from the individual, direct measurements of anthracene and phenanthrene (150 mg/L each in chloroform) by CP-MIMS-LEI/CI. Signal intensities are normalized for 100% $M^{+\bullet}$ abundance.

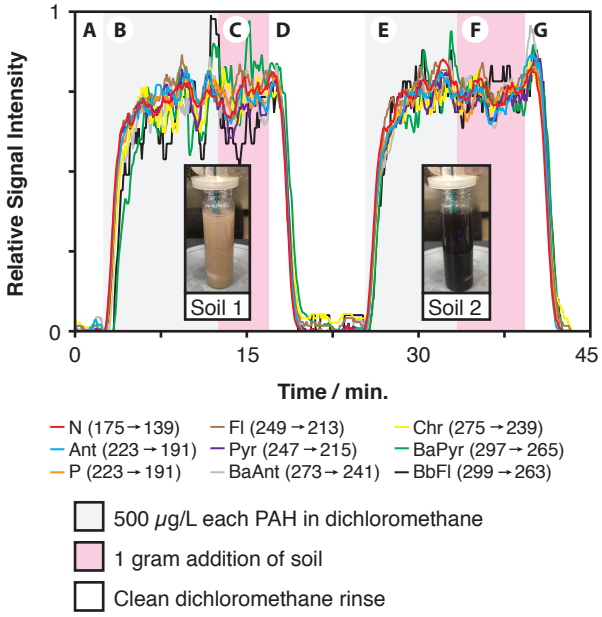

Figure 6.5.4: Online addition of clean soils to PAH dichloromethane standards (500 µg/L each naphthalene, anthracene, phenanthrene, fluoranthene, pyrene, benz[*a*]anthracene, chrysene, benzo[*a*]pyrene, benzo[*b*]fluoranthene, and perylene). Order of events: A) t = 0 min.; 7.0 mL dichloromethane rinse. B) t =2.5 min.; PAH spike, 500 µg/L each. C) t = 12.4 min.; Addition of 1 gram 1.85% organic matter clean soil. D) t = 16.8 min.; 7.0 mL dichloromethane rinse. E) t = 25.2 min.; PAH spike, 500 µg/L each. F) t = 33.4 min.; Addition of 1 gram 5.96% organic matter clean soil. G) t = 39.3 min.; 7.0 mL dichloromethane rinse. Soils were purchased from and verified to have no PAH contamination by Sigma Aldrich (Oakville, ON, Canada).

Chapter 7

Conclusions

7.1 Summary

Previous generations of CP-MIMS systems predominantly used atmospheric pressure ionization sources, most often electrospray. While inherently successful, such pairings represented a fundamental incompatibility as discussed earlier: PDMS membrane extraction (*i.e.*, CP-MIMS) is ideal for hydrophobic molecules, whereas electrospray ionization is ideal for polar, hydrophilic molecules. This thesis represents the development of coupling CP-MIMS with both EI and CI (*i.e.*, CP-MIMS-LEI/CI), as such ionization strategies are more ideal for hydrophobic molecules. The CP-MIMS-LEI/CI methodology resulted in rapid sample throughput, and allowed for the quantitative analyses of complex, heterogeneous samples (soils, dust, etc.) while obviating sample preparation, cleanup, and concentration steps. The technique was furthermore shown to be highly sensitive, and the eventual use of CI allowed for additional selectivity. Additional advantages of the CP-MIMS-LEI/CI pairing as discussed in this thesis are summarized below.

Chapter 2 explored the use of co-solvents in the PDMS membrane to improve permeability (*i.e.*, increased sensitivity and lessened signal risetime) for a CP-MIMS and ESI-based system. A mixture of heptane and methanol, used as the CP-MIMS acceptor phase, formed a polymer inclusion membrane (PIM) with the PDMS, and allowed for improved analytical performance for model compounds relative to previous CP-MIMS designs. The same acceptor phase system was applied in Chapter 3, where PAHs were quantitated directly from both aqueous and soil samples using CP-MIMS-LEI. The ideal pairing of CP-MIMS with LEI for PAH detection resulted in high sensitivity, and the use of a PIM allowed for high sample throughput. The successful analysis of hydrophobic molecules from complex, heterogeneous samples was applied further in Chapter 4 to the on-line monitoring of synthetic reactions. In Chapter 5, the solvent naturally present solvent at the LEI source was serendipitously used as a CI reagent for phthalate analyses (*i.e.*, CP-MIMS-LEI/CI). Finally, in Chapter 6, a dichloromethane and methanol reagent system/acceptor phase was used with CP-MIMS-LEI/CI for isomer-specific PAH quantitation directly from soils, where the advantages of previous CP-MIMS-LEI/CI designs (sensitivity, elimination of sample cleanup, minimal matrix effects, etc.) were maintained.

7.2 Recommendations for Future Work

While successful, the combination of direct measurement and *in situ* chemical ionization for isomer differentiation of PAHs in soils should continue to be improved. The CI processes should be further optimized, through means such as alternate reagent selection and source improvements, for the improvement of both sensitivity and further selectivity. CP-MIMS-LEI/CI should also be further explored and developed on simpler mass spectrometry systems (*i.e.*, single quadrupoles, ion traps) for the purposes of mobilization and in-field measurements. While the work in this thesis for PAH isomer differentiation was dependent upon tandem mass spectrometry experiments, the presence of multiple PAH adducts species formed at reproducible relative intensities may still allow for isomer differentiation while using a non-tandem mass analyzer. This simpler, robust instrumental design may therefore be taken more easily outside of the laboratory and applied to challenging in-field measurements.

More broadly, the use of CP-MIMS-LEI/CI should continue to be applied a direct mass spectrometry solution for analytes that are otherwise challenging for atmospheric pressure techniques, such as polychlorinated biphenyls, dioxins, furans, polybrominated diphenyl ethers, and other hydrophobic molecules. CP-MIMS-LEI/CI should also be further applied to other classes of analytes that otherwise exhibit extensive EI fragmentation (such as the phthalates explored in Chapter 5), where CI behaviour may assist preservation of the molecular ion signal, allowing for enhanced sensitivity and selectivity. CP-MIMS-LEI/CI should be further applied to other sample types/phases for synthetic reaction monitoring and environmental sample screening. The use of a variety of *in situ* CI strategies should be further explored, particularly for direct measurements of increasingly complex matrices for bettered selectivity. In support of further CP-MIMS-LEI/CI application to samples of increasing complexity, Figure 7.1 shows preliminary work for the direct analyses of fruit juice, dogfish liver, window sealant, and a powdered flooring tile.

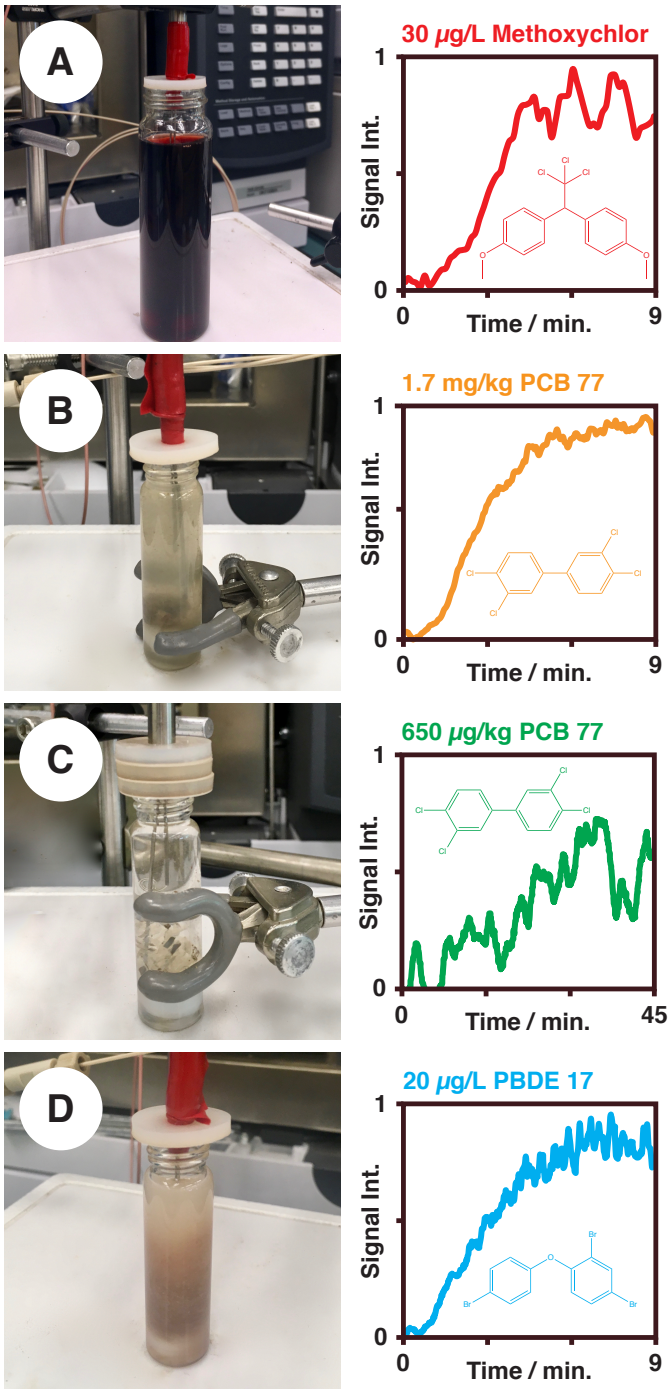

Figure 7.1: Online contaminant analyses by CP-MIMS. (A) Methoxychlor spiked into fruit juice. (B) Polychlorinated biphenyl 77 from dogfish liver. (C) Polychlorinated biphenyl 77 from window sealant. (D) Polybrominated diphenyl ether 17 spiked into powdered flooring tile slurry.

More studies aimed at better understanding of CP-MIM-LEI/CI fundamental processes should be conducted. For example, the correlation of space charging effects for various solvent systems with increasing liquid flowrates should be investigated for both LEI and LEI/CI source designs. For purposes of library matching at 70 eV, different LEI source constructions (permitting improved solvent venting) may be explored in order to minimize CI behaviour. To further capitalize on the strengths of CI as shown in the latter chapters of this thesis, alternative means of introducing effective CI reagents to the CP-MIMS-LEI/CI system should be explored. These studies will allow for reagent introduction that is not simply limited to liquids that are compatible as sample and acceptor phases. The dimensions of the CP-MIMS system, notably the direct immersion/sampling probe, should be reduced to nanoscale where possible in an effort to reduce or completely eliminate the passive flow splitter. This miniaturization would therefore allow the liquid flows from CP-MIMS to be directly and more simply coupled to LEI/CI sources.

It the belief of the author that the examples of CP-MIMS-LEI/CI presented in this thesis are only the surface of potential applications with respect to both analyte and sample types. As the field of atmospheric pressure/ambient ionization direct mass spectrometry techniques continues to advance, CP-MIMS-LEI/CI should also continue to be developed in parallel as a complimentary and sometimes situationally more ideal analytical strategy.

Appendix

Paper Spray Mass Spectrometry for the Direct, Semi-Quantitative Measurement of Fentanyl and Norfentanyl in Complex Matrices

Reproduced with minor changes and permission from Vandergrift, G.W.; Hessels, A.J.; Palaty, J.; Krogh, E.T.; Gill, C.G. "Paper spray mass spectrometry for the direct, semi-quantitative measurement of fentanyl and norfentanyl in complex matrices." *Clinical Biochemistry*, **2018**, *54*, 106-111. G.W. Vandergrift primarily designed the experiments and analyzed the data. G.W. Vandergrift and J. Palaty primarily collected the data, with contributions from A.J. Hessels. C.G Gill designed and constructed the sampling interface, with contributions from A.J. Hessels. G.W. Vandergrift drafted the manuscript, with intellectual and editorial contributions from J. Palaty, E.T. Krogh and C.G. Gill.

A.1 Introduction

Fentanyl (N-(1-phenethyl-4-piperidyl) propionanilide) is a potent synthetic opioid at the center of an international health crisis. Originally synthesized by Paul Janssen in 1960, fentanyl is widely used in the health system for chronic pain relief, anesthesia, and pre-surgery due to low health risk (if correctly monitored), fast action, and high potency (50 to 100 times more effective than morphine).[152-154] Unfortunately, it has also become increasingly attractive for illicit drug suppliers to lace fentanyl into other substances, notably heroin, oxycodone, and methylenedioxymethamphetamine (MDMA). This is largely due to fentanyl's significantly cheaper production costs, availability, and higher potency compared to other illicit substances.[152-153, 155] The high potency of fentanyl, along with the crude production methods and lack of precise dose control of street suppliers, results in a very high risk of fatal overdose for users. The fentanyl crisis is of particular concern in the province of British Columbia, Canada, where the percentage of overdoses in which fentanyl was detected has risen from 4% in 2012 to 81% in 2017. In British Columbia, there were 12 fentanyl related deaths in 2012, 656 deaths in 2016, and a record 1156 fentanyl related deaths in 2017.[156]

To date, most quantitative analytical methods for the detection of fentanyl are based on mass spectrometry (MS), with liquid chromatography (LC),[154, 157-159] or gas chromatography (GC)[160-162] introduction systems, focusing on analyses in blood and/or urine. While sensitive and selective, these techniques are typically used to detect fentanyl in a biological matrix after the drug has already been consumed. This may be too late for the patient, showing the need for measurements to be made in the street drugs themselves. Furthermore, conventional sample introduction methods (*i.e.* chromatography) are costly, time-consuming, and require highly trained professionals, making such methods unsuitable for point-of-care testing. Conventional methods may therefore fail to effectively support a strategy aimed at harm reduction, which may be the best course of action to help prevent overdoses and save lives.[153] The ideal analytical pre-screening technique for this approach should be sensitive (*i.e.* requiring minimal sample), selective, and capable of producing at least semi-quantitative results. In addition, the technique needs to be inexpensive and easy for untrained personnel to use.

Paper spray mass spectrometry (PS-MS) is an emerging ambient ionization technique, taking advantage of a simple direct sampling strategy in combination with the powerful analytical capabilities of mass spectrometry. Briefly, a strip of paper with a pointed tip is loaded with a small amount of sample (< 10 μL), wetted with a solvent, and connected to high voltage (3–5 kV). Ions are directly generated from the tip of the paper by a mechanism akin to electrospray,[163-164] and are subsequently detected by a mass spectrometer.[164-169] Results are produced in seconds, and detection limits have been reported in the low picograms of material.[165] PS-MS has been used for a wide variety of analytes, including illicit substances,[165, 168-169] therapeutic substances,[166] herbicides,[170] and chemical warfare agents.[171] Sampling may be accomplished by spotting the sample onto the paper, or by simply swabbing a contaminated substance with the paper itself, obviating the need for any sample pretreatment. While semi-quantitative in nature, satisfactory measurements may be obtained using PS-MS through the use of an internal standard.[165, 169] Due to the low cost of consumables, simple sampling protocols, small sample requirement, applicability to a wide variety of sample types and high sensitivity/selectivity, PS-MS has excellent potential for pre-screening street drugs for opioids such as fentanyl, as well as monitoring post-drug use in blood or urine. This is especially significant when combined with the growing availability of mass spectrometers intended for field use.[17, 172-174]

Presented here is the development and characterization of a PS-MS method for the semi-quantitative measurement of fentanyl and norfentanyl in complex matrices such as urine and analgesic slurries that mimic street drug preparations. The analysis of whole blood samples was purposely not explored, as this would not be the route taken at a harm reduction clinic. We demonstrate the use and optimization of a custom PS interface, showing how interface position and paper strip quality can significantly affect quantitative results. Comparable calibrations across different matrices are presented, as well as data showing low picogram detection limits.

A.2 Materials and Methods

A.2.1 Standard Solution and Sample Preparation

Stock solutions of fentanyl (1.0 mg/mL), fentanyl-d_5 (100 µg/mL), norfentanyl oxalate (1.0 mg/mL, as free base), and norfentanyl-d_5 oxalate (100 µg/mL, also as free base) in methanol were obtained from Cerilliant Corporation (Round Rock, TX, USA). Methanol samples were prepared by gravimetric dilution using HPLC grade methanol (Fisher Scientific, Ottawa, ON, Canada). Calibration samples in diluted urine were prepared by gravimetric dilution using a sample of clean, unfiltered human urine and 18MΩ de-ionized (DI) water (Model MQ Synthesis A10, Millipore Corp., Billerica, MA, USA). These samples were prepared such that the urine comprised 10% of the final sample by mass. Care was also taken to ensure that urine calibrator samples were < 0.1% methanol by mass. Anonymized patient urine samples (LifeLabs Medical Laboratories, Burnaby, BC, Canada) were gravimetrically diluted ten-fold with DI. A commercially available analgesic tablet containing several active (acetaminophen, guaifenesin, pseudoephedrine, dextromethorphan) and inactive (cellulose, corn starch) ingredients was ground to a powder with a mortar and pestle, and a slurry was prepared by suspending 50 mg of analgesic powder in 1 mL of methanol spiked with fentanyl standard.

Paper strips were fashioned from Whatman #1 filter paper (Fisher Scientific, Ottawa, ON, Canada), manually cut into 2.6cm×0.9cm strips using a carbide razor blade (Fatmax® Carbide Utility Blades, Stanley Canada Inc., Mississauga, ON, Canada) and 3D printed cutting template. All 3D printed parts were made using a stereolithographic printer (Form 2, Formlabs Inc., New Castle, DE, USA). The paper was cut to have a tapered point 0.9 cm from the end of the strip, such that the tip formed a 60 degree angle (Figure A.1). Acetonitrile has previously been found to be an effective wash solvent for paper spray paper.[170] Before analysis, cut paper strips were exhaustively cleaned with HPLC grade acetonitrile for a minimum of 2 h by Soxhlet extraction to remove any contaminants.

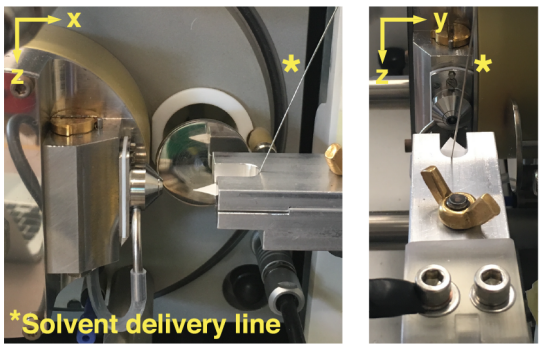

Figure A.1: Photographic details of the custom PS-MS interface, illustrating the positioning of the paper strip and solvent delivery line.

For all PS-MS measurements presented, 10 μL unfiltered samples were spotted on individual paper strips 0.7 cm from the tip using a micropipettor. Spotting location on the paper was kept consistent across samples through the use of a 3D printed guide (Supplemental information, Figure A.5.1). Deuterated fentanyl and norfentanyl internal standard solutions (in methanol) were subsequently spotted on the paper strips in a similar fashion (1.3 ng and 3.0 ng of internal standard, respectively, for each analysis). For the urine standard addition experiments, 85 pg of fentanyl and 690 pg of norfentanyl were also spiked on the strips with the sample. Internal standards and standard additions were spiked separately on the paper to simplify the analysis, consistent with PS-MS methodology employed by others.[170] To minimize sample preparation time, a forced air heat gun (Jobmate, Waterloo, ON, Canada) was used to gently evaporate water/solvent from the paper until dry (approximately 30s). The paper temperature reached 90°C, as measured by an infrared thermometer (TG165 Spot Thermal Camera, FLIR Systems, Wilsonville, OR, USA). As a control to investigate any possible analyte loss due to volatility, paper strips were left to air dry (3 h) and then compared to identical samples dried by the forced air heat gun. Similar quantitative results were obtained for both drying methods.

A.2.2 Paper Spray Mass Spectrometry (PS-MS) System

A triple quadrupole mass spectrometer (Micromass Quattro Ultima LC, Waters-Micromass, Altrincham, UK) fitted with an in-house constructed paper spray source was used for all work presented (Figures A.5.2, A.5.3, A.5.4). The MS inlet design was a second-generation Z-Spray geometry (Waters-Micromass). No nitrogen curtain gas flow at the inlet cones was used, as there was no significant effect upon signal intensity. Argon (UHP grade, Praxair, Nanaimo, Canada) was maintained at approximately 3 mTorr in the collision cell for tandem mass spectrometry (MS/MS) experiments. Positive ion mode was used for all analyses. The MS dwell time was set to 50 ms for all analytes, and the appropriate MS/MS parameters are given in Table A.5.1.

When sample loading was complete, the paper strips were mounted on an in-house constructed paper spray interface (Figures A.1, A.5.2, A.5.3, A.5.4) consisting of an aluminum clamping block (electrical conductor) and a 3D printed mounting arm (electrical insulator), which was then mounted on a three-axis translational stage. High voltage (+4.5 kV), supplied by the mass spectrometer ESI power supply, was connected to the clamping block of the interface, which in turn contacted the paper strip. A methanol/water/formic acid (90:10:0.1 v/v) solvent mix was continuously supplied at 20 μL/min to the top of the paper strip behind the sample spot via a short length of 22 gauge stainless steel hypodermic stock (Vita Needle Co., Needham, MA, USA). Solvent delivery was achieved using a syringe pump (Harvard Apparatus Pump 11 Elite, St. Laurent, QC, Canada) and gastight syringe (10 mL, Hamilton Corporation, Reno, NV, USA). For all analyses, the pointed tip of the paper was maintained at an optimized distance of 0.7 cm from the MS inlet cone. A new strip of paper was used for each analysis. All analyses were performed at ambient temperatures and pressures (~25°C and ~101 kPa).

A.2.3 Liquid Chromatography-Mass Spectrometry

Fentanyl in patient urine samples was determined at LifeLabs by screening with immunoassay (Enzyme Multiplied Immunoassay Technique, Thermo Scientific, Waltham, MA, USA; cut-off 1 ng/mL) run on a high volume chemistry analyzer (Cobas Integra 800, Roche Diagnostics, Mannheim, Germany) followed by confirmation of positive results by salt-assisted liquid-liquid extraction, followed by LC-MS. Fentanyl is eliminated in the urine primarily as norfentanyl and the unchanged free drug.[175-176] Enzyme hydrolysis is not strictly necessary, but was performed as the LC-MS assay included other drugs (e.g. buprenorphine) where glucuronide hydrolysis is required. In brief, 125 µL urine was hydrolyzed with 250 µL of abalone enzyme (KURA Biotec, Los Angeles, CA, USA) in 10 mM pH 5 sodium acetate buffer containing fentanyl-d_5 and norfentanyl-d_5 for 15 min at 60 °C, following which brine (100 µL) and acetonitrile (700 µL) were added. The mixture was vortexed and centrifuged. The supernatant was decanted and evaporated to dryness prior to reconstitution with 0.2% formic acid in methanol-water (1:9, v/v, 200 µL), analyzed using a 2.1 × 50 mm Kinetex Biphenyl column (Phenomenex, Torrance, CA, USA) used with a binary liquid chromatographic system (1200 Series, Agilent Technologies, Santa Clara, CA, USA) interfaced to a triple quadrupole mass spectrometer (Model 6410, Agilent Technologies). The same MRM transitions as listed in Table A.5.1 were used. The analytical measurement range was 0.5 to 40 ng/mL for both fentanyl and norfentanyl.

A.2.4 Data Analysis

Microscopic images were obtained using a dissection microscope (Model MDG 17, Wild Heerbrugg, Switzerland) equipped with a digital camera imaging system (Model MD500, Amscope, Irvine, CA, USA). For the presentation of data only, four-point moving boxcar smoothing was applied to the signal chronograms. Signal intensities were processed as peak heights from the raw, unsmoothed data. All signals for PS-MS were normalized to that of the corresponding internal standard. Signal ratios of the quantifier to qualifier ions for all urine sample analyses are presented in Table A.5.2. All measurements were conducted in triplicate, with uncertainties/error bars given as standard deviations unless otherwise noted. Detection limits were estimated as the concentration needed to produce a signal 3 times that of the standard deviation of the signals obtained from blank, clean paper strips (6 replicates).

A.3 Results and Discussion

A.3.1 Paper Strip Position Optimization

It has previously been shown that satisfactory analytical performance for cocaine analysis by PS-MS is not strongly dependent on positioning of the PS interface in front of the MS inlet.[165] However, there do not appear to be many other positional PS optimization studies published for different analytes in the literature. Rather, PS interfaces are typically fixed at a single distance

from the MS inlet for the analyses of multiple compounds.[171, 177-178] Figure A.2 shows an optimization of the distance between the MS entrance cone and tip of the paper strip along the x-axis (see Figure A.1) for the simultaneous measurement of 10 µL samples containing 85 pg fentanyl and 970 pg norfentanyl. Figure A.2 shows a strong dependence of paper tip position (linear distance from the cone over the range of 0 to 1.5 cm) on analytical sensitivity for norfentanyl but not fentanyl. This suggests that optimal PS interface positioning may have a dramatic impact on signal intensity and that optimum distances may be analyte-specific. All analyses described here were conducted with a distance of 0.7 cm between MS cone and paper tip, the best position for both fentanyl and norfentanyl measurements (Figure A.2).

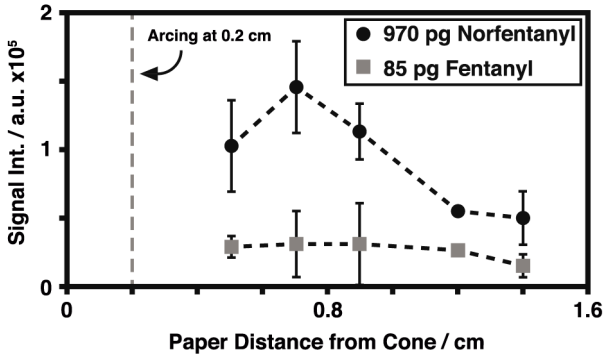

Figure A.2: Paper strip position optimization for the analyses of fentanyl and norfentanyl in a methanol standard by PS-MS. When the paper tip is positioned within 0.2 cm of the MS entrance cones, arcing is observed. All measurements were made in triplicate, and error bars represent two standard deviations.

A.3.2 Paper Preparation Optimization

In addition to paper position and paper cleaning (to reduce background[170]), the precision of the paper's cut was found to significantly affect analytical performance of PS-MS. Figure A.3 shows a comparison of the raw signals obtained for a loading of 85 pg fentanyl and 1.3 ng fentanyl-d_5 using 'good' and 'poorly' cut paper (Figure A.3 panels A and B, respectively). For 'poor' cuts (intentionally made using an older carbide razor blade), ions may be emitted and lost from sharp defects along the frayed edges, reducing the number available at the tip of the paper for transfer to the mass spectrometer, resulting in the reduction or even absence of analytical signals. Cutting via a sharp carbide razor blade was found to be effective, and all paper strips were visually inspected for quality of cut before use in all presented studies. Future studies will employ a more precise and consistent method of making PS strips, such as laser cutting. While Figure A.3 shows data collection for approximately 5 min, it should be noted that quantitative results are obtained in the first few seconds of a measurement, and all results were based upon the maximum observed signal intensities.

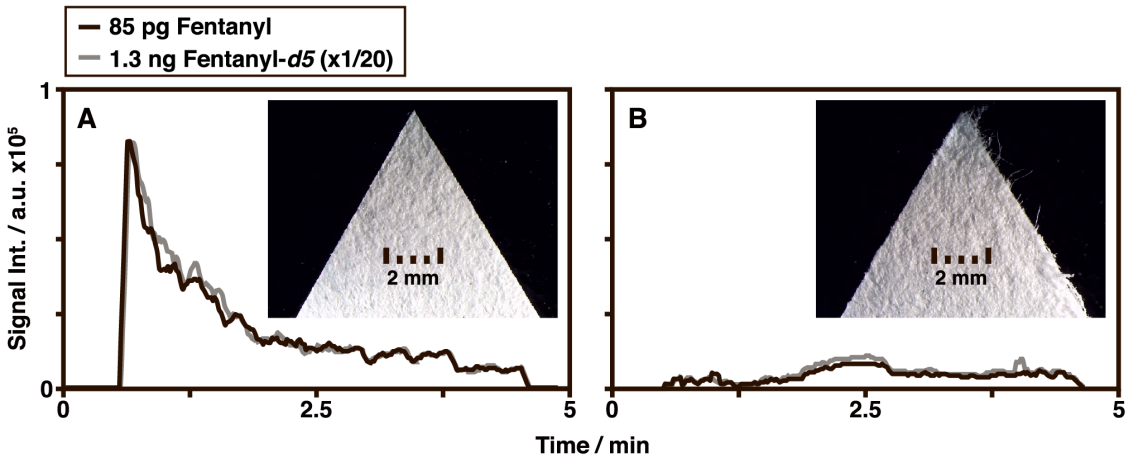

Figure A.3: Comparison of the raw signal traces for the PS-MS measurement of trace levels of fentanyl and fentanyl-d_5 (data scaled as noted for clarity) with 'good' (panel A) and 'poor' (panel B) quality paper cuts.

A.3.3 Internal Standard Correction for Matrix Effects

Figure A.3 also illustrates how closely the PS-MS internal standard signal mirrors the analyte signal, and the internal standard is therefore appropriate for signal correction. Furthermore, Figure A.5.5 shows a constant and nearly identical signal response (*i.e.* signal per unit concentration ratio of fentanyl to internal standard) for the PS-MS analysis of similar concentrations of fentanyl in three different matrices (methanol, analgesic slurry, and diluted urine) over time. The constant response across the different complex matrices indicates that any possible matrix effects in this study are mitigated by the use of the internal standard. Inter-day variability is also minimized by internal standard correction.

A.3.4 Quantitation in Complex Samples

To simulate fentanyl added to a street drug, 50 mg of over-the- counter analgesic tablet powder was suspended in 1 mL of fentanyl-spiked methanol for each individual calibration standard as described above. Calibration results are presented in Figure A.4, demonstrating a linear range of 30 to 600 ng/mL fentanyl. Remarkably, Figure A.4 also shows that the least squares fit of the calibration data for analgesic slurry samples is very similar to the data obtained using methanol standards (0.5 to 600 ng/mL; calibration slopes for methanol and analgesic slurry samples are only 6.6% different, presented in Table A.5.3). Detection limits for fentanyl in all the complex matrices studied are given in Table A.1. In the context of this study and for the measurement of fentanyl in illicit substances, Figure A.4 illustrates that it is not strictly necessary for the calibrator matrix to match that of complex samples, suggesting that the same calibration, obtained using clean analytical standards (*i.e.*, methanol instead of a slurry), may be applied to semi- quantitative measurements made in a variety of complex matrices. Instead of freshly preparing new calibrators on a regular basis, the calibration may be stored and recalled for some

time because normalization with an internal standard corrects for matrix effects and reduces inter-replicate and inter-day variability. These features provide the operational simplicity that is crucial for the use of PS-MS (or any other technique) in clinical harm reduction strategies. Lastly, a few milligrams of sample is required for each analysis. This is an important issue and essential for harm reduction, as the typical patient will not willingly part with a large fraction of a street drug they have just purchased.[153]

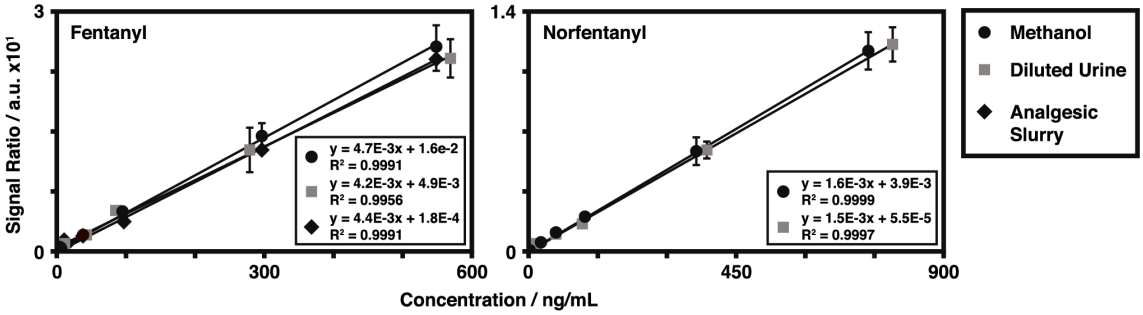

Figure A.4: Direct calibration data for fentanyl and norfentanyl in methanol, diluted urine, and an analgesic slurry. Signal ratio is calculated by dividing the analyte signal by its respective labeled internal standard signal. All measurements were made in triplicate, and error bars represent two standard deviations.

Table A.1: Estimated detection limits (concentrations and absolute amounts) for fentanyl and norfentanyl in complex matrices.

Target analyte	Methanol		Diluted urine		Analgesic slurry	
	pg/mL	pg	pg/mL	pg	pg/mL	pg
Fentanyl	49	0.4	270	3.5	660	5.3
Norfentanyl	440	3.5	6600	52	-	-

Detection limits estimated as the concentration needed to produce a signal 3 times that of the standard deviation of signals obtained from blank, clean paper strips (6 replicates).

When distinguishing recent from remote drug use, it is not sufficient to detect the presence of fentanyl alone. This distinction may, however, be provided by the relative levels of fentanyl's principal metabolite, norfentanyl, produced by hepatic and intestinal cytochrome P450 3A4.[175-176, 179] A low metabolite (norfentanyl) to parent (fentanyl) ratio in the urine suggests a shorter residence time for fentanyl in the human body.[180] Combined with high levels of both compounds, a low ratio indicates recent use, or a higher likelihood that any observed symptoms are due to fentanyl.[180] As fentanyl may be detected in urine for well over a week since last ingestion (LifeLabs, unpublished data), the concentration ratio of fentanyl to norfentanyl is also important for overdose assessment. Direct calibrations obtained for fentanyl and norfentanyl in ten-fold diluted urine are presented in Figure A.4. As before, analytical calibration in dilute urine

is comparable to that obtained for methanol standards (11% different for fentanyl, 2.6% different for norfentanyl, see Figure A.4, Table A.5.3). As emphasized earlier, the internal standard correction therefore adequately corrects for matrix effects across the complex matrices studied here. Norfentanyl detection limits are given in Table A.1. In summary, PS-MS appears to be a satisfactory direct, semi-quantitative measurement technique for both fentanyl and norfentanyl in urine.

Due to its low cost, simplicity, and potential high sample throughput, PS-MS may be used as a point-of-care screening tool in advance of or in combination with more conventional analytical techniques (*i.e.*, LC-MS). Table A.2 summarizes the measurement of fentanyl and norfentanyl in real urine samples by both LC-MS and PS-MS, where both standard addition and direct calibration quantitation techniques were used with PS-MS. Acceptable quantifier to qualifier ion ratio agreement was observed using PS-MS ($\leq$ 20% for 9 of 10 urine samples tested) for both fentanyl and norfentanyl measurements in urine (Table A.5.2). As indicated by Table A.2, the comparison of direct sampling PS-MS methods with LC-MS results shows a negative bias. Many of the LC-MS values exceed the upper limit of quantitation (40 ng/mL) and should be viewed as approximate only. Therefore, these results appear satisfactory in the context of a semi-quantitative analysis for harm reduction applications. As a negative control, no fentanyl or norfentanyl was detected by either PS-MS and LC-MS in 25 additional human urine samples.

Table A.2: Comparison of the measurement of fentanyl and norfentanyl in urine by liquid chromatography-mass spectrometry and paper spray-mass spectrometry.

Sample	Target analyte	LC-MS	PS-MS			
			Standard addition[a]		Direct calibration[b]	
		ng/mL	ng/mL	% Bias[c]	ng/mL	% Bias[c]
1	Fentanyl	49[d]	30 ± 10	-32	34 ± 19	-30
	Norfentanyl	2275[d]	900 ± 250	-61	1100 ± 200	-50
2	Fentanyl	323[d]	910 ± 240	+181	200 ± 47	-38
	Norfentanyl	1464[d]	1030 ± 230	-30	850 ± 110	-42
3	Fentanyl	12	7 ± 1	-44	9 ± 9	-28
	Norfentanyl	458[d]	310 ± 70	-33	220 ± 12	-52
4	Fentanyl	149[d]	70 ± 10	-48	53 ± 17	-65
	Norfentanyl	5654[d]	3520 ± 730	-38	3130 ± 13	-45
5	Fentanyl	81[d]	120 ± 50	+48	71 ± 31	-13
	Norfentanyl	758[d]	510 ± 130	-33	360 ± 80	-52
6	Fentanyl	11	7 ± 1	-40	10 ± 10	-9
	Norfentanyl	59[d]	60 ± 14	+2	82 ± 19	+39
7	Fentanyl	5.0	4 ± 1	-21	8 ± 8	+51
	Norfentanyl	42[d]	23 ± 8	-45	17 ± 14	-61
8	Fentanyl	37	27 ± 4	-28	24 ± 12	-36
	Norfentanyl	354[d]	180 ± 20	-49	186 ± 14	-47
9	Fentanyl	135[d]	110 ± 16	-18	90 ± 11	-33
	Norfentanyl	1873[d]	790 ± 130	-58	740 ± 14	-60
10	Fentanyl	99[d]	47 ± 16	-53	38 ± 12	-62
	Norfentanyl	1756[d]	2460 ± 360	+40	860 ± 14	-51

		Average	Average
		% Bias	% Bias
	Fentanyl	-6 ± 72[e]	-31 ± 31[e]
	Norfentanyl	-26 ± 33[e]	-42 ± 29[e]

[a] Mean ± standard deviation (n = 3)

[b] Uncertainties calculated by the method of least squares (n = 3)

[c] % Bias calculated as (PS result - LC result)/LC result ×100%

[d] Above the analytical measurement range for the LC-MS assay (0.5–40 ng/mL)

[e] Uncertainties represent standard deviations in the % Biases

To examine if a statistical difference exists between the PS-MS results obtained using standard addition and direct calibration, a paired *t*-test was conducted. The calculated *t* values for fentanyl and norfentanyl analyses were 1.13 and 0.827, respectively. Both are below the tabulated *t* value of 2.262 (95% confidence), indicating that the two PS-MS measurement methods do not produce significantly different results. While both quantitation strategies (standard addition and direction calibration) are feasible, it is more likely that direct calibration would be the route taken for a harm reduction setting as discussed earlier. Furthermore, we

believe the magnitude of bias for PS-MS measurements compared with LC-MS results (Table A.2) is acceptable given the cost, speed, and simplicity of PS-MS, and because many of the reported LC-MS results are above the analytical measurement range. While the discrepancies for some samples would not be acceptable for a candidate quantitative method, we believe the clinical need in harm reduction is for semi-quantitative analysis only: in that context, the performance of PS-MS is more than sufficient, especially when combined with its speed and simplicity.

A.4 Conclusions

Fentanyl and norfentanyl were analyzed in complex sample matrices by both PS-MS and LC-MS. The results demonstrate that PS-MS is a sensitive and selective direct detection method for trace levels in a variety of complex matrices, including urine and an analgesic tablet slurry. Because of its simplicity, selectivity and sensitivity, PS-MS is a promising candidate analytical technique for implementation in point-of-care opioid harm reduction strategies. It is important to note that PS- MS may also be of equal value for use in enforcement as well as emergency room scenarios where rapid, specific results can provide life-saving information. PS-MS also shows high potential as a rapid semi-quantitative pre-screening technique in advance of more comprehensive (and regulated) LC-MS or GC–MS methods. Current and future work is focused on expanding the suite of opioids and metabolites detected (including a wide range of fentanyl analogs), system and data handling automation, and incorporating PS with portable and field operable mass spectrometer systems for on-site use.

A.5 Supporting Information

Table A.5.1: MS scan parameters.

Target analyte	Molar mass g/mol	MS transition *m/z*	Inlet cone V	Collision energy eV
Fentanyl	336.47	337→188[a]	40	25
		337→105[b]	40	40
Fentanyl-d_5	341.51	342→188	40	25
Norfentanyl	232.33	233→84[a]	35	20
		233→55[b]	35	35
Norfentanyl-d_5	237.36	238→84	35	20

[a] Quantifier ion
[b] Qualifier ion

Table A.5.2: Signal ratios of quantifier to qualifier ions for fentanyl and norfentanyl.

	Fentanyl Signals				Norfentanyl Signals			
	337→188	337→105	Ratio[b]		233→84	233→55	Ratio[b]	
Analytical standard[a]								
Trial 1	8.7×10^3	7.9×10^3	1.1		4.7×10^4	8.8×10^3	5.4	
Trial 2	1.3×10^5	1.2×10^5	1.1		2.0×10^5	4.0×10^4	5.0	
Trial 3	4.2×10^4	3.7×10^4	1.1		2.2×10^5	3.6×10^4	6.1	
Trial 4	1.3×10^5	1.3×10^5	0.99		2.6×10^5	4.6×10^4	5.5	
Trial 5	1.2×10^4	1.3×10^4	0.95		2.2×10^5	3.3×10^4	6.6	
Trial 6	6.1×10^4	5.2×10^4	1.2		2.9×10^5	5.3×10^3	5.5	
Average			1.1				5.7	
% RSD			7.6				10	
	337→188	337→105	Ratio[b]	% Diff.[c]	233→84	233→55	Ratio[b]	% Diff.[c]
Urine samples								
1	1.6×10^4	1.3×10^4	1.2	9.3	4.8×10^4	8.6×10^3	6.0	6.1
2	1.9×10^4	1.5×10^4	1.3	16	1.6×10^4	2.7×10^3	5.9	4.3
3	5.5×10^2	5.5×10^2	1.0	7.5	3.6×10^3	6.6×10^2	5.4	5.6
4	1.1×10^3	1.0×10^3	1.1	5.0	1.3×10^5	2.2×10^4	6.0	6.1
5	4.4×10^3	4.2×10^3	1.0	2.6	1.0×10^4	2.2×10^3	4.6	21
6	1.7×10^2	3.0×10^2	0.59[d]	59	2.7×10^3	8.2×10^2	3.3[d]	54
7	8.7×10^2	1.0×10^3	0.88	20	1.4×10^4	6.5×10^2	5.4	5.6
8	1.9×10^3	2.1×10^3	0.93	15	3.3×10^3	6.4×10^2	5.1	12
9	4.9×10^3	4.1×10^3	1.2	10	2.1×10^4	3.5×10^3	5.9	4.3
10	5.2×10^3	5.5×10^3	0.95	12	4.3×10^4	6.8×10^3	6.2	9.4

[a] Mixed standard containing 11 ng/mL fentanyl and 89 ng/mL norfentanyl in methanol

[b] Calculated as the ratio of signal from the quantifier ion to that of the qualifier ion

[c] Percent difference between the ion ratio for a particular urine sample and the average analytical standard ion ratio

[d] Excessive deviation the combined result of possible isobaric interference (complex sample) and low signal intensities

Table A.5.3: Percent differences of calibration curve slopes in complex matrices relative to calibration curve slopes in methanol

Target analyte	Diluted Urine	Analgesic Slurry
	% Difference	% Difference
Fentanyl	11	6.6
Norfentanyl	4.7	-

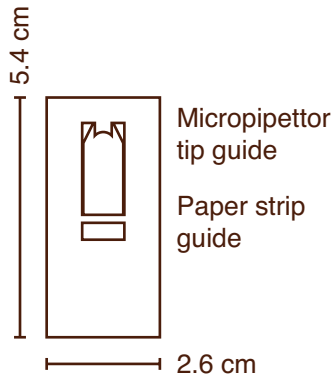

Figure A.5.1: Schematic diagram of 3D printed guide for consistent sample spotting on paper strips. The guide is placed over top of a paper strip. The bottom of the paper strip is aligned with the 'paper strip guide,' while the micropipettor tip is aligned with the 'micropipettor tip guide' while spotting the sample.

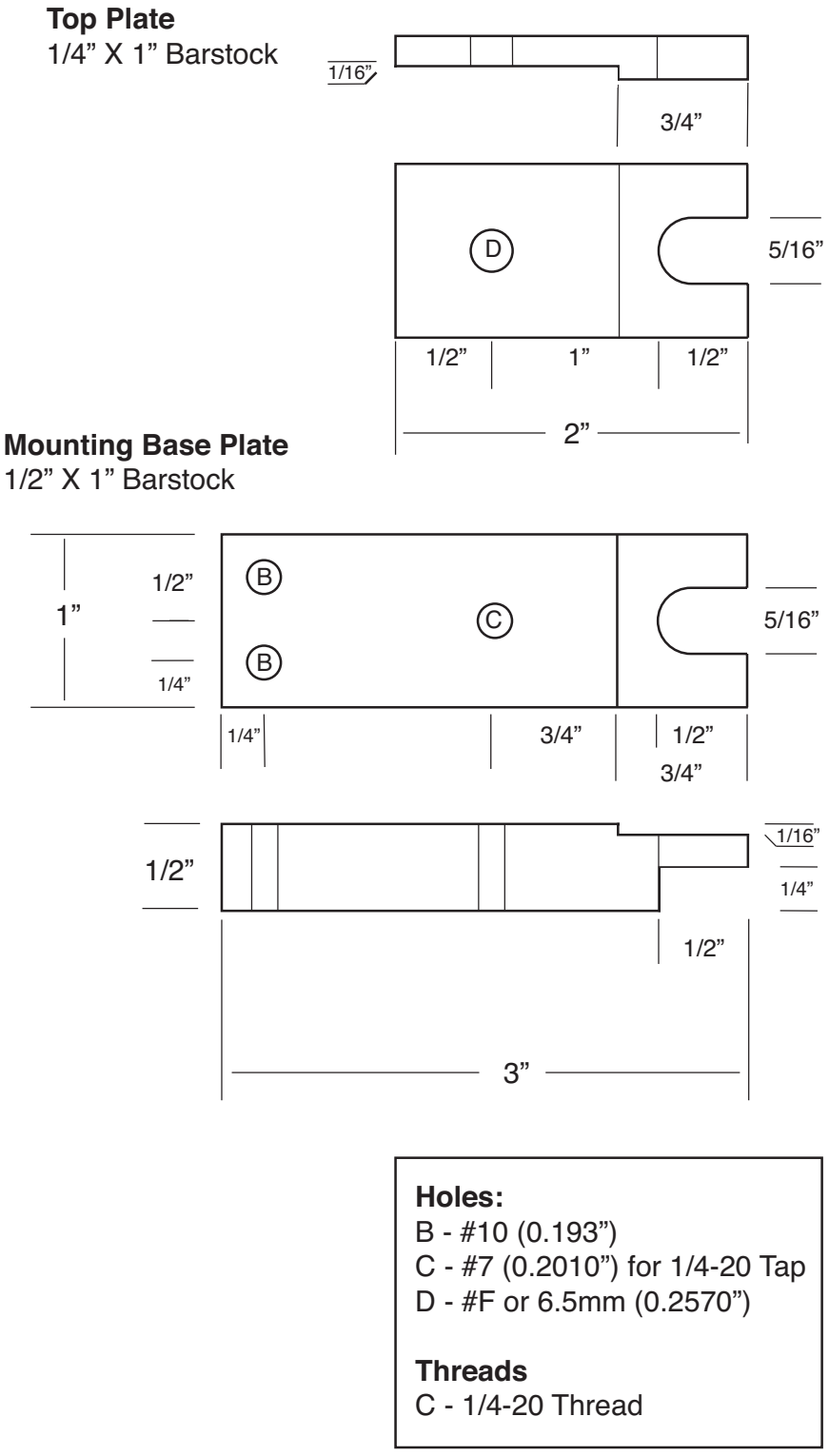

Figure A.5.2: Schematic diagram of the aluminum paper spray sample mount.

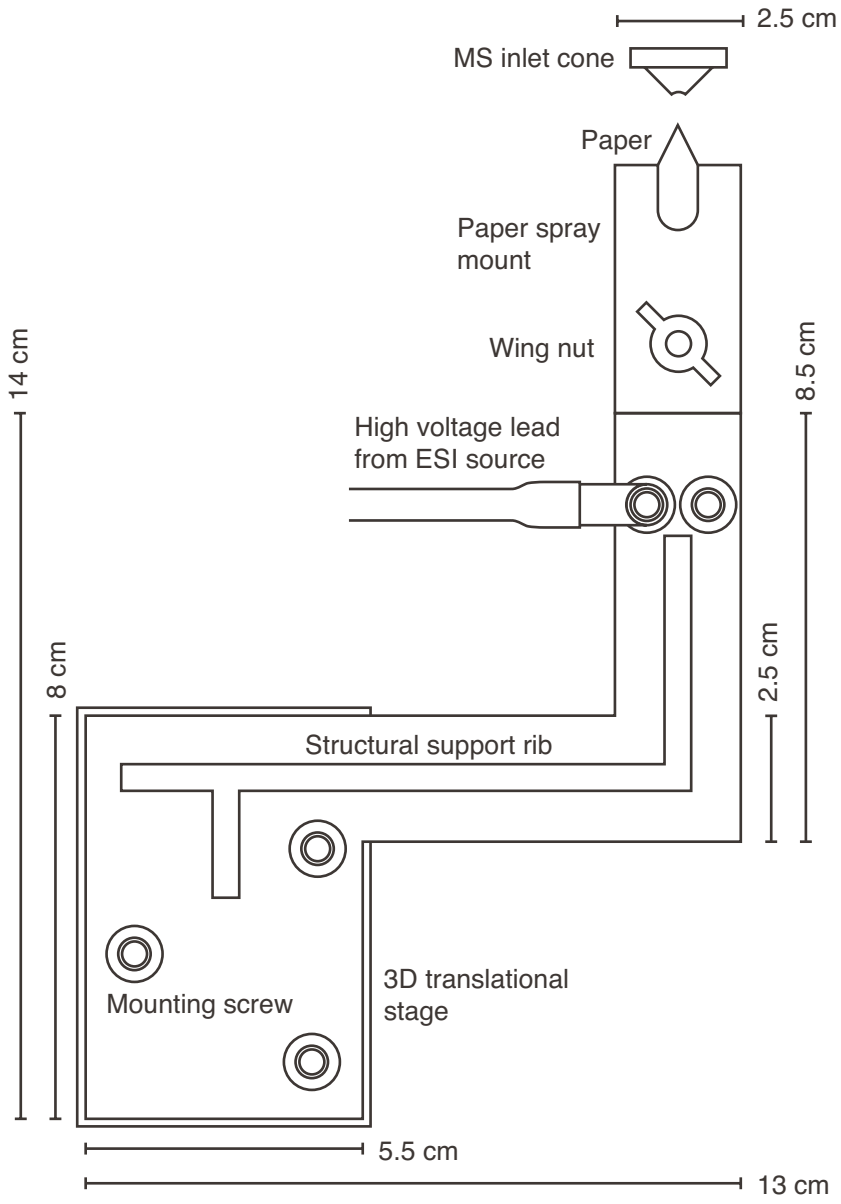

Figure A.5.3: Schematic of 3D printed mounting arm for the paper spray sample mount.

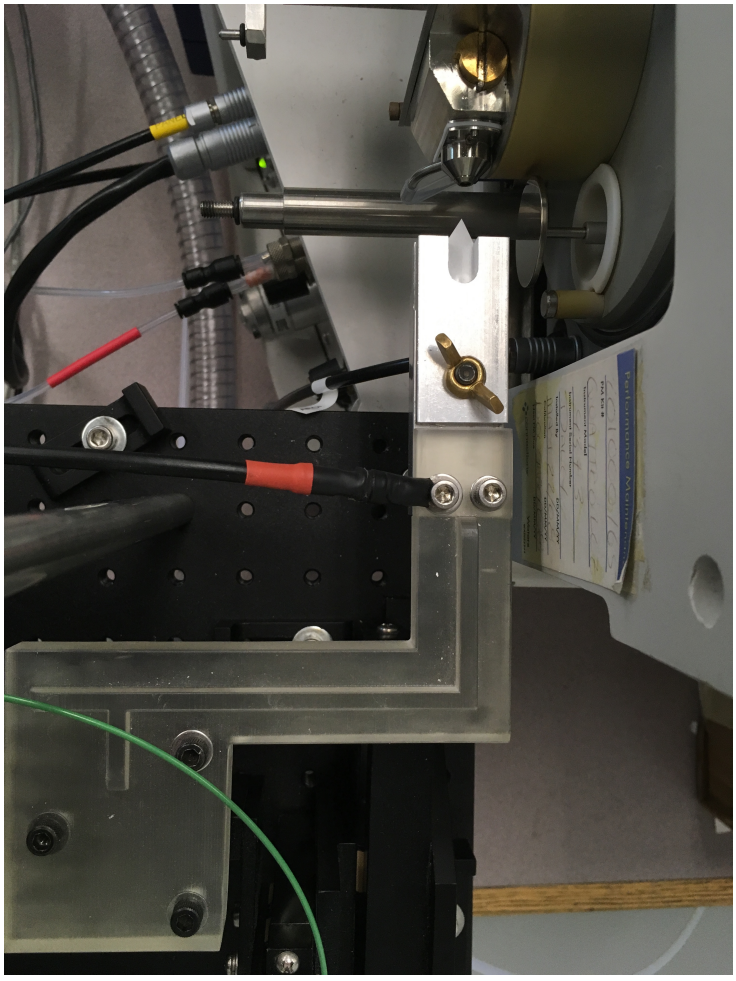

Figure A.5.4: Photograph of PS-MS interface mounted on the mass spectrometer system.

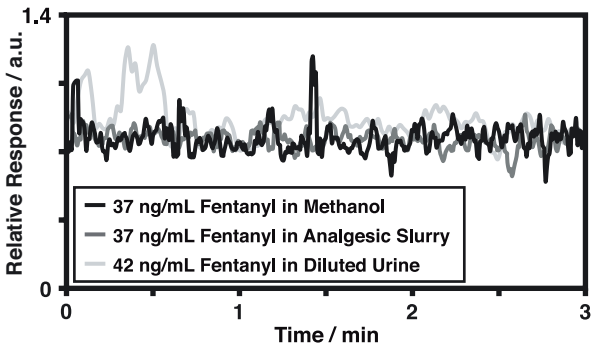

Figure A.5.5: Relative fentanyl response plots for continuous measurements made in complex matrices using PS-MS. The similar relative response over time indicates that pre-spiking the paper strip with internal standard (10 μL of 169 ng/mL fentanyl-d_5) sufficiently corrects for any matrix effects for the complex matrices examined. Relative response is calculated as [(fentanyl signal)/(fentanyl concentration)]/[(fentanyl-d_5 signal)/(fentanyl-d_5 concentration)].

Bibliography

1. Kondrat, R. W.; Cooks, R. G. Direct Analysis of Mixtures by Mass Spectrometry. *Anal. Chem.* **1978**, *50*, 81A-92A.
2. Monge, M. E.; Harris, G. A.; Dwivedi, P.; Fernández, F. M. Mass Spectrometry: Recent Advances in Direct Open Air Surface Sampling/Ionization. *Chem. Rev.* **2013**, *113*, 2269-2308.
3. Cooks, R. G.; Ouyang, Z.; Takats, Z.; Wiseman, J. M. Ambient Mass Spectrometry. *Science* **2006**, *311*, 1566-1570.
4. Gross, J. H., *Mass Spectrometry*. 2nd ed.; Springer: Heidelburg, Germany, 2011.
5. Byliński, H.; Gębicki, J.; Dymerski, T.; Namieśnik, J. Direct Analysis of Samples of Various Origin and Composition Using Specific Types of Mass Spectrometry. *Crit. Rev. Anal. Chem.* **2017**, *47*, 340-358.
6. Duncan, K. D.; McCauley, E. P. B.; Krogh, E. T.; Gill, C. G. Characterization of a condensed-phase membrane introduction mass spectrometry (CP-MIMS) interface using a methanol acceptor phase coupled with electrospray ionization for the continuous on-line quantitation of polar, low-volatility analytes at trace levels in complex aqueous samples. *Rapid Commun. Mass Spectrom.* **2011**, *25*, 1141-1151.
7. Willis, M. D.; Duncan, K. D.; Krogh, E. T.; Gill, C. G. Delicate polydimethylsiloxane hollow fibre membrane interfaces for condensed phase membrane introduction mass spectrometry (CP-MIMS). *Rapid Commun. Mass Spectrom.* **2014**, *28*, 671-681.
8. Duncan, K. D.; Vandergrift, G. W.; Krogh, E. T.; Gill, C. G. Ionization suppression effects with condensed phase membrane introduction mass spectrometry: methods to increase the linear dynamic range and sensitivity. *J. Mass Spectrom.* **2015**, *50*, 437-443.
9. Vandergrift, G. W.; Krogh, E. T.; Gill, C. G. Polymer Inclusion Membranes with Condensed Phase Membrane Introduction Mass Spectrometry (CP-MIMS): Improved Analytical Response Time and Sensitivity. *Anal. Chem.* **2017**, *89*, 5629-5636.
10. Vandergrift, G. W.; Monaghan, J.; Krogh, E. T.; Gill, C. G. Direct Analysis of Polyaromatic Hydrocarbons in Soil and Aqueous Samples Using Condensed Phase Membrane Introduction Tandem Mass Spectrometry with Low-Energy Liquid Electron Ionization. *Anal. Chem.* **2019**, *91*, 1587-1594.
11. Termopoli, V.; Torrisi, E.; Famiglini, G.; Palma, P.; Zappia, G.; Cappiello, A.; Vandergrift, G. W.; Zvekic, M.; Krogh, E. T.; Gill, C. G. Mass Spectrometry Based Approach for Organic Synthesis Monitoring. *Anal. Chem.* **2019**, *91*, 11916-11922.
12. Vandergrift, G. W.; Lattanzio-Battle, W.; Krogh, E. T.; Gill, C. G. Condensed Phase Membrane Introduction Mass Spectrometry with In Situ Liquid Reagent Chemical Ionization in a Liquid Electron Ionization Source (CP-MIMS-LEI/CI). *J. Am. Soc. Mass Spectrom.* **2020**, *31*, 908-916.
13. Vandergrift, G. W.; Hessels, A. J.; Palaty, J.; Krogh, E. T.; Gill, C. G. Paper spray mass spectrometry for the direct, semi-quantitative measurement of fentanyl and norfentanyl in complex matrices. *Clin. Biochem.* **2018**, *54*, 106-111.
14. Johnson, R. C.; Cooks, R. G.; Allen, T. M.; Cisper, M. E.; Hemberger, P. H. Membrane introduction mass spectrometry: trends and applications. *Mass Spectrom. Rev.* **2000**, *19*, 1.

15. Ketola, R. A.; Kotiaho, T.; Cisper, M. E. Environmental applications of membrane introduction mass spectrometry. *J. Mass Spectrom.* **2002**, *37*, 457-476.
16. Davey, N. G.; Krogh, E. T.; Gill, C. G. Membrane-introduction mass spectrometry (MIMS). *Trends Anal. Chem.* **2011**, *30*, 1477-1485.
17. Krogh, E. T.; Gill, C. G. Membrane introduction mass spectrometry (MIMS): a versatile tool for direct, real-time chemical measurements. *J. Mass Spectrom.* **2014**, *49*, 1205-1213.
18. Cussler, E. L., *Diffusion, Mass transfer in fluid systems*. Cambridge University Press: New York, NY, 1984.
19. VanHassel, E.; Bier, M. E. An electrospray membrane probe for the analysis of volatile and semi-volatile organic compounds in water. *Rapid Comm. Mass Spectrom.* **2007**, *21*, 413-420.
20. LaPack, M. A.; Tou, J. C.; Enke, C. G. Membrane mass spectrometry for the direct trace analysis of volatile organic compounds in air and water. *Anal. Chem.* **1990**, *62*, 1265-1271.
21. Alberici, R.; Sparrapan, R.; Eberlin, M. N.; Windmoller, D.; Augusti, R. Polyetherimide-silicon: a 10 um ultrathin composite membrane for faster and more sensitive membrane introduction mass spectrometry analysis. *Anal. Commun.* **1999**, *36*, 221-223.
22. Sgarlata, C.; Arena, G.; Longo, E.; Zhang, D.; Yang, Y.; Bartsch, R. A. Heavy metal separation with polymer inclusion membranes. *J. Membr. Sci.* **2008**, *323*, 444-451.
23. Kaya, A.; Onac, C.; Alpoguz, H. K.; Agarwal, S.; Gupta, V. K.; Atar, N.; Yilmaz, A. Reduced graphene oxide based a novel polymer inclusion membrane: Transport studies of Cr(VI). *J. Mol. Liq.* **2016**, *219*, 1124-1130.
24. Yildiz, Y.; Manzak, A.; Tutkun, O. Selective extraction of cobalt ions through polymer inclusion membrane containing Aliquat 336 as a carrier. *Desalin. Water Treat.* **2016**, *57*, 4616-4623.
25. Gelotte, K. M.; Lostritto, R. T. Solvent Interaction with Polydimethylsiloxane Membranes and Its Effects on Benzocaine Solubility and Diffusion. *Pharm. Res.* **1990**, *7*, 523-529.
26. Jánská, M.; Lehotay, S. J.; Mastovská, K.; Hajslova, J.; Alon, T.; Amirav, A. A simple and inexpensive "solvent in silicone tube extraction" approach and its evaluation in the gas chromatographic analysis of pesticides in fruites and vegetables. *J. Sep. Sci.* **2006**, *29*, 66-80.
27. Garcia-Rodríguez, A.; Matamoros, V.; Kolev, S. D.; Fontàs, C. Development of a polymer inclusion membrane (PIM) for the preconcentration of antibiotics in environmental water samples. *J. Membr. Sci.* **2015**, *492*, 32-39.
28. Zeng, W.; Du, Y.; Xue, Y.; Frisch, H. L., Solubility Parameters. In *Physical Properties of Polymers*, 2nd ed.; Mark, J. E., Ed. American Chemical Society: Washington, DC, 1993; pp 289-303.
29. Duncan, K. D.; Letourneau, D. R.; Vandergrift, G. W.; Jobst, K. J.; Reiner, E. J.; Gill, C. G.; Krogh, E. T. A semi-quantitative approach for the rapid screening and mass profiling of naphthenic acids directly in contaminated aqueous samples. *J. Mass Spectrom.* **2015**, *51*, 44-52.
30. SRC Physical Properties Database. http://esc.syrres.com/fatepointer/search.asp (accessed August 1, 2018).
31. Twist, J. N.; Zatz, J. L. *J. Pharm. Sci.* **1988**, *77*, 536-540.
32. Iribarne, J. V.; Thomson, B. A. On the evaporation of small ions from charged droplets. *J. Chem. Phys.* **1975**, *64*, 2287-2294.
33. Pape, J.; Vikse, K. L.; Janusson, E.; Taylor, N.; McIndoe, J. S. Solvent effects on surface activity of aggregate ions in

electrospray ionization. *Int. J. Mass Spectrom.* **2014**, *373*, 66-71.
34. Duncan, K. D.; Willis, M. D.; Krogh, E. T.; Gill, C. G. A miniature condensed-phase membrane introduction mass spectrometry (CP-MIMS) probe for direct and on-line measurements of pharmaceuticals and contaminants in small, complex samples. *Rapid Commun. Mass Spectrom.* **2013**, *27*, 1213-1221.
35. Duncan, K. D.; Volmer, D. A.; Gill, C. G.; Krogh, E. T. Rapid Screening of Carboxylic Acids from Waste and Surface Water by ESI-MS/MS Using Barium Ion Chemistry and On-Line Membrane Sampling. *J. Am. Soc. Mass. Spectrom.* **2015**, *27*, 443-450.
36. Termopoli, V.; Famiglini, G.; Palma, P.; Cappiello, A.; Vandergrift, G. W.; Krogh, E. T.; Gill, C. G. Condensed Phase Membrane Introduction Mass Spectrometry with Direct Electron Ionization: On-line Measurement of PAHs in Complex Aqueous Samples. *J. Am. Soc. Mass. Spectrom.* **2015**, *27*, 301-308.
37. King, R.; Bonfiglio, R.; Fernandez-Metzler, C.; Miller-Stein, C.; Olah, T. Mechanistic investigation of ionization suppression in electrospray ionization. *J. Am. Soc. Mass. Spectrom.* **2000**, *11*, 942-950.
38. Annesley, T. M. Ion suppression in mass spectrometry. *Clin. Chem.* **2003**, *49*, 1041-1044.
39. Matuszewski, B. K.; Constanzer, M. L.; Chavez-Eng, C. M. Strategies for the assessmenet of matrix effect in quantitative bioanalytical methods based on HPLC-MS/MS. *Anal. Chem.* **2003**, *75*, 3019-3030.
40. Taylor, P. J. Matrix effects: The Achilles heel of quantitative high-performance liquid chromatography-electrospray-tandem mass spectrometry. *Clin. Biochem.* **2005**, *38*, 328-334.
41. Headley, J. V.; Peru, K. M.; Barrow, M. P.; Derrick, P. J. Characterization of Naphthenic Acids from Athabasca Oil Sands Using Electrospray Ionization: The Significant Influence of Solvents. *Anal. Chem.* **2007**, *79*, 6222-6229.
42. Barrow, M. P.; Witt, M.; Headley, J. V.; Peru, K. M. Athabasca Oil Sands Process Water: Characterization by Atmospheric Pressure Photoionization and Electrospray Ionization Fourier Transform Ion Cyclotron Resonance Mass Spectrometry. *Anal. Chem.* **2010**, *82*, 3727-3735.
43. Headley, J. V.; Barrow, M. P.; Peru, K. M.; Fahlman, B.; Frank, R. A.; Bickerton, G.; McMaster, M. E.; Parrott, J.; Hewitt, L. M. Preliminary fingerprinting of Athabasca oil sands polar organics in environmental samples using electrospray ionization Fourier transform ion cyclotron resonance mass spectrometry. *Rapid Commun. Mass Spectrom.* **2011**, *25*, 1899-1909.
44. Headley, J. V.; Peru, K. M.; Barrow, M. P. Mass spectrometric characterization of naphthenic acids in environmental samples: A review. *Mass Spectrom. Rev.* **2009**, *28*, 121-134.
45. Headley, J. V.; Peru, K. M.; Barrow, M. P. Advances in mass spectrometric characterization of naphthenic acids fraction compounds in oil sands environmental samples and crude oil—a review. *Mass Spectrom. Rev.* **2015**, *35*, 311-328.
46. Headley, J. V.; Peru, K. M.; McMartin, D. W.; Winkler, M. Determination of Dissolved Naphthenic Acids in Natural Waters by Using Negative-Ion Electrospray Mass Spectrometry. *J. AOAC Int.* **2002**, *85*, 182-187.
47. United States Environmental Protection Agency Priority Pollutant List. http://www.epa.gov/sites/production/files/2015-09/documents/priority-pollutant-list-epa.pdf (accessed July 10, 2018).
48. Slezakova, K.; Pires, J. C. M.; Castro, D.; Alvim-Ferraz, M. C. M.;

Delerue-Matos, C.; Morais, S.; Pereira, M. C. PAH air pollution at a Portuguese urban area: carcinogenic risks and sources identification. *Environ. Sci. Pollut. Res.* **2013**, *20*, 3932-3945.
49. Mirabelli, M. F.; Zenobi, R. Solid-Phase Microextraction Coupled to Capillary Atmospheric Pressure Photoionization-Mass Spectrometry for Direct Analysis of Polar and Nonpolar Compounds. *Anal. Chem.* **2018**, *90*, 5015-5022.
50. Krüger, O.; Christoph, G.; Kalbe, U.; Berger, W. Comparison of stir bar sorptive extraction (SBSE) and liquid-liquid extraction (LLE) for the analysis of polycyclic aromatic hydrocarbons (PAH) in complex aqueous matrices. *Talanta* **2011**, *85*, 1428-1434.
51. Law, R. J.; Dawes, V. J.; Woodhead, R. J.; Matthiessen, P. Polycyclic Aromatic Hydriocarbons (PAH) in Seawater around England and Wales. *Mar. Pollut. Bull.* **1997**, *34*, 306-322.
52. García-Falcón, M. S.; Cancho-Grande, B.; Simal-Gándara, J. Stirring bar sorptive extraction in the determination of PAHs in drinking waters. *Water Res.* **2004**, *38*, 1679-1684.
53. Kolahgar, B.; Hoffmann, A.; Heiden, A. C. Application of stir bar sorptive extraction to the determination of polycyclic aromatic hydrocarbons in aqueous samples. *J. Chromatogr. A* **2002**, *963*, 225-230.
54. Prieto, A.; Telleria, O.; Etxebarria, N.; Fernández, L. A.; Usobiaga, A.; Zuloaga, O. Simultaneous preconcentration of a wide variety of organic pollutants in water samples. Comparison of stir bar sorptive extraction and membrane-assisted solvent extraction. *J. Chromatogr. A* **2008**, *1214*, 1-10.
55. Rodil, R.; Schellin, M.; Popp, P. Analysis of polycyclic aromatic hydrocarbons in water and beverages using membrane-assisted solvent extraction in combination with large volume injection-gas chromatography-mass spectrometric detection. *J. Chromatogr. A* **2007**, *1163*, 288-297.
56. Egli, S. N.; Butler, E. D.; Bottaro, C. S. Selective extraction of light polycyclic aromatic hydrocarbons in environmental water samples with pseudo-template thin-film molecularly imprinted polymers. *Anal. Methods* **2015**, *7*, 2028-2035.
57. Cresswell, S. L.; Haswell, S. J. Evaluation of on-line methodology for microwave-assisted extraction of polycyclic aromatic hydrocarbons (PAHs) from sediment samples. *Analyst* **1999**, *124*, 1361-1366.
58. Shu, Y. Y.; Lao, R. C.; Chiu, C. H.; Turle, R. Analysis of polycyclic aromatic hydrocarbons in sediment reference materials by microwave-assisted extraction. *Chemosphere* **2000**, *41*, 1709-1716.
59. Afanasov, I. M.; Kepman, A. V.; Morozov, V. A.; Seleznev, A. N.; Avdeev, V. V. Determination of Polyaromatic Hydrocarbons in Coal Tar Pitch. *J. Anal. Chem.* **2009**, *64*, 361-365.
60. Yamada, T. M.; Souza, D. A.; Morais, C. R.; Mozeto, A. A. Validation of a Method for the Analysis of PAHs in Bulk Lake Sediments Using GC-MS. *J. Chromatogr. Sci.* **2009**, *47*, 794-799.
61. Hawthorne, S. B.; Grabanski, C. B.; Martin, E.; Miller, D. J. Comparisons of Soxhlet extraction, pressurized liquid extraction, supercritical fluid extraction and subcritical water extraction for environmental solids: recovery, selectivity and effects on sample matrix. *J. Chromatogr. A* **2000**, *892*, 421-433.
62. Ramos, L.; Vreuls, J. J.; Brinkman, U. A. T. Miniaturised pressurised liquid extraction of polycyclic aromatic hydrocarbons from soil and sediment with subsequent large-volume injection-gas chromatography. *J. Chromatogr. A* **2000**, *891*, 275-286.

63. Fuoco, R.; Ceccarini, A.; Onor, M.; Marrara, L. Analysis of priority pollutants in environmental samples by on-line supercritical fluid chromatography cleanup–cryo-trap–gas chromatography–mass spectrometry. *J. Chromatogr. A* **1999**, *846*, 387-393.
64. Tomy, G. T.; Halldorson, T.; Chernomas, G.; Bestvater, L.; Danegerfield, K.; Ward, T.; Pleskach, K.; Stern, G.; Atchison, S.; Majewski, A.; Reist, J. D.; Palace, V. P. Polycyclic Aromatic Hydrocarbon Metabolites in Arctic Cod (Boreogadus saida) from the Beaufort Sea and Associative Fish Health Effects. *Environ. Sci. Technol.* **2014**, *48*, 11629-11636.
65. Coelho, E.; Ferreira, C.; Almeida, C. M. M. Analysis of polynuclear aromatic hydrocarbons by SPME-GC-FID in environmental and tap waters. *J. Braz. Chem. Soc.* **2008**, *19*, 1084-1097.
66. Poster, D. L.; Schantz, M. M.; Sander, L. C.; Wise, S. A. Analysis of polycyclic aromatic hydrocarbons (PAHs) in environmental samples: a critical review of gas chromatographic (GC) methods. *Anal. Bioanal. Chem.* **2006**, *386*, 859-881.
67. Crompton, T. R., *Determination of Organic Compounds in Natural and Treated Waters*. E & FN Spon: London New York, 2000.
68. Frandsen, H.; Janfelt, C.; Lauritsen, F. R. Fast and direct screening of polyaromatic hydrocarbon (PAH)-contaminated sand using a miniaturized membrane inlet mass spectrometer (mini-MIMS). *Rapid Comm. Mass Spectrom.* **2007**, *21*, 1574-1578.
69. Mirabelli, M. F.; Gionfriddo, E.; Pawliszyn, J.; Zenobi, R. A quantitative approach for pesticide analysis in grape juice by direct interfacing of a matrix compatible SPME phase to dielectric barrier discharge ionization-mass spectrometry. *Analyst* **2018**, *143*, 891-899.
70. Seemann, B.; Alon, T.; Tsizin, S.; Fialkov, A. B.; Amirav, A. Electron ionization LC-MS with supersonic molecular beams—the new concept, benefits and applications. *J. Mass Spectrom.* **2015**, *50*, 1252-1263.
71. Cappiello, A.; Famiglini, G.; Palma, P.; Pierini, E.; Termopoli, V.; Trufelli, H. Overcoming Matrix Effects in Liquid Chromatography - Mass Spectrometry. *Anal. Chem.* **2008**, *80*, 9343-9348.
72. Termopoli, V.; Famiglini, G.; Palma, P.; Piergiovanni, M.; Cappiello, A. Atmospheric Pressure Vaporization Mechanism for Coupling a Liquid Phase with Electron Ionization Mass Spectrometry. *Anal. Chem.* **2017**, *89*, 2049-2056.
73. Krogh, E. T.; Gill, C. G., Condensed Phase Membrane Introduction Mass Spectrometry - Continuous, Direct and Online Measurements in Complex Samples. In *Advances in the Use of Liquid Chromatography Mass Spectrometry (LC-MS): Instrumentation Developments and Applications*, Cappiello, A.; Palma, P., Eds. Elsevier: Amsterdam, NL, 2018; pp 173-200.
74. Russ, C. W.; Prest, H. F.; Kernan, J. T. Axial magnetic ion source and related ionization methods. 2015.
75. Mason, E. A.; McDaniel, E. W., *Transport Properties of Ions in Gases*. Wiley-VCH Verlag GmbH & Co. KGaA: Weinheim, Germany, 1988.
76. Jiménez-González, C.; Curzons, A. D.; Constable, D. J. C.; Cunningham, V. L. Expanding GSK's solvent selection guide - application of life cycle assessment to enhance solvent selections. *Clean Technol. Environ. Policy* **2004**, *7*, 42-50.
77. Boden, A. R.; Reiner, E. J. Development of an isotope-dilution gas chromatographic-mass spectrometric method for the analysis of polycyclic aromatic compounds in environmental

matrices. *Polycyclic Aromat. Compd.* **2004**, *24*, 309-323.
78. Mosi, A. A.; Cullen, W. R.; Eigendorf, G. K. Ion–Molecule Reactions of Halocarbon Cations with Polycyclic Aromatic Hydrocarbons in a Quadrupole Ion Trap Part I—Differentiation of Structural Isomers. *J. Mass Spectrom.* **1997**, *32*, 864-874.
79. Powell, J. R.; Voisinet, D.; Salazar, A.; Acree Jr., W. E. Solubility of Pyrene in Organic Nonelectrolyte Solvents - Comparison of Observed versus Predicted Values based upon Mobile Order Theory. *Phys. Chem. Liq.* **1994**, *28*, 269-276.
80. Roy, L. E.; Hernandez, C. E.; Acree Jr., W. E. Thermodynamics of Mobile Order Theory. Part 3. Comparison of Experimental and Predicted Solubilities for Fluoranthene and Pyrene. *Polycyclic Aromat. Compd.* **1999**, *13*, 205-219.
81. Chen, L.-A.; Sung, K. Direct UV Observation and Kinetic Studies of a α-Alkoxy Benzyloxy Radical. *Org. Lett.* **2009**, *11*, 3370-3373.
82. Marchetti, F.; Pampaloni, G.; Pinzino, C. Room-temperature long-lived [Nb2F11]− salts of radical cations of simple arenes: EPR, UV–Vis and DFT results. *J. Organomet. Chem.* **2011**, *696*, 1294-1300.
83. Herrera, A.; Fernández-Valle, E.; Martínez-Álvarez, R.; Molero-Vílchez, D.; Pardo-Botero, Z. D.; Sáez-Barajas, E. Monitoring organic reactions by UF-NMR spectroscopy. *Magn. Reson. Chem.* **2015**, *53*, 952-970.
84. Chen, C.-C.; Lin, P.-C. Monitoring of chemical transformations by mass spectrometry. *Anal. Methods* **2015**, *7*, 6947-6959.
85. Santos, J. C.; Reis, M. M.; Machado, R. A. F.; Bolzan, A.; Sayer, C.; Giudici, R.; Araújo, P. H. H. Online Monitoring of Suspension Polymerization Reactions Using Raman Spectroscopy. *Ind. Eng. Chem. Res.* **2004**, *43*, 7282-7289.
86. Drexler, M. T.; Foley, D. A.; Ward, H. W.; Clarke, H. J. IR and NMR Reaction Monitoring Techniques for Nucleophilic Addition Reactions: In Situ Monitoring of the Addition of Benzimidazole to a Pyridinium Salt. *Org. Process Res. Dev.* **2015**, *19*, 1119-1127.
87. Pulliam, C. J.; Bain, R. M.; Osswald, H. L.; Snyder, D. T.; Fedick, P. W.; Ayrton, S. T.; Flick, T. G.; Cooks, R. G. Simultaneous Online Monitoring of Multiple Reactions Using a Miniature Mass Spectrometer. *Anal. Chem.* **2017**, *89*, 6969-6975.
88. Luo, J.; Wu, Y.; Zijlstra, H. S.; Harrington, D. A.; McIndoe, J. S. Mass transfer and convection effects in small-scale catalytic hydrogenation. *Catal. Sci. Technol.* **2017**, *7*, 2609-2615.
89. Theron, R.; Wu, Y.; Yunker, L. P. E.; Hesketh, A. V.; Pernik, I.; Weller, A. S.; McIndoe, J. S. Simultaneous Orthogonal Methods for the Real-Time Analysis of Catalytic Reactions. *ACS Catal.* **2016**, *6*, 6911-6917.
90. Yunker, L. P. E.; Ahmadi, Z.; Logan, J. R.; Wu, W.; Li, T.; Martindale, A.; Oliver, A. G.; McIndoe, J. S. Real-Time Mass Spectrometric Investigations into the Mechanism of the Suzuki–Miyaura Reaction. *Organometallics* **2018**, *37*, 4297-4308.
91. Yan, X.; Sokol, E.; Li, X.; Li, G.; Xu, S.; Cooks, R. G. On-Line Reaction Monitoring and Mechanistic Studies by Mass Spectrometry: Negishi Cross-Coupling, Hydrogenolysis, and Reductive Amination. *Angew. Chem. Int. Ed.* **2014**, *53*, 5931-5935.
92. Huang, G.; Li, G.; Ducan, J.; Ouyang, Z.; Cooks, R. G. Synchronized Inductive Desorption Electrospray Ionization Mass Spectrometry. *Angew. Chem. Int. Ed.* **2011**, *50*, 2503-2506.
93. Cody, R. B.; Laramée, J. A.; Durst, H. D. Versatile New Ion Source for the

Analysis of Materials in Open Air under Ambient Conditions. *Anal. Chem.* **2005**, *77*, 2297-2302.
94. Crawford, E. A.; Esen, C.; Volmer, D. A. Real Time Monitoring of Containerless Microreactions in Acoustically Levitated Droplets via Ambient Ionization Mass Spectrometry. *Anal. Chem.* **2016**, *88*, 8396-8403.
95. Brodbelt, J. S.; Cooks, R. G. An exceedingly simple mass spectrometer interface with application to reaction monitoring and environmental analysis. *Anal. Chem.* **1985**, *57*, 1153-1155.
96. Johnson, R. C.; Koch, K.; Cooks, R. G. On-Line Monitoring of Reactions of Epichlorohydrin in Water Using Liquid Membrane Introduction Mass Spectrometry. *Ind. Eng. Chem. Res.* **1999**, *38*, 343-351.
97. Nelson, J. H. L.; Friesen, D. A.; Gill, C. G.; Krogh, E. T. On-line measurement of oxidative degradation kinetics for trace gasoline contaminants in aqueous solutions and natural water by membrane introduction tandem mass spectrometry. *J. Environ. Sci. Health., Part A* **2010**, *45*, 1720-1731.
98. Letourneau, D. R.; Gill, C. G.; Krogh, E. T. Photosensitized degredation kinetics of trace halogenated contaminants in natural waters using membrane introduction mass spectrometry as an *in situ* reaction monitor. *Photochem. Photobiol. Sci.* **2015**, *14*, 2108-2118.
99. Clinton, R.; Creaser, C. S.; Bryant, D. Real-time monitoring of a pharmaceutical process reaction using a membrane interface combined with atmospheric pressure chemical ionisation mass spectrometry. *Anal. Chim. Acta* **2005**, *539*, 133-140.
100. Termopoli, V.; Famiglini, G.; Palma, P.; Piergiovanni, M.; Rocio-Bautista, P.; Ottaviani, M. F.; Cappiello, A.; Saeed, M.; Perry, S. Evaluation of a liquid electron ionization liquid chromatography–mass spectrometry interface. *J. Chromatogr. A* **2019**, *1591*, 120-130.
101. Borden, S. A.; Damer, H. N.; Krogh, E. T.; Gill, C. G. Direct quantitation and characterization of fatty acids in salmon tissue by condensed phase membrane introduction mass spectrometry (CP-MIMS) using a modified donor phase. *Anal. Bioanal. Chem.* **2019**, *411*, 291-303.
102. Yamashita, A.; Norton, E. B.; Williamson, R. T.; Ho, D. M.; Sinishtaj, S.; Mansour, T. S. Use of Bis-(chiral α-methylbenzyl)glycine Esters for Synthesis of Enantiopure β-Hydroxyamino Esters. *Org. Lett.* **2003**, *5*, 3305-3308.
103. Jahnsen, R. D.; Sandberg-Schaal, A.; Vissing, K. J.; Nielsen, H. M.; Frimodt-Møller, N.; Franzyk, H. Tailoring Cytotoxicity of Antimicrobial Peptidomimetics with High Activity against Multidrug-Resistant Escherichia coli. *J. Med. Chem.* **2014**, *57*, 2864-2873.
104. Eller, K.; Henkes, E.; Rossbacher, R.; Höke, H., Amines, Aliphatic. In *Ullmann's Encyclopedia of Industrial Chemistry*, Wiley-VCH: Weinheim, 2005.
105. Porzi, G.; Sandri, S. Enantioselective synthesis of (R)-and (S)-α-aminoacids using (6S)- and (6R)-6-methyl-morpholine-2,5-dione derivatives. *Tetrahedron: Asymmetry* **1996**, *7*, 189-196.
106. Abb, M.; Heinrich, T.; Sorkau, E.; Lorenz, W. Phthalates in house dust. *Environ. Int.* **2009**, *35*, 965-970.
107. Miao, Y.; Wang, R.; Lu, C.; Zhao, J.; Deng, Q. Lifetime cancer risk assessment for inhalation exposure to di(2-ethylhexyl) phthalate (DEHP). *Environ. Sci. Pollut. Res.* **2017**, *24*, 312-320.
108. Heudorf, U.; Mersch-Sundermann, V.; Angerer, J. Phthalates: Toxicology and exposure. *Int. J. Hyg. Environ. Health* **2007**, *210*, 623-634.
109. Hirosawa, N.; Yano, K.; Suzuki, Y.; Sakamoto, Y. Endocrine disrupting effect of di-(2-ethylhexyl)phthalate on female rats and proteome analyses of their pituitaries. *PROTEOMICS* **2006**, *6*, 958-971.

110. Net, S.; Delmont, A.; Sempéré, R.; Paluselli, A.; Ouddane, B. Reliable quantification of phthalates in environmental matrices (air, water, sludge, sediment and soil): A review. *Sci. Tot. Environ.* **2015**, *515-516*, 162-180.
111. Self, R. L.; Wu, W.-H. Rapid qualitative analysis of phthalates added to food and nutraceutical products by direct analysis in real time/orbitrap mass spectrometry. *Food Control* **2012**, *25*, 13-16.
112. Hajslova, J.; Cajka, T.; Vaclavik, L. Challenging applications offered by direct analysis in real time (DART) in food-quality and safety analysis. *TrAC, Trends Anal. Chem.* **2011**, *30*, 204-218.
113. Rothenbacher, T.; Schwack, W. Rapid identification of additives in poly(vinyl chloride) lid gaskets by direct analysis in real time ionisation and single-quadrupole mass spectrometry. *Rapid Commun. Mass Spectrom.* **2010**, *24*, 21-29.
114. Schulz, S.; Wagner, S.; Gerbig, S.; Wächter, H.; Sielaff, D.; Bohn, D.; Spengler, B. DESI MS based screening method for phthalates in consumer goods. *Analyst* **2015**, *140*, 3484-3491.
115. Miao, M.; Zhao, G.; Xu, L.; Dong, J.; Cheng, P. Direct determination of trace phthalate esters in alcoholic spirits by spray-inlet microwave plasma torch ionization tandem mass spectrometry. *J. Mass Spectrom.* **2018**, *53*, 189-194.
116. Su, H.; Huang, M.-Z.; Chou, J.-H.; Chang, T.-H.; Jiang, Y.-M.; Cho, Y.-T.; Cheng, S.-C.; Wu, M.-T.; Shiea, J. High-throughput screening of phthalate-containing objects in the kindergartens by ambient mass spectrometry. *Anal. Chim. Acta* **2018**, *1039*, 65-73.
117. Bergh, C.; Torgrip, R.; Östman, C. Simultaneous selective detection of organophosphate and phthalate esters using gas chromatography with positive ion chemical ionization tandem mass spectrometry and its application to indoor air and dust. *Rapid Commun. Mass Spectrom.* **2010**, *24*, 2859-2867.
118. Jeilani, Y. A.; Cardelino, B. H.; Ibeanusi, V. M. Positive chemical ionization triple-quadrupole mass spectrometry and ab initio computational studies of the multi-pathway fragmentation of phthalates. *J. Mass Spectrom.* **2010**, *45*, 678-685.
119. Harvan, D. J.; Hass, J. R.; Albro, P. W.; Friesen, M. D. Mass spectrometry of di-(2-ethylhexyl)phthalate metabolites. *Biomed. Mass. Spectrom.* **1980**, *7*, 242-246.
120. Cappiello, A.; Famiglini, G.; Palma, P.; Mangani, F. Trace Level Determination of Organophosphorus Pesticides in Water with the New Direct-Electron Ionization LC/MS Interface. *Anal. Chem.* **2002**, *74*, 3547-3554.
121. Cappiello, A.; Famiglini, G.; Mangani, F.; Palma, P. A simple approach for coupling liquid chromatography and electron ionization mass spectrometry. *J. Am. Soc. Mass Spectrom.* **2002**, *13*, 265-273.
122. Cappiello, A.; Famiglini, G.; Palma, P.; Pierini, E.; Termopoli, V.; Trufelli, H. Direct-EI in LC-MS: towards a universal detector for small-molecule applications. *Mass Spectrom. Rev.* **2011**, *30*, 1242-1255.
123. Tsizin, S.; Bokka, R.; Keshet, U.; Alon, T.; Fialkov, A. B.; Tal, N.; Amirav, A. Comparison of electrospray LC–MS, LC–MS with Cold EI and GC–MS with Cold EI for sample identification. *Int. J. Mass Spectrom.* **2017**, *422*, 119-125.
124. Keshet, U.; Alon, T.; Fialkov, A. B.; Amirav, A. Open Probe fast GC–MS — combining ambient sampling ultra-fast separation and in-vacuum ionization for real-time analysis. *J. Mass Spectrom.* **2017**, *52*, 417-426.
125. Amirav, A.; Keshet, U.; Alon, T.; Fialkov, A. B. Open Probe fast GC–MS— Real time analysis with separation. *Int. J. Mass Spectrom.* **2014**, *371*, 47-53.

126. Creba, A. S.; Weissfloch, A. N. E.; Krogh, E. T.; Gill, C. G. An enzyme derivatized polydimethylsiloxane (PDMS) membrane for use in membrane introduction mass spectrometry (MIMS). *J. Am. Soc. Mass Spectrom.* **2007**, *18*, 973-979.
127. Angelstad, M. A.; Krogh, E. T.; Agnes, G. R.; Gill, C. G. Online measurement of phthalate–particulate matter interactions by membrane introduction mass spectrometry (MIMS). *J. Environ. Sci. Health, Part A* **2018**, *53*, 702-707.
128. NIST Chemistry WebBook. https://webbook.nist.gov/chemistry/ (accessed August 9, 2019).
129. Moneti, G.; Pieraccini, G.; Favretto, D.; Traldi, P. Acetonitrile in chemical ionization of monounsaturated hydrocarbons: a 13C and 2H labeling study. *J. Mass Spectrom.* **1998**, *33*, 1148-1149.
130. Mosi, A. A.; Cullen, W. R.; Eigendorf, G. K. Ion-Molecule Reactions of Halocarbon Cations with Polycyclic Aromatic Hydrocarbons in a Quadrupole Ion Trap. Part II - applications to environmental analysis. *J. Mass Spectrom.* **1998**, *33*, 250-263.
131. Hunter, E. P.; Lias, S. G. Evaluated Gas Phase Basicities and Proton Affinites of Molecules: An Update. *J. Phys. Chem. Ref. Data* **1998**, *27*, 413-656.
132. Boström, C.-E.; Gerde, P.; Hanberg, A.; Jernström, B.; Johansson, C.; Kyrklund, T.; Rannug, A.; Törnqvist, M.; Victorin, K.; Westerholm, R. Cancer Risk Assessment, Indicators, and Guidelines for Polycyclic Aromatic Hydrocarbons in the Ambient Air. *Environ. Health Perspect.* **2002**, *110*, 451-488.
133. *PAHs and Related Compounds*. Springer: 1998; Vol. 3.
134. Ahad, J. M. E.; Macdonald, R.; Parrot, J.; Yang, Z.; Zhang, Y.; Siddique, T.; Kuznetsova, A.; Rauert, C.; Galarneau, E.; Studabaker, W.; Evans, M.; McMaster, M.; Shang, D. Polycyclic aromatic compounds (PACs) in the Canadian environment: A review of sampling techniques, strategies and instrumentation. *Environ. Pollut.* **2020**, 114988.
135. Dale, M. J.; Jones, A. C.; Pollard, S. J. T.; Langridge-Smith, P. R. R. Direct determination of polycyclic aromatic hydrocarbons in environmental matrices using laser desorption laser photoionization time-of-flight mass spectrometry. *Analyst* **1994**, *119*, 571-578.
136. Specht, A. A.; Blades, M. W. Direct determination of polycyclic aromatic hydrocarbons in solid matrices using laser desorption/laser photoionization ion trap mass spectrometry. *J. Am. Soc. Mass Spectrom.* **2003**, *14*, 562-570.
137. Rodgers, R. P.; Lazar, A. C.; Reilly, P. T. A.; Whitten, W. B.; Ramsey, J. M. Direct Determination of Soil Surface-Bound Polycyclic Aromatic Hydrocarbons in Petroleum-Contaminated Soils by Real-Time Aerosol Mass Spectrometry. *Anal. Chem.* **2000**, *72*, 5040-5046.
138. Jjunju, F. P. M.; Maher, S.; Li, A.; Badu-Tawiah, A. K.; Taylor, S.; Graham Cooks, R. Analysis of Polycyclic Aromatic Hydrocarbons Using Desorption Atmospheric Pressure Chemical Ionization Coupled to a Portable Mass Spectrometer. *J. Am. Soc. Mass Spectrom.* **2015**, *26*, 271-280.
139. Castellanos, A.; Benigni, P.; Hernandez, D. R.; DeBord, J. D.; Ridgeway, M. E.; Park, M. A.; Fernandez-Lima, F. Fast screening of polycyclic aromatic hydrocarbons using trapped ion mobility spectrometry – mass spectrometry. *Anal. Methods* **2014**, *6*, 9328-9332.
140. Simonsick, W. J.; Hites, R. A. Analysis of isomeric polycyclic aromatic hydrocarbons by charge-exchange chemical ionization mass spectrometry. *Anal. Chem.* **1984**, *56*, 2749-2754.
141. Lee, M. L.; Hites, R. A. Mixed charge exchange-chemical ionization mass spectrometry of polycyclic aromatic

hydrocarbons. *J. Am. Chem. Soc.* **1977**, *99*, 2008-2009.
142. Ming Ng, K.; Ling Ma, N.; Wai Tsang, C. Differentiation of isomeric polyaromatic hydrocarbons by electrospray Ag(I) cationization mass spectrometry. *Rapid Comm. Mass Spectrom.* **2003**, *17*, 2082-2088.
143. Keough, T. Dimethyl ether as a reagent gas for organic functional group determination by chemical ionization mass spectrometry. *Anal. Chem.* **1982**, *54*, 2540-2547.
144. Burinsky, D. J.; Campana, J. E. Gas-phase electrophilic addition reaction of chlorinated alkyl ions. *Org. Mass Spectrom.* **1988**, *23*, 613-619.
145. Eftekhari, M.; Ismail, A. I.; Zare, R. N. Isomeric differentiation of polycyclic aromatic hydrocarbons using silver nitrate reactive desorption electrospray ionization mass spectrometry. *Rapid Comm. Mass Spectrom.* **2012**, *26*, 1985-1992.
146. Wang, Z.; Zhu, H.; Huang, G. Ion suppression effect in desorption electrospray ionization and electrospray ionization mass spectrometry. *Rapid Commun. Mass Spectrom.* **2017**, *31*, 1957-1962.
147. Li, L.; Wang, Q.; Li, W.; Yao, Y.-N.; Wu, L.; Hu, B. Comprehensive comparison of ambient mass spectrometry with desorption electrospray ionization and direct analysis in real time for direct sample analysis. *Talanta* **2019**, *203*, 140-146.
148. Modelli, A.; Mussoni, L. Rapid quantitative prediction of ionization energies and electron affinities of polycyclic aromatic hydrocarbons. *Chem. Phys.* **2007**, *332*, 367-374.
149. United States Environmental Protection Agency Regional Screening Levels. http://www.epa.gov/risk/regional-screening-levels-rsls-users-guide (accessed July 22, 2020).
150. Canada, P. T. Test Group Summary Report C18 PAHs in Soil January 2020 PT Round. http://www.ptcanada.org/pt-resources/general-pt-reports/ (accessed June 18, 2020).
151. PubChem. https://pubchem.ncbi.nlm.nih.gov/ (accessed May 15, 2020).
152. Giorgetti, A.; Centola, C.; Giorgetti, R. Fentanyl novel derivative-related deaths. *Hum. Psychopharmacol. Clin. Exp.* **2017**, *32*, 2605-2616.
153. Frank, R. G.; Pollack, H. A. Adressing the Fentanyl Threat to Public Health. *N. Engl. J. Med.* **2017**, *376*, 605-607.
154. Bista, S. R.; Lobb, M.; Haywood, A.; Hardy, J. Development, validation and application of an HPLC-MS/MS method for the determination of fentanyl and nor-fentanyl in human plasma and saliva. *J. Chromatogr. B* **2014**, *960*, 27-33.
155. Voelker, R. Fentanyl-fueled overdoses. *JAMA* **2017**, *317*, 2055-2055.
156. Service, B. C., Fentanyl-Detected Illicit Drug Overdose Deaths. August 4, 2017 ed.; Burnaby, BC, 2017; pp 1-6.
157. Mahlke, N. S.; Ziesenitz, V.; Mikus, G.; Skopp, G. Quantitative low-volume assay for simultaneous determination of fentanyl, norfentanyl, and minor metabolites in human plasma and urine by liquid chromatography-tandem mass spectrometry (LC-MS/MS). *Int. J. Legal Med.* **2014**, *128*, 771-778.
158. Meyer, M. R.; Dinger, J.; Schwaninger, A. E.; Wissenbach, D. K.; Zapp, J.; Fritschi, G.; Maurer, H. H. Qualitative studies on the metabolism and toxicological detection of the fentanyl-derived designer drugs 3-methylfentanyl and isofentanyl in rats using liquid chromatography-linear ion trap-mass spectrometry (LC-MSn). *Anal. Bioanal. Chem.* **2012**, *402*, 1249-1255.
159. Hisada, T.; Katoh, M.; Hitoshi, K.; Kondo, Y.; Fujioka, M.; Toyama, Y.; Ieda, H.; Gocho, S.; Nadai, M. A Simple Liquid

Chromatogrpahy-Tandem Mass Spectrometry Method for Determination of Plasma Fentanyl Concentration in Rats and Patients with Cancer Pain. *Biol. Parm. Bull.* **2013**, *26*, 412-416.
160. Nishikawa, R. K.; Bell, S. C.; Kraner, J. C.; Callery, P. S. Potential Biomarkers of Smoked Fentanyl Utilizing Pyrolysis Gas Chromatography-Mass Spectrometry. *J. Anal. Toxicol.* **2009**, *33*, 418-422.
161. Gillespie, T. J.; Gandolfi, A. J.; Maiorino, R. M.; Vaughan, R. W. Gas Chromatographic Determination of Fentanyl and its Analogues in Human Plasma. *J. Anal. Toxicol.* **1981**, *5*, 133-137.
162. Goldberger, B. A.; Chronister, C. W.; Merves, M. L. Quantitation of fentanyl in blood and urine using gas chromatography-mass spectrometry (GC-MS). *Methods Mol. Biol.* **2010**, *603*, 245-252.
163. Fenn, J. B., Method and apparatus for electrospray ionization. Google Patents: 2001.
164. Espy, R. D.; Muliadi, A. R.; Ouyang, Z.; Cooks, R. G. Spray mechanism in paper spray ionization. *Int. J. Mass Spectrom.* **2012**, *325-327*, 167-171.
165. Liu, J.; Wang, H.; Manicke, N. E.; Lin, J.; Cooks, R. G.; Ouyang, Z. Development, Characterization, and Application of Paper Spray Ionization. *Anal. Chem.* **2010**, *82*, 2463-2471.
166. Manicke, N. E.; Abu-Rabie, P.; Spooner, N.; Ouyang, Z.; Cooks, R. G. Quanititative analysis of therapeutic drugs in dried blood spot samples by paper spray mass spectrometry: an avenue to therapeutic drug monitoring. *J. Am. Soc. Mass. Spectrom.* **2011**, *22*, 1501-1507.
167. Wang, H.; Manicke, N. E.; Yang, Q.; Zheng, L.; Shi, R.; Cooks, R. G.; Ouyang, Z. Direct Analysis of Biological Tissue by Paper Spray Mass Spectrometry. *Anal. Chem.* **2011**, *83*, 1197-1201.
168. Wang, H.; Ren, Y.; McLuckey, M. N.; Manicke, N. E.; Park, J.; Zheng, L.; Shi, R.; Cooks, R. G.; Ouyang, Z. Direct Quantitative Analysis of Nicotine Alkaloids from Biofluid Samples using Paper Spray Mass Spectrometry. *Anal. Chem.* **2013**, *85*, 11540-11544.
169. Wang, H.; Liu, J.; Cooks, R. G.; Ouyang, Z. Paper Spray for Direct Analysis of Complex Mixtures Using Mass Spectrometry. *Angew. Chem.* **2010**, *122*, 889-892.
170. Reeber, S. L.; Gadi, S.; Huang, S.-B.; Glish, G. L. Direct analysis of herbicides by paper spray ionization mass spectrometry. *Anal. Methods* **2015**, *7*, 9808-9816.
171. McKenna, J.; Dhummakupt, E. S.; Connell, T.; Demond, P. S.; Miller, D. B.; Nilles, J. M.; Manicke, N. E.; Glaros, T. Detection of chemical warfare agent simulants and hydrolysis products in biological samples by paper spray mass spectrometry. *Analyst* **2017**, *142*, 1442-1451.
172. Cooks, R. G.; Mueller, T. Through a glass darkly: glimpses into the future of mass spectrometry. *Mass Spectrom. (Tokyo)* **2013**, *2*, S0001.
173. Ouyang, Z.; Noll, R. J.; Cooks, R. G. Handheld Miniature Ion Trap Mass Spectrometers. *Anal. Chem.* **2009**, *81*, 2421-2425.
174. Bell, R. J.; Davey, N. G.; Martinsen, M.; Collin-Hansen, C.; Krogh, E. T.; Gill, C. G. A Field-Portable Membrane Introduction Mass Spectrometer for Real-time Quantitation and Spatial Mapping of Atmospheric and Aqueous Contaminants. *J. Am. Soc. Mass. Spectrom.* **2014**, *26*, 212-223.
175. Mather, L. E. Clinical pharmacokinetics of fentanyl and its newer derivatives. *Clin. Pharmacokinet.* **1983**, *8*, 422-446.

176. Baselt, R. C., *Disposition of Toxic Drugs & Chemicals in Man*. 11th ed.; Biomedical Publications: Seal Beach, California, 2011.
177. Chen, S.; Chang, Q.; Yin, K.; He, Q.; Deng, Y.; Chen, B.; Liu, C.; Wang, Y.; Wang, L. Rapid Analysis of Bisphenol A and Its Analogs in Food Packaging Products by Paper Spray Ionization Mass Spectrometry. *J. Agric. Food Chem.* **2017**,
178. Shen, L.; Zhang, J.; Yang, Q.; Manicke, N. E.; Ouyang, Z. High throughput paper spray mass spectrometry analysis. *Clin. Chim. Acta* **2013**, *420*, 28-33.
179. Labroo, R. B.; Paine, M. F.; Thummel, K. E.; Kharasch, E. D. Fentanyl metabolism by human hepatic and intestinal cytochrome P450 3A4: implications for interindividual variability in disposition efficacy, and drug interactions. *Drug Metab. Dispos.* **1997**, *25*, 1072-1080.
180. Ruan, X.; Chiravuri, S.; Kaye, A. D. Using postmortem blood and urine norfentanyl/fentanyl ratios in the investigation of fentanyl-related deaths. *Clin. Toxicol.* **2016**, *54*, 893.